The net exchange of carbon greenhouse gases with high Arctic terrestrial and aquatic ecosystems

by

Craig Andrew Emmerton

A thesis submitted in partial fulfillment of the requirements for the degree of

Doctor of Philosophy

in

Ecology

Department of Biological Sciences
University of Alberta

Abstract

Accelerated climate warming of Canada's sparsely vegetated high Arctic has resulted in rapid environmental changes including loss of glacial ice, permafrost thaw, decreased snow cover and changing plant communities. These responses are causing mostly unknown changes to the natural cycling of the greenhouse gases (GHGs) carbon dioxide (CO_2) and methane (CH_4) between northern landscapes and the atmosphere, therefore potentially perturbing global carbon feedbacks. From 2005-2012 at Lake Hazen, Quttinirpaaq National Park, Nunavut, Canada (82ºN), we investigated growing season (June-September) exchange of atmospheric CO_2 and CH_4 with high Arctic landscapes and aquatic systems, and scaled these ground-level measurements to larger regions to more broadly apply our findings.

We used multi-year eddy covariance and static chamber measurements on contrasting high Arctic dry semidesert and meadow wetland landscapes to quantify their net exchange of CO_2 and CH_4 with the atmosphere. We used these rare high latitude data with ground and satellite productivity measurements (Normalized Difference Vegetation Index; NDVI) to evaluate the effectiveness of upscaling local to regional exchange of CO_2. During the growing season, the semidesert landscape was a weak CO_2 source to the atmosphere (+0.05 g C m^{-2} d^{-1}) which was primarily driven by increasing surface soil respiration and moisture. However, rising soil temperatures and environmental conditions suitable for gas diffusion resulted in considerable consumption of atmospheric CH_4 (-0.001±0.000 g-CH_4 m^{-2} d^{-1}) in semidesert soils. Greater access to water and resulting plant growth at the nearby wetland resulted in considerable uptake of CO_2 (-0.63 g C m^{-2} d^{-1}) relative to the semidesert during the growing season, rivaling rates observed at Arctic wetlands much further to the south. Emission of CH_4 from the wet soils,

however, was weak ($+0.001\pm0.000$ g-CH_4 m^{-2} d^{-1}) compared to other high Arctic sites likely because of shallow permafrost depths and limited microbial substrate. Our upscaling assessment found that semidesert ground NDVI was low and similar to satellite measurements, however, faint seasonal changes and poor relationships between CO_2 exchange and measured NDVI suggested that high Arctic landscapes were too sparsely vegetated currently to accurately upscale ground measurements of productivity to broader regions.

We also quantified dissolved CO_2 and CH_4 concentrations and fluxes of common aquatic systems in the Lake Hazen watershed by collecting water samples and deploying automated systems. Gas concentrations in oligotrophic Lake Hazen were near atmospheric equilibrium and associated closely with carbonate concentrations in the water and turbulence, resulting in near-zero exchange of each GHG with the atmosphere. Lakes higher in the watershed emitted CO_2 in relation to heterotrophic signatures, while CH_4 emission was low and declined with increasing incidence of dissolved sulfate in water columns. Shoreline ponds bordering Lake Hazen transitioned from weak CO_2 sinks during drier conditions, to strong sources of CH_4 when flooded by Lake Hazen.

Finally, we weighted mean seasonal GHG exchange rates from measured landscapes and aquatic systems by total land cover in the Lake Hazen watershed. We found that despite existence of environments capable of exchanging considerable amounts of GHGs with the atmosphere (e.g., shoreline ponds, meadow wetlands), Lake Hazen watershed cycling of GHGs was dominated by exchange at the expansive, but relatively unproductive, semidesert soils and Lake Hazen. Therefore, we estimated that the watershed effectively transferred net-zero amounts of carbon GHGs (CO_2: 20 ± 267, CH_4: -0.76 ± 0.80 mg C m^{-2} d^{-1}) with the atmosphere during the

growing season. Continued climate warming in the watershed is expected to support greater vegetation growth and productivity in Lake Hazen. However, poor soil moisture retention and limited nutrient availability in soils and in Lake Hazen may hinder short-term changes in productivity and GHG exchange, at least until plant reproductive success improves, vegetation cover expands and accumulation of organic matter and moisture in soils occurs.

These studies report the most northerly eddy covariance data in the literature and also concurrently compare GHG cycling between two contrasting high Arctic ecosystems, which has only been achieved at a small handful of high Arctic site globally. This important baseline data set may be important for the global carbon modeling community which has only rare high Arctic CO_2 and CH_4 exchange data to validate simulations.

Preface

Most scientific studies require collaborations with other researchers and technical professionals to achieve scientific goals. Research contained within this thesis is not an exception to this practice. Credit has therefore been given, by way of authorship, to people who provided scientific direction, analytical expertise and supporting data to the three manuscripts that have been, or will be, published from this thesis.

Chapter 2: Emmerton, C.A.; St. Louis, V.L.; Humphreys, E.R.; Barker, J.D.; Gamon, J.A.; Pastorello, G.Z. Net ecosystem production of polar semidesert and wetland landscapes in the rapidly changing Canadian high Arctic. To be submitted to *Global Change Biology* in 2015.

Chapter 3: Emmerton, C.A.; St. Louis, V.L.; Lehnherr, I.; Humphreys, E.R.; Rydz, E.; Kosolofski, H.R. The net exchange of methane with high Arctic landscapes during the summer growing season. *Biogeosciences* 2014, *11*, 3095-3106.

Chapter 4: Emmerton, C.A.; St. Louis, V.L.; Lehnherr, I., Graydon, J.A.; Rondeau, K.; Kirk, J.L.; Barker J.D. The net exchange of carbon greenhouse gases with aquatic systems in a high Arctic watershed and its role in whole-ecosystem carbon transfer. To be submitted to *Environmental Science & Technology* in 2015.

Acknowledgments

Table of Contents

List of Tables

Table of Figures

Chapter 1. General Introduction

Rapid Arctic climate change

From initial hypothesis (Arrhenius, 1896) to weather analyses (Brooks, 1949) and modeling (Manabe and Stouffer, 1980), pioneering climate change studies indicated a disproportionate heating of polar latitudes is, or will be, occurring as releases of anthropogenic carbon greenhouse gases (GHGs) continue. During natural atmospheric conditions, the Earth receives most solar energy in equatorial regions, where absorbed and re-emitted radiation (as heat) is transferred toward high latitude regions via air and oceanic currents. Under atmospheric conditions perturbed by human activity (Stocker *et al.*, 2013), more energy is trapped and transferred to the poles (Spielhagen, 2011) where the heat-sensitive cryosphere is most prominent. Resultant high-latitude warming of the atmosphere and oceans, above that of mean global temperature change, is known as Arctic or polar amplification (Serreze and Barry, 2011) and it is a distinct symptom of global climate change.

Multiple lines of evidence support the existence of Arctic amplification and its strengthening into the future. First, despite the general paucity of long-term weather observations from remote polar regions with extreme cold, wind and winter darkness, existing records indicate consistent warming has occurred in many locations throughout the Arctic. For example, Bekryaev *et al.* (2010) found that several northern (>60ºN) continental weather stations measured mean increases of 1.36ºC per century from 1875-2008; a rate twice that of the Northern Hemisphere. Second, reconstructions of past weather, via tree ring analysis or lake sediment coring (e.g., Kaufman, 2009), effectively broaden instrumental weather records and have shown evidence of greater warming today compared to the past. Using environmental archives to model historical air temperature, Overpeck (1997) found that the since 1840, the Arctic had warmed to its highest temperature in four centuries. Finally, calibrated climate models have consistently predicted a greater rate of warming at high latitudes into the future compared to mean planetary temperatures, though the estimated magnitude of heating is highly variable (Serreze and Barry, 2011). Most heating was expected to occur over the Arctic Ocean where projected sea-ice loss would allow for warming of the water column, especially during later summer and autumn during annual sea ice coverage minimum. When considering the wealth of

1

evidence, we now have high confidence that Arctic amplification is occurring and will continue into the future and result in significant changes to the Arctic environment (Stocker *et al.*, 2013).

Among the most prominent environmental responses to Arctic amplification has been the recent rapid decline of sea ice thickness and areal coverage across the Arctic Ocean. Mean sea-ice thickness has declined between 1.3 and 2.3 m and areal coverage has reduced by more than 50% since 1980 (Stroeve *et al.* 2007; Stocker *et al.*, 2013). Especially evident has been the loss of multi-year ice cover which has been replaced by annual ice which melts each summer season (Kwok *et al.*, 2009). Disappearance of sea ice is particularly crucial for polar regions because that process drives the Arctic albedo feedback, where high-albedo ice cover is replaced by low-albedo ocean water capable of absorbing more heat (Serreze *et al.*, 2000). The resulting increase in ocean warming further impacts sea ice thickness and coverage and potentially accelerates Arctic amplification further. Melting or thawing of the polar terrestrial cryosphere has also been substantial. Glacier cover has declined rapidly in the North, particularly in Greenland and the Canadian high Arctic, contributing directly to sea level rise (Pritchard *et al.*, 2009; Gardner *et al.*, 2011). Snow cover across the Arctic has declined rapidly and extensively since 2009 (AMAP, 2011), reducing approximately 50%, while snow-free growing seasons have extended by several days at different sites throughout the Arctic (Post *et al.*, 2009). Permafrost in northern soils, defined as soils continuously below 0ºC for consecutive years, is thawing in most regions, with a mean increase in permafrost temperature of 0.5-2ºC since the 1970s (AMAP, 2011). Permafrost extent is expected to continue declining in the future in Canada, Alaska, Scandinavia and Russia, with possibly up to 20% loss of permafrost coverage in some areas by the end of the 21st century (AMAP, 2011). Loss of permafrost and thickening of active layers can have effects not only on dry land in the form of slumps and mass flows (Kokelj *et al.*, 2013), but also on lakes which have been documented to shrink or drain because of permafrost degradation (Smith *et al.*, 2005; Smol and Douglas, 2007). Thermokarst lakes can also develop where destabilization of permafrost gives way to depressions and accumulation of runoff water (Smith *et al.*, 2005). Other observed consequences of a warming Arctic include northward migration of southern plant and animal species and diseases (e.g, Post *et al.*, 2009), increased evaporation, precipitation, runoff and river discharge (Peterson *et al.*, 2002; Bintanja and Selten, 2014), more extensive spring-summer cloud cover and trapping of infrared heat (Schweiger, 2004), and a host of behavioral changes in

the biosphere (e.g., Post and Forchhammer, 2008). The multitude of atmospheric, hydrological and biological changes resulting from the continuing amplification of temperatures in the Arctic, have considerable effects on the Arctic carbon cycle and its role in global carbon feedbacks, which have the potential to disturb climate further.

Response of the carbon cycle to Arctic warming

Global carbon feedbacks, as opposed to albedo or energy feedbacks, describe processes which, once affected by changing environmental or climate conditions, either release or absorb carbon GHGs relative to the atmosphere (Callaghan *et al.*, 2011). These feedbacks directly modify concentrations of GHGs in the atmosphere and have the potential to enhance or buffer anthropogenic climate change. The most abundant carbon GHG in the atmosphere is carbon dioxide (CO_2; 398 parts-per-million [ppm] as of 2015; NOAA, 2015), followed by much less abundant methane (CH_4; ~1.8 ppm; CDIAC, 2014), which is more powerful per molecule than CO_2 at trapping infrared radiation (Stocker *et al.*, 2013). These GHGs naturally cycle between the circulating atmosphere and terrestrial, freshwater and marine ecosystems through processes such as diffusion and weathering, photosynthesis and respiration, methanotrophy and methanogenesis, and sediment burial in aquatic and soil systems, among others. However, Arctic amplification can perturb these processes and potentially affect natural carbon feedbacks which help to stabilize the Earth's climate over millennia (ACIA, 2005). Positive feedbacks are described as processes which release a balance of GHGs to the atmosphere and intensify the trapping of heat, further supporting climate warming. An example of a positive feedback affected by Arctic amplification might be temperature-controlled heterotrophic respiration of previously frozen organic soils in permafrost and increased release of CO_2 to the atmosphere (ACIA, 2005). Alternatively, negative feedbacks are described as processes which absorb and effectively trap a balance of GHGs from the atmosphere, therefore reducing concentrations and undermining climate warming. An example of a negative feedback in a warming Arctic might be the northward expansion of the boreal tree line, which may promote greater uptake and sequestration of CO_2 from the atmosphere as organic carbon (ACIA, 2005). However, quantifying the net GHG exchange between Arctic ecosystems and the atmosphere, let alone understanding its

changes, is a complex puzzle in part because of the Arctic's harsh and variable climate, and its extensive, heterogeneous land cover.

The magnitude and direction of GHG exchange (as mass fluxes; i.e., mass per area per time) between Arctic ecosystems and the global atmosphere vary considerably in response to the harsh temperature and moisture conditions in the North. Cold Arctic temperatures are well known to reduce heterotrophic decomposition rates (Davidson and Janssens, 2006), resulting in reduced CO_2 emission to the atmosphere, and accumulation of organic matter in soils (Tarnocai *et al.*, 2009). However, cold air also restricts autotrophic productivity and uptake of atmospheric CO_2, resulting in, for example, a close relationship between the positions of the mean 10°C July air temperature isotherm and the circumpolar boreal tree line (AMAP, 1998). Frost fronts in cold northern soils can even physically force accumulated GHGs at depth to the atmosphere during shoulder seasons (e.g., Mastepanov *et al.*, 2008). Extremes in soil moisture can also supplement or weaken GHG fluxes in the Arctic. Ample standing water and saturated soils in the Arctic due to low relief and permafrost barriers at depth, promote anaerobic decomposition and emissions of CH_4 to the atmosphere (ACIA, 2005). High concentrations of dissolved organic carbon in streams and lakes can be readily respired or photodegraded, resulting in release of CO_2 to the atmosphere (Laurion and Mladenov, 2013). Alternatively, cold and dry polar air at the highest latitudes can desiccate soils both restricting plant CO_2 uptake due to water starvation, but also promoting uptake/oxidation of CH_4 in aerated soils. Though the Arctic carbon cycle responds variably to different heating and moisture regimes, the timing and intensity of various GHG fluxes is ultimately shaped by temporal changes in weather and light, which can change substantially from hours to days to seasons in the Arctic (Elberling and Brandt, 2003; Elberling *et al.*, 2008).

GHG emissions and uptake also vary considerably in space across the Arctic, and at very resolved scales. For example, emissions of CH_4 from some wet tundra environments in the Arctic can vary by a magnitude or more at the meter scale, making it extremely challenging to measure gas fluxes from these landscapes (Moosavi *et al.*, 1996). Though seasonal exchange of CO_2 may be more predictable to measure than the typically episode-driven exchange of CH_4, heterogeneous distribution of vegetation, water and soil types across Arctic landscapes can

complicate even the predictable seasonal flux pattern of CO_2. For example, temperature and moisture conditions can change substantially over the square meter scale of patterned ground, often leading to much different GHG exchanges in small space (Fox *et al.*, 2008). However, though GHG fluxes may change considerably across small scales in the Arctic, these differences may be unimportant compared to the dramatic land cover, albedo, energy balance and climate differences between the low and high Arctic ecoregions.

Contrasting low and high Arctic landscapes

Above the boreal tree line, the North can effectively be divided into the low Arctic and the high Arctic (AMAP, 1998), each with particularly distinct environments with large differences in GHG fluxes. In general step with the 10ºC July isotherm, large conifers of the boreal forest disappear leaving less productive lowland tundra (~65-75 ºN). The low Arctic has accumulated substantial amounts of organic carbon in soils (Tarnocai *et al.*, 2009) and has some of the most extensive cover of lakes and wetlands on Earth (Lehner and Doll, 2004), and is therefore a potential global hot spot for both CO_2 (Tarnocai *et al.*, 2009) of CH_4 (Corradi *et al.*, 2005) exchange. However, a much different ecoregion occurs north of the lowland tundra. Because of prevailing high pressure at high Arctic latitudes, very cold and dry air washes over landscapes, leaving only hearty and well-adapted vegetation present, though as only sparse cover. This has resulted in relatively poor organic carbon and nutrient accumulation, and thus little vegetation cover, resulting in the polar desert (or semidesert; ~65-85 ºN), which harbors some of the least productive landscapes on Earth. Consequently exchange of CO_2 (0.060±0.036 g C m^{-2} d^{-1} uptake during the growing season; Soegaard *et al.*, 2000; Lloyd, 2001, Lund *et al.*, 2012) is extremely low, and wet ecosystems are rare. Interestingly, dry soils at this latitude typically take up atmospheric CH_4 (Jorgensen *et al.*, 2015), rather than emitting as is the case throughout lower Arctic latitudes (Christensen et al, 1995). Though exchange of GHGs in the high Arctic is gaining more attention (Stocker *et al.*, 2013), still very few studies at very few sites across the polar semidesert exist, resulting in an unclear picture as to the magnitude, seasonality and net direction of GHG fluxes with the atmosphere there. Further, we are only beginning to understand the environmental factors which control the generation or uptake of GHGs in this extreme environment, or how effectively hectare-scale measurements of GHG

exchange can be applied to broader regions of the high Arctic. These topics form the basis of my thesis research.

The first research chapter, *Chapter 2: Net ecosystem production of polar semidesert and wetland landscapes in the rapidly changing Canadian high Arctic*, presents a three to five year data set of hectare-scale, near real-time measurements of CO_2 exchange between the atmosphere and contrasting high Arctic landscapes. We also used several supporting meteorological and environmental measurements to better understand which factors influenced the measured exchange of CO_2. We then used these rare data with ground and satellite productivity measurements to evaluate the effectiveness of upscaling local to regional measurements of CO_2 exchange.

The second research chapter, *Chapter 3: The net exchange of methane with high Arctic landscapes during the summer growing season*, presents three to five years of static chamber measurements of terrestrial CH_4 exchange between contrasting high Arctic landscapes and the atmosphere. These data are enhanced by one growing season of rare hectare-scale, near real-time measurements of CH_4 exchange between a wetland and the atmosphere. We investigated environmental and weather factors which associated closely with changes in CH_4 fluxes to better understand influential conditions contributing to the release or storage of the potent GHG. At the wetland, we integrated measurements of terrestrial CH_4 exchange with aquatic transport of CH_4 to construct a mass balance of the GHG within the wetland, something not done previously in the high Arctic.

The third research chapter, *Chapter 4: The net exchange of carbon greenhouse gases with aquatic systems in a high Arctic watershed and its role in whole-ecosystem carbon transfer*, presents the exchange of both CO_2 and CH_4 from fully-aquatic environments in a high Arctic setting. We used both manual water collection and in-situ measurements by automated systems at different lake types in the high Arctic to quantify aqueous exchange of the GHGs with the atmosphere. The five year dataset also contains general chemical measurements of each lake where GHG samples were collected, to better understand the biogeochemical conditions influencing GHG exchange in high Arctic lakes. We then placed our aquatic and terrestrial GHG exchange findings (from all three chapters) into a regional context to understand the relative

contributions of each terrestrial and aquatic environment to the watershed-scale exchange of these gases with the atmosphere.

Finally, a general conclusion (*Chapter 5: General conclusion*) is presented to both summarize the findings of the thesis as an entirety, but also provide guidance for future research in this area and discuss its implications for global climate change.

References

ACIA. 2005. Arctic climate impact assessment—scientific report, 1st ed. New York: Cambridge University Press.

AMAP. 1998. AMAP Assessment Report: Arctic Pollution Issues. Arctic Monitoring and Assessment Programme (AMAP), Oslo, Norway. xii+859 pp.

AMAP. 2011. Snow, Water, Ice and Permafrost in the Arctic (SWIPA): Climate Change and the Cryosphere. Arctic Monitoring and Assessment Programme (AMAP), Oslo, Norway. xii + 538 pp.

Arrhenius, S. 1896. On the influence of carbonic acid in the air upon the temperature of the ground. Philos. Mag. J. Sci., 5, 237–276.

Bekryaev, R.V., Polyakov, I.V., Alexeev, V.A. 2010. Role of polar amplification in longterm surface air temperature variations and modern Arctic warming. J. Climate, 23, 3888–3906.

Bintanja R., Selten F.M. 2014. Future increases in Arctic precipitation linked to local evaporation and sea-ice retreat. Nature, 509, 479-482.

Brooks, C.E.P. 1949. Climate through the ages, 2nd edition. Ernest Benn Ltd., London. 395 pp.

Callaghan, T.V., Johansson, M., Key, J., Prowse, T., Ananicheva, M., Klepikov, A. 2011. Feedbacks and interactions: From the Arctic cryosphere to the climate system. Ambio, 40, 75-86.

CDIAC (Carbon Dioxide Information and Analysis Center). 2014. Current greenhouse gas concentrations. From: http://cdiac.ornl.gov/pns/current_ghg.html, DOI: 10.3334/CDIAC/atg.032.

Christensen, T.R., Jonasson, S., Callaghan, T.V., Havstrom, M. 1995. Spatial Variation in High-Latitude Methane Flux Along a Transect across Siberian and European Tundra Environments. Journal of Geophysical Research-Atmospheres, 100, 21035-21045.

Corradi, C., Kolle, O., Walter, K., Zimov, S.A., Schulze, E.D. 2005. Carbon dioxide and methane exchange of a north-east Siberian tussock tundra. Global Change Biology, 11, 1910-1925.

Davidson, E.A., Janssens, I.A. 2006. Temperature sensitivity of soil carbon decomposition and feedbacks to climate change. Nature, 440, 165-173.

Elberling, B., Brandt, K.K. 2003. Uncoupling of microbial CO_2 production and release in frozen soil and its implications for field studies of Arctic C cycling. Soil Biology & Biochemistry, 35, 263-272.

Elberling, B., Nordstrom, C., Grondahl, L., Sogaard, H., Fridborg, T., Christensen, T.R., Strom, L., Marchand, F., Nijs, I. 2008. High-Arctic soil CO_2 and CH_4 production controlled by temperature, water, freezing and snow. Advances in Ecological Research, 40, 441-472.

Fox, A.M., Huntley, B., Lloyd, C.R., Williams, M., Baxter, R. 2008. Net ecosystem exchange over heterogeneous Arctic tundra: Scaling between chamber and eddy covariance measurements. Global Biogeochemical Cycles, 22, GB2027.

Gardner, A.S., Moholdt, G., Wouters, B., Wolken, G.J., Burgess, D.O., Sharp, M.J., Cogley, J.G., Braun, C., Labine, C. 2011. Sharply increased mass loss from glaciers and ice caps in the Canadian Arctic Archipelago. Nature 473, 357-360.

Jorgensen, C.J., Johansen, K.M.L., Westergaard-Nielsen, A., Elberling, B. 2015. Net regional methane sink in High Arctic soils of northeast Greenland. Nature Geoscience, 8, 20-23.

Kaufman, D.S., Schneider, D.P., McKay, N.P., Ammann, C.M., Bradley, R.S., Briffa, K.R., Miller, G.H., Otto-Bliesner, B.L., Overpeck, J.T., Vinther, B.M. 2009. Recent warming reverses long-term Arctic cooling. Science, 325(5945), 1236-1239.

Kokelj, S.V, Lacelle, D., Lantz, T.C., Tunnicliffe, J., Malone, L., Clark, I.D., Chin, K.S. 2013. Thawing of massive ground ice in mega slumps drives increases in stream sediment and solute flux across a range of watershed scales. Journal of Geophysical Research-Earth Surface, 118(2), 681-692.

Kwok, R., Cunningham, G.F., Wensnahan, M., Rigor, I., Zwally, H.J., Yi, D. 2009. Thinning and volume loss of the Arctic Ocean sea ice cover: 2003-2008. Geophysical Research Letters, 114, C07005.

Laurion, I., Mladenov, N. 2013. Dissolved organic matter photolysis in Canadian arctic thaw ponds. Environ. Res. Lett., 8, 1-12.

Lehner, B., Doll, P. 2004. Development and validation of a global database of lakes, reservoirs and wetlands, J. Hydrol., 296, 1–22.

Lloyd, C. R. 2001. The measurement and modelling of the carbon dioxide exchange at a high arctic site in Svalbard. Global Change Biology, 7(4), 405-426.

Lund, M., Falk, J.M., Friborg, T., Mbufong, H.N., Sigsgaard, C., Soegaard, H., Tamstorf, M.P. 2012. Trends in CO2 exchange in a high arctic tundra heath, 2000-2010. Journal of Geophysical Research-Biogeosciences, 117, G02001.

Manabe, S., Stouffer, R.J. 1980. Sensitivity of a global climate model to an increase of CO2 concentration in the atmosphere. J. Geophys. Res. 85, 5529–5554.

Mastepanov, M., Sigsgaard, C., Dlugokencky, E.J., Houweling, S., Ström, L., Tamstorf, M.P., Christensen, T.R. 2008. Large tundra methane burst during onset of freezing. Nature, 456, 628-631.

Moosavi, S.C., Crill, P.M., Pullman, E.R., Funk, D.W., Peterson, K.M. 1996. Controls on CH4 flux from an Alaskan boreal wetland. Global Biogeochemical Cycles, 10(2), 287-296.

NOAA (National Oceanic and Atmospheric Administration). 2015. From: http://www.esrl.noaa.gov/gmd/ccgg/trends/.

Overpeck, J., Hughen, K., Hardy, D., Bradley, R., Case, R., Douglas, M., Finney, B., Gajewski, K., Jacoby, G., Jennings, A., Lamoureux, S., Lasca, A., MacDonald, G., Moore, J., Retelle, M., Smith, S., Wolfe, A., Zielinski, G. 1997. Arctic environmental change of the last four centuries. Science, 278(5341), 1251-1256.

Peterson, B. J., Holmes, R. M., McClelland, J.W., Vorosmarty, C.J., Lammers, R.B., Shiklomanov, A.I., Shiklomanov, I. A., Rahmstorf, S. 2002. Increasing river discharge to the Arctic Ocean. Science, 298, 2171−2173.

Post, E., Forchhammer, M.C. 2008. Climate change reduces reproductive success of an Arctic herbivore through trophic mismatch. Philosophical Transactions of the Royal Society B-Biological Sciences, 363(1501), 2369-2375.

Post, E., Forchhammer, M.C., Bret-Harte, M.S., Callaghan, T.V., Christensen, T.R., Elberling, B., Fox, A.D., Gilg, O., Hik, D.S., Hoye, T.T., Ims, R.A., Jeppesen, E., Klein, D.R., Madsen, J., McGuire, A.D., Rysgaard, S., Schindler, D.E., Stirling, I., Tamstorf, M.P., Tyler, N.J.C., van der Wal, R., Wlker, J., Wookey, P.A., Schmidt, N.M., Aastrup, P. 2009. Ecological dynamics across the Arctic associated with recent climate change. Science 325: 1355-1358.

Pritchard, H.D., Arthern, R.J., Vaughan, D.G., Edwards, L.A. 2009. Extensive dynamic thinning on the margins of the Greenland and Antarctic ice sheets. 461, 971-975.

Schweiger, A.J. 2004. Changes in seasonal cloud cover over the Arctic seas from satellite and surface observations. Geophysical Research Letters, 31, L2207.

Serreze, M.C., Walsh, J.E., Chapin III, F.S., Osterkamp, T., Dyurgerov, M., Romonovsky, V., Oechel,W.C., Morison, J., Zhang, T., Barry, R.G. 2000. Observational evidence of recent change in the northern high latitude environment. Climatic Change, 46, 159–207.

Serreze, M.C., Barry, R.G. 2011. Processes and impacts of Arctic amplification: A research synthesis. Global and Planetary Change, 77, 85-96.

Smith, L.C., Sheng, Y., MacDonald, G.M., Hinzman, L.D. 2005. Disappearing Arctic lakes. Science. 308, 1429.

Smol, J.P., Douglas, M.S.V. 2007. Crossing the final ecological threshold in high Arctic ponds. PNAS, 104(3), 12395-12397.

Spielhagen, R.F., Werner, K., Sørensen, S.A., Zamelczyk, K., Kandiano, E., Budeus, G., Husum, K., Marchitto, T.M., Hald, M. 2011. Enhanced modern heat transfer to the Arctic by warm Atlantic water. Science, 331, 450-453.

Soegaard, H.; Nordstroem, C.; Friborg, T.; Hansen, B. U.; Christensen, T.R.; Bay, C. 2000. Trace gas exchange in a high-arctic valley 3. Integrating and scaling co2 fluxes from canopy to landscape using flux data, footprint modeling, and remote sensing. Global Biogeochemical Cycles, 14(3), 725-744.

Stocker, T.F., Qin, D., Plattner, G,-K., Alexander, L.V., Allen, S.K., Bindoff, N.L., Bréon, F.-M., Church, J.A., Cubasch, U., Emori, S., Forster, P., Friedlingstein, P., Gillett, N., Gregory, J., Hartmann, D.L., Jansen, E., Kirtman, B., Knutti, R., Krishna Kumar, K., Lemke, P., Marotzke, J., Masson-Delmotte, V., Meehl, G.A., Mokhov, I.I., Piao, S., Ramaswamy, V., Randall, D., Rhein, M., Rojas, M., Sabine, C., Shindell, D., Talley, L.D., Vaughan, D.G., Xie, S.-P., 2013. Technical Summary. In: Climate Change 2013: The Physical Science Basis. Contribution of Working Group I to the Fifth Assessment Report of the Intergovernmental Panel on Climate Change [Stocker, T.F., Qin, D., Plattner, G.-K., Tignor, M., Allen, S.K., Boschung, J., Nauels, A., Xia, Y., Bex, V., Midgley, P.M. (eds.)]. Cambridge University Press, Cambridge, United Kingdom and New York, NY, USA.

Stroeve, J., Holland, M.M., Meier, W., Scambos, T., Serreze, M. 2007. Arctic sea ice decline: Faster than forecast. Geophysical Research Letters, 34, L09501.

Tarnocai, C., Canadell, J.G., Schuur, E.A.G., Kuhry, P., Mazhitova, G., Zimov, S. 2009. Soil organic carbon pools in the northern circumpolar permafrost region. Global Biogeochemical Cycles, 23, GB2023.

Chapter 2. Net ecosystem production of polar semidesert and wetland landscapes in the rapidly changing Canadian high Arctic

Introduction

Nearly half of global below-ground organic carbon (OC) stores are located within northern terrestrial ecosystems, particularly in the low Arctic (defined by AMAP, 1998; Tarnocai *et al.*, 2009). Cold temperatures, short growing seasons, nutrient scarcity, and poorly draining soils in the Arctic are robust barriers to heterotrophic decomposition of OC by soil microbes and release of the greenhouse gas carbon dioxide (CO_2) to the atmosphere (Oechel *et al.*, 2000; Mack *et al.*, 2004). However, a rapidly warming Arctic climate and regional hydrological changes (Spielhagen *et al.*, 2011; Parmentier *et al.*, 2013; Lupascu *et al.*, 2014; Bintanja and Selten, 2014) are disturbing the relative balance of CO_2 between northern landscapes and the atmosphere and are affecting global carbon feedbacks (Arneth *et al.*, 2010). For example, declining snow cover and landscape albedo, warming soils and permafrost degradation (Serreze *et al.*, 2000; Post *et al.*, 2009; Callaghan *et al.*, 2011) may support increased microbial decomposition of contemporary and archived OC and release of CO_2 to the atmosphere (Oechel *et al.*, 1993). Alternatively, longer growing seasons and northward migration of more productive vegetation from southern latitudes may increase landscape accumulation of OC and therefore reduce atmospheric CO_2 concentrations (Sala *et al.*, 2000; Barichivich *et al.*, 2013; Pearson *et al.*, 2013). These transformations may be further modified by hydrological changes driven by regional surface wetting or drying (Zhang *et al.*, 2012). Ultimately, the net result of landscape changes, driven by heating and moisture, influence future carbon storage in the Arctic.

Net ecosystem production (NEP) is a critical ecosystem measurement used to describe net carbon uptake on landscapes and is often measured at the hectare-scale using eddy covariance (EC) flux towers (Baldocchi, 2003). NEP is defined here as the difference between CO_2 uptake by gross ecosystem productivity (GEP) and CO_2 release via ecosystem respiration (R_{ECO}) ($NEP = GEP - R_{ECO}$). GEP is the gross sum of an ecosystem's CO_2 fixation by vascular, bryophytic and microbial photoautotrophs. R_{ECO} includes aerobic and anaerobic respiration by vegetation, microbial communities, secondary consumers and abiotic contributions. Over a defined period of time, net uptake of CO_2 by a landscape (+NEP) means it is in a state of

autotrophy, whereas net release of CO_2 to the atmosphere from a landscape (-NEP) means it is in a state of heterotrophy.

Assessments of NEP in northern ecosystems using EC and other techniques have focused mostly on landscapes of the low Arctic (e.g., Marushchak *et al.*, 2013). Plant growth is considerable there, but enhanced soil respiration is expected to play a globally significant role by increasing atmospheric CO_2 concentrations as permafrost degrades (Callaghan *et al.*, 2011). In contrast, high Arctic landscapes, which currently cover over one million square kilometers (Brummell *et al.*, 2012), support minimal rates of plant growth and microbial respiration due to colder weather and soils low in moisture, nutrients and OC. However, our understanding of integrative CO_2 cycling at high Arctic locations is limited by low measurement frequency at relatively few sites, and is therefore underrepresented within global-scale carbon assessments (Lafleur *et al.*, 2012). This is particularly notable because the high Arctic is expected to experience substantial climate and hydrological changes relative to most of the globe (Bintanja and Selten, 2014).

High Arctic NEP has only been measured at a handful of sites using EC, including a fen and heath site at Zackenburg, Greenland (74.5ºN; e.g., Rennermalm *et al.*, 2005; Lund *et al.*, 2012) and polar semidesert locations at Svalbard, Norway (79.6ºN; Lloyd, 2001; Lüers *et al.*, 2014) and in the Canadian Arctic Archipelago (63.8-74.9ºN; Lafleur *et al.*, 2012). Though the wet Zackenburg fen was consistently autotrophic each growing season because of the efficiency of plant growth there (Soegaard *et al.*, 2000), drier semidesert sites were either net autotrophic or heterotrophic depending on seasonal heating or moisture conditions (Lloyd, 2001; Lund *et al.*, 2012; Lupascu *et al.*, 2014). Dry sites are particularly widespread in the high Arctic, so it is critical to better understand not only how heat influences contemporary NEP, but also moisture, so as to better predict the future role of these landscapes within the global carbon cycle. However, it is also critical to develop methods of upscaling local studies to larger regions. One way to assess NEP over areas larger than what EC towers can measure is by taking a top-down approach to measuring ecosystem productivity using aircraft or satellite measurements, typically within a modeling framework (Cheng *et al.*, 2006). However, the Arctic presents a challenging environment for assessing ecosystem CO_2 exchange with optical remote sensing due to sparse

plant growth, and the confounding influences of clouds, surface water, and snow and ice (Stow *et al.*, 2004; Gamon *et al.*, 2013). Without an accurate link across scales of NEP measurements, the true role of high Arctic landscapes in the global cycling of CO_2 will remain rather speculative.

Our research aimed to clarify the role of heating and moisture on high Arctic terrestrial NEP and assess how well these findings "on the ground" associated with similar biome-level measurements by satellites. Specifically, the first objective was to quantify growing season NEP, R_{ECO} and GEP on contrasting dry high Arctic semidesert and meadow wetland landscapes using multi-season EC measurements at the highest-latitude location measured to date (81.8°N, 71.4°W). The second objective was to examine how moisture, heating and other environmental conditions affect NEP, both between and within sites. The final objective was to compare ground and remotely-sensed ecosystem productivity measurements with the goal of evaluating upscaling methods for high Arctic sites. We predicted that during the June to August, high Arctic growing and senescence season (herein "growing season"), a sparse, inland dry semidesert landscape would be a net emitter of CO_2 to the atmosphere depending on moisture conditions, while net CO_2 uptake would occur at a meadow wetland and productivity would benefit more from heating and advantageous high Arctic growing conditions. We also expected that the clear optical conditions of a specific high Arctic watershed would enable a comparison of ground-level productivity to satellite greenness measurements as a means of upscaling.

Methods

Site description

Lake Hazen camp is located in central Quttinirpaaq National Park (QNP), Canada's most northerly and remote protected area, on northern Ellesmere Island, Nunavut (Figure A1.1). The lower reach of the lake's watershed is considered a high Arctic thermal oasis (France, 1993) because it is protected from colder coastal weather by the adjacent Grant Land Mountains and the Hazen Plateau. We studied two distinct and hydrologically dissimilar high Arctic landscape types in the watershed, the common unproductive semidesert comprised of dry upland mineral soils, and the less common moist productive meadow wetlands that occur on the landscape where water flows and pools (Figure A1.1). Semidesert ground cover is classified as graminoid,

12

prostrate dwarf-shrub forb tundra (Walker *et al.*, 2005) consisting of cryptogamic crust (56.1%), lichen spp. (11.8%), *Dryas integrifolia* Vahl (4.8%), moss spp. (1.9%), *Carex nardina* Fr.+*Kobresia myosuroides* Willd. (1.3%), *Salix arctica* Pall. (0.6%), litter (3.5%) and bare ground (20.5%, Tarnocai *et al.*, 2001). Wetland ground cover is classified as sedge/grass, moss meadow wetland (Walker *et al.*, 2005) consisting of *Carex* spp., *Eriophorum* spp., bryophytes and graminoids (Edlund, 1994). Canopy height is ~2 cm at the semidesert and ~5-10 cm at the wetland. Dry soil ecosystems, like the semidesert described here, comprise over 99% of the ice-free land area in QNP, while only ~1% is poorly-drained wet soils (Edlund, 1994).

A typical growing season at the Lake Hazen watershed began with the onset of snowmelt in late May following over eight months of <0ºC temperatures. Peak snowmelt occurred when mean daily air temperature approached 5 ºC and concluded a few days later. Afterwards, the nearly barren semidesert soils were spongy and wet (33% v v^{-1} at 5 cm below the surface) before drying later in June to a stable summer moisture of 13-16% v v^{-1}. Semidesert soil temperature (at 5 cm depth) warmed to summer daily means of 7-12 ºC (max. 18 ºC). Wetland soils typically remained near saturation (70-90% v v^{-1}) except when streamflow was restricted through the wetland. Wetland daily mean soil temperature (Jun.-Aug.) was cooler than the semidesert (~5-10 ºC). Watershed conditions changed rapidly into September as mean daily air temperature decreased below freezing and soils froze by mid-September. Mean daily photosynthetically-active radiation (PAR) ranged from 577 μmol m^{-2} s^{-1} on June 21st (summer solstice) to only 25 μmol m^{-2} s^{-1} on September 22nd (autumn equinox).

Growing season NEP

NEP - Identical EC flux towers were deployed to measure NEP at the two adjacent landscapes (Figure A1.1; Table A1.1). The semidesert tower (~188 masl; 1 km SW of camp) was positioned within a broad area of a semidesert landscape and operated from 2008 to 2012. The wetland tower (~231masl; 1 km N of camp) was positioned on the western edge (leeward of prevailing wind direction) of a 2.9 ha portion of the Skeleton Creek meadow wetland complex and operated from 2010 to 2012. Each tower was equipped with Campbell Scientific Inc. (CSI; Logan, US) CSAT3 three-dimensional sonic anemometers and LI-COR (Lincoln, US) LI-7500 (open-path; all years) and LI-7200 (enclosed-path; 2011-12 only) CO_2\water vapor infrared gas

analyzers (Table A1.1, A1.2). The LI-7500 itself, and the LI-7200 intake, were positioned 12 cm from either side of the center of the CSAT3 sensors, and all EC sensors were positioned approximately 2 m above the canopy at each site. Sensors to quantify water and energy budgets, and weather and soil conditions were also fixed to each tower (Table A1.2). Signals from EC (10 Hz) and other meteorological sensors (half - hour means) were collected on CSI CR3000-XT dataloggers. EC towers were usually deployed in May each year when the landscape was still snow covered. For logistical reasons, measurements typically ceased in early to mid-August, except in 2012 when towers were left operating until solar-charged batteries powering the sensors expired in diminishing daylight in early October.

EddyPro (LI-COR, v. 5.0) was used to calculate half-hour CO_2, water vapor, momentum, sensible heat (H) and latent heat fluxes from 10 Hz signals and was used to QA/QC data, remove outliers and apply standard flux corrections (see Appendix 1). All corrections resulted in removal of 41% (LI-7500) and 24% (LI-7200) of all flux measurements at the semidesert and 49% (LI-7500) and 33% (LI-7200) of all flux measurements at the wetland. Each half-hour, NEP was calculated as the sum of the CO_2 flux and the rate of change in CO_2 storage below the height of the EC measurements using the CO_2 concentration measured at ~2 m. CO_2 storage was typically much less than 1% of the measured CO_2 fluxes at our sites. Total evaporation (ET, mm) for each half hour, a measure of transpiration and evaporation from moist soil and plant surfaces, was converted from the latent heat flux and the latent heat of vaporization. We used linear interpolation to fill half-hour and one-hour gaps in the NEP record at both sites. To fill larger gaps (NEP_F), we used a light response and respiration model (Reichstein *et al.*, 2012):

$$NEP_F(\mu mol\ CO_2\ s^{-1}m^{-2}) \ = \frac{\alpha * \beta * PAR}{\alpha * PAR + \beta} - \ R_{ECO} \qquad [1]$$

where fitted parameters are α (initial slope of the light-response curve) and β (maximum GEP), R_{ECO} represents ecosystem respiration (see Equation [2]) and the measured variable is PAR ($\mu mol\ s^{-1}\ m^{-2}$; Table A1.3). Gaps in the measurement records of H and ET at both towers were filled using linear relationships with net radiation (R_N) measurements.

Heating of the air inside the measurement path by internal electronics of the early generation LI-7500s can falsely measure CO_2 uptake, particularly in cold conditions. To correct

for this, we applied a common heating correction (Burba *et al.*, 2008) to all LI-7500 data at each site using site-specific parameterizations developed using the 2011 and 2012 data when the LI-7200 was running concurrently (Table A1.4). All subsequent analyses presented use corrected LI-7500 results or when available, LI-7200 results (unaffected by heating issues; e.g., 2011, 2012). When analyzing our NEP data for diurnal effects, relationships with environmental variables, or total seasonal NEP, we used 2010-12 data when both towers were operational (Figure A1.2).

Daily mean NEP (as $g C m^{-2} d^{-1}$) and random uncertainty (as calculated by EddyPro using the method of Finkelstein and Sims [2001]) were calculated by summing 48, gap-filled, half-hour periods each day and converting to mass units using $12 g$ carbon mol^{-1} of CO_2. Because it was not logistically possible to collect full growing seasons of NEP data during any given year, we calculated mean NEP for each day from 2010-12 to construct an NEP time series of a "typical" growing season (1-June to 31-August). Typical daily NEP was summed to estimate growing season carbon accumulation and uncertainty was estimated by propagating daily random uncertainties. To estimate frozen period carbon accumulation (1-Sep to 31-May), we multiplied the daily negative NEP value closest to zero when the ground was snow-covered and frozen by the number of days in that "typical" non-growing season period (273).

R_{ECO} - Normally EC data can be used to quantify R_{ECO} during suitable night-time conditions. However these measurements were not possible at our location during the 24-hour daylight growing season. Therefore, R_{ECO} was independently measured using partially-buried collars and a LI-COR portable photosynthesis sensor (model LI-6400) configured as a dark soil flux chamber. At the start of each season, and at the same locations each year, we set four to nine 10.5 cm-diameter white PVC collars 5 cm into the soil, where they remained for the remainder of the field season (Figure A1.3). Semidesert collars were placed within 50 m of the EC tower and enclosed either bare (n=2-7 collars) or vegetated soils consisting of *Salix*, *Dryas* or *Ericaceae* (n=2-3 collars). At the wetland, collars were placed along its margin within 50 m of the EC tower (n=4 collars) because a boardwalk was not permitted in QNP to access the centre of the wetland. However, collars enclosed soil and vegetation similar to the rest of the wetland. The dark soil chamber was deployed onto collars at each landscape every 2-4 days between June and

August each year when we were on-site (Table A1.1). Most measurements were taken between 10:00 and 18:00, though some were performed later to investigate diurnal changes. Diurnal trends in R_{ECO} were weak at both sites, so all measurements taken each day were assumed to be representative of the mean daily dark soil respiration rate. Mean daily R_{ECO} (μmol CO_2 m^{-2} s^{-1}) at the semidesert during each sampling period was calculated by weighting fluxes obtained from bare and vegetated collars by the approximate percent ground cover represented by these collar locations (bare soil+cryptogamic crust = 76.6%; vegetated = 23.4%; Tarnocai *et al.*, 2001). Mean daily R_{ECO} at the wetland was calculated as the arithmetic mean of all collar measurements because vegetation cover was similar within each collar and throughout the wetland. To compare with more complete daily records of NEP, gaps of R_{ECO} between measurement days were filled using a Q_{10}- temperature response model (Lloyd and Taylor, 1994) using air temperature (T) with a modifier related to ET measured at each site using the EC systems as a proxy for near surface water (and energy) availability (Figure A1.4):

$$R_{ECO} = (a + b\mathrm{ET} + c/10) * R_{10}Q_{10}^{(T-10)/10}$$ [2]

where R_{10} is base ecosystem respiration at 10ºC, Q_{10} is the temperature sensitivity parameter for a 10ºC increase in temperature, and *a*, *b*, and *c* are fitted parameters (Table A1.5). Other studies typically model chamber respiration using soil temperature and moisture measurements (e.g., Gaumont-Guay *et al.* 2006) but our soil moisture and temperature measurement at 5 cm depth where sensors were positioned appeared to have weak relationship to chamber measurements (i.e., a disconnect between conditions at the surface where plants and cryptogams resided, with those at depth).

GEP - Daily GEP was determined by summing daily NEP and R_{ECO} on days when chamber measurements were performed. Full-season GEP was estimated using the same approach but included gap-filled R_{ECO} fluxes.

NEP in response to changing environmental conditions

We used classification and regression tree (CART) analysis (Systat v13; Systat Software, Inc.) to identify the daily environmental variables that were most closely associated with daily NEP from each EC tower. CART uses repeated partitioning of multivariate data sets to determine the strongest associations between a dependent variable (e.g., NEP) and multiple

independent variables (e.g., environmental conditions). CART is robust to data with interactions, thus it is an approach suitable for multivariate time-series data sets. For a partition of the data to occur, a minimum of five daily values were required with a minimum model improvement of 0.05. Daily gap-filled data from each site were used during unfrozen conditions (June-August) between 2010 and 2012. NEP was considered the dependent variable while surface ET and H fluxes, soil volumetric water content, temperature and heat fluxes at 5 cm depth, air pressure and T, wind speed, R_N and PAR were the independent variables. Variables explaining the largest portion of variability within the models were considered key factors affecting the daily variations in NEP of each site.

Site and regional relationships of NEP

Vegetation indices can be used as proxies for green biomass, leaf area index, and autotrophic ecosystem production (GEP, NEP) from small (e.g., plots) to large (e.g., satellites) scales, and have been widely used in the Arctic (Stow *et al.*, 2004; Street *et al.*, 2007; Huemmrich *et al.*, 2010). We used variants of the Normalized Difference Vegetation Index (NDVI) to compare seasonal trends and absolute values of ecosystem productivity at ground and satellite scales at both sites via:

$$\text{NDVI} = \frac{\rho_{\text{NIR}} - \rho_{\text{VIS}}}{\rho_{\text{NIR}} + \rho_{\text{VIS}}}$$ [3]

where ρ_{NIR} and ρ_{VIS} are reflectances (outgoing/incoming radiation) of near-infrared and red wavelengths, respectively. A common variation is to substitute a broadband visible (i.e., PAR) sensor for the red band (400-700 nm), providing a robust, proxy NDVI (Huemmrich *et al.*, 1999, Gamon *et al.*, 2010). At the semidesert tower only, we used reflectance from paired PAR and pyrometer optical sensors (PAR Smart Sensor S-LIA-M003, 400-700 nm; Silicon pyranometer S-LIB-M003, 300-1100 nm; Onset; Cape Cod, U.S.A.) to establish a growing season trend of proxy NDVI in 2012. The optical sensors were attached to the tower by an extension at 3 m height to provide an unobstructed view of the semidesert landscape ("tower area NDVI"). Raw data were collected every five minutes between June and August.

To evaluate spatial NDVI around EC towers ("landscape NDVI"), we took hyperspectral reflectance scans (~300-1100 nm) of each landscape twice during the 2012 growing season (once

at peak NEP; once at senescence) using a portable spectrometer (UniSpec DC, PP Systems; Amesbury, USA). Several transects were walked in a grid pattern around each EC flux tower and measurements were taken every 8-10 m. Tower area NDVI was also measured during August using the spectrometer. Calibration white and dark scans were performed periodically during all measurements and spectral data were analyzed using MultiSpec (v. 5.0). Landscape NDVI was calculated using reflectances at 800 nm (ρ_{NIR}) and 680 nm (ρ_{VIS}).

To provide an independent, satellite-based ecosystem productivity measurement, NDVI from the Moderate Resolution Imaging Spectroradiometer (MODIS) on the National Aeronautics and Space Administration (NASA) Terra and Aqua orbiting satellites were acquired from NASA's online Reverb tool for the periods when EC towers were operational. Composite 16-day measurements of NDVI (ρ_{NIR}: 841-876 nm; ρ_{VIS} 620-670 nm) from up to two, 6.3 ha pixels surrounding each EC tower ("Satellite NDVI") were used and compared to ground-level measurements.. The wetland, however, was smaller in area (2.9 ha) compared to a MODIS pixel (6.3 ha). No data points were removed by filtering procedures; however quality flags were noted.

Results

Growing season NEP

NEP - At both our landscapes across all years, we observed consistent growing season trends of NEP but with evident differences in the magnitude of the fluxes (Figure 2.1; Table 2.1). Site moisture status was a clear determinant of NEP. At the semidesert, NEP was near zero throughout the measurement period, with neither CO_2 loss nor uptake exceeding 0.6 g C m^{-2} d^{-1} in 90% of all daily measurements (Figure 2.2). In contrast, the wetland site had both larger uptake and losses varying from ~ -2.5 to +4.5 g C m^{-2} d^{-1}. During frozen conditions in late May and after August, NEP fluxes at both sites were on average just below zero with slightly greater CO_2 loss during spring compared to autumn. Through snowmelt in June, NEP was mostly negative at both sites with a greater range in values relative to other periods as the ecosystems transitioned from having a net loss to a net uptake of CO_2. Maximum NEP in summer among growing seasons at both sites was considerably different in magnitude and timing (0.28-0.44 g C m^{-2} d^{-1}; 22 June to 29 July at the semidesert; 3.66-4.54 g C m^{-2} d^{-1} between 6-12 July at the
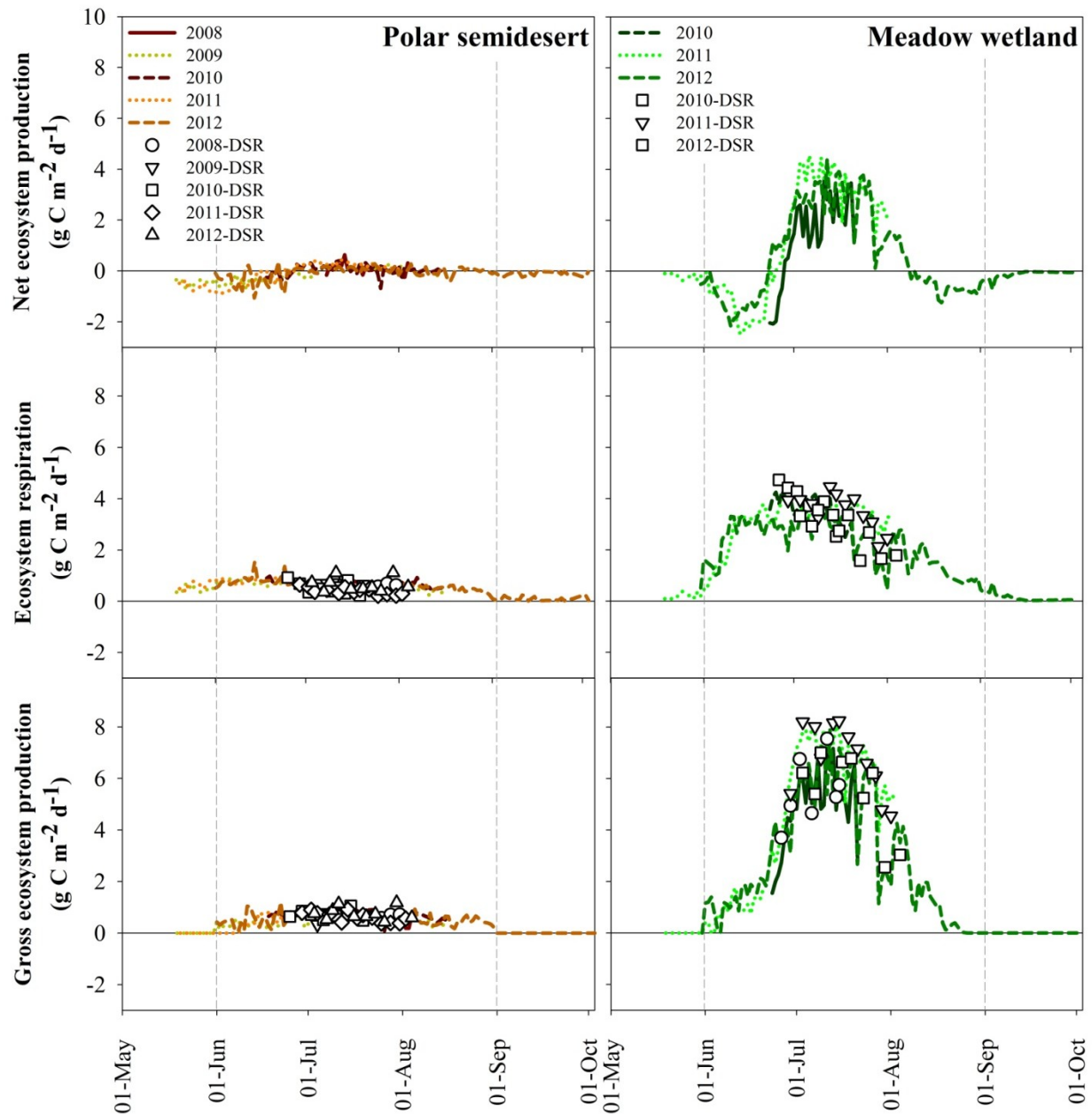
Figure 2.1 Measured mean daily net ecosystem production (NEP; top panels), and modelled net ecosystem respiration (middle panels) and gross ecosystem production (GEP; lower panels) at the polar semidesert (left panels) and wetland (right panels) sites. Points overlain on the net ecosystem respiration plot represent direct measurements of mean daily dark soil respiration (DSR) while points on the GEP plot are modelled based on differences of NEP and DSR measurements. Dashed vertical lines indicated transition between frozen and growing season conditions (June - September). Note: Showing corrected LI-7500 NEP fluxes for 2008-10 and September-October 2012, otherwise showing LI-7200 NEP fluxes.

19

Table 2.1 Mean (±1SE) of net ecosystem production (NEP) fluxes (where positive values indicate net CO_2 uptake by the ecosystem) and daily environmental measurements during snow-covered, frozen conditions (F) and during the growing season when eddy covariance flux towers were operational at the polar semidesert (2008-12) and meadow wetland (2010-12) sites.

	Period (no. days)	NEP (g C m^{-2} d^{-1})	H (W m^{-2})	ET (mm hr^{-1})	W_S (m s^{-1})	Air$_P$ (kPa)	Air$_T$ (°C)	Rn (W m^{-2})	PAR (μmol m^{-2} s^{-1})	SHF[#] (W m^{-2})	VWC[#] (% v v^{-1})	Soil$_T$[#] (°C)
P. semidesert	F (58)	-0.29±0.03	3±1	0.01±0.00	1.8±0.1	98.7±0.1	-4±0	12±4	329±39	-1±1	6±0	-5±1
	Jun. (103)	-0.28±0.03	42±2	0.06±0.00	2.9±0.2	99.4±0.1	5±0	112±3	697±15	35±2	16±1	7±1
	Jul. (148)	0.12±0.01	50±1	0.02±0.00	2.9±0.1	98.8±0.1	8±0	82±2	597±12	25±1	15±0	12±0
	Aug. (68)	-0.01±0.02	21±1	0.02±0.00	2.7±0.2	98.7±0.1	6±0	37±2	387±15	14±1	13±0	7±0
M. wetland	F (46)	-0.16±0.02	-1±1	0.01±0.00	1.2±0.1	98.3±0.2	-5±0	-3±2	244±38	-1±0	25±3	-5±1
	Jun. (68)	-0.66±0.14	42±2	0.05±0.00	2.2±0.2	98.8±0.1	7±1	106±5	672±15	9±1	56±4	5±1
	Jul. (83)	2.84±0.11	41±2	0.06±0.00	2.1±0.2	98.1±0.1	10±0	93±3	593±16	7±0	75±2	10±0
	Aug. (33)	-0.04±0.17	15±2	0.02±0.00	2.0±0.3	98.2±0.1	5±1	37±4	329±20	3±0	69±1	5±1

Notes: [#] measured at 5 cm depth; H: sensible heat flux; ET: total evaporation; W_S: wind speed; AIR$_P$: air pressure; Air$_T$: air temperature; Rn: net radiation; PAR: photosynthetically active radiation; SHF: soil heat flux; VWC: volumetric water content; Soil$_T$: soil temperature.
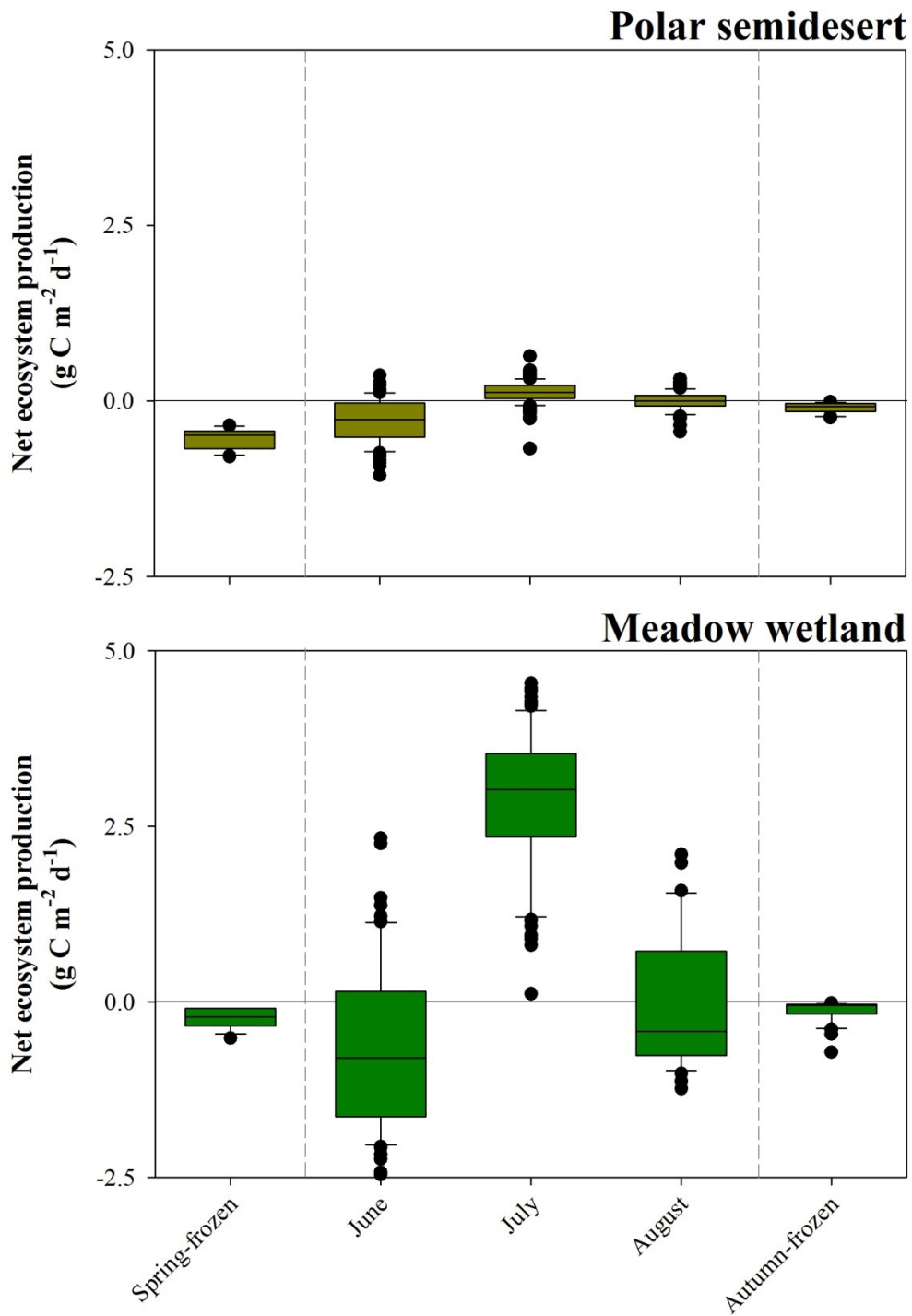
Figure 2.2 Monthly summaries of net ecosystem production fluxes from the polar semidesert (2008-12) and meadow wetland (2010-12) during frozen and growing periods. Mid-bar=median; box borders: 25th, 75th percentiles; whiskers: 10th, 90th percentiles; filled circles: outliers.

wetland). As semidesert soils dried after snowmelt, all years converged around an NEP of ~0.1 g C m^{-2} d^{-1} in later July before decreasing toward zero in September. At the wetland, NEP clearly transitioned from net CO_2 uptake to net emission through August as senescence progressed. Mean diurnal NEP patterns for both sites for the 2010-12 unfrozen periods showed the sharp contrast between landscape types (Figure 2.3). Considering uncertainty about mean NEP at the semidesert (see below), the diurnal pattern of NEP was likely not different than zero. Positive NEP was most apparent between 6:30 and 8:30 while negative NEP was strongest between 9:30 and 15:30, despite average PAR that remained above 300 µmol m^{-2} s^{-1} at all times (Figure 2.3). At the wetland, a more typical diurnal pattern existed with a defined peak in NEP between 10:00 and 11:30 and lower NEP toward the margins of the day. Only at the wetland did mean PAR fall below 300 µmol m^{-2} s^{-1} (due to a mountain shadow at 21:00), resulting in decreased NEP fluxes.

Integrated daily CO_2 accumulation during a "typical" growing season (2010-12) was -0.05 g C m^{-2} d^{-1} at the semidesert and 0.63 g C m^{-2} d^{-1} at the wetland, resulting in over 16 times more wetland carbon accumulation during the growing season (58.1±20.5 g C m^{-2}, ±random error vs. -4.1±11.8 g C m^{-2}). However, when including estimates of NEP during frozen conditions (Sep. to Jun.; 273 days), there was an estimated net loss of CO_2 at the semidesert (-8.7 g C m^{-2}) compared to an overall CO_2 accumulation at the wetland (52.4 g C m^{-2}), however these estimates were based on shoulder season respiration rates, rather than true winter measurements.

R_{ECO} - Semidesert soil R_{ECO} rates (Jun.-Aug. mean±SE) were significantly lower (0.52±0.08 µmol CO_2 m^{-2} s^{-1}) than wetland soil rates (3.17±0.12 µmol CO_2 m^{-2} s^{-1}; 2-sample t-test; $t_{(16)}$= -10.0, $p<0.001$; Figure A1.5a.,d.). R_{ECO} was generally low and stable throughout each growing season except just after snowmelt and rain events (Figure A1.6). R_{ECO} was strongly affected by vegetation cover. Collars enclosing *Dryas*, *Salix* and *Ericaceae* had significantly higher CO_2 emission rates (1.21±0.23 µmol CO_2 m^{-2} s^{-1}) compared to collars enclosing cryptogamic bare soil or sparse graminoids (0.30±0.04 µmol CO_2 m^{-2} s^{-1}; 2-sample t-test; $t_{(12)}$=-5.8, $p<0.001$; Figure A1.3, A1.5b). This suggested that ~0.90 µmol CO_2 m^{-2} s^{-1} was attributed to plant-related respiration, and when weighted by actual landscape cover, comprised about 40% of all R_{ECO} at the semidesert. Wetland R_{ECO} declined from late June to early August each year, in concert with declining plant productivity (Figure 2.1, A1.6). Soil respiration rates were similar
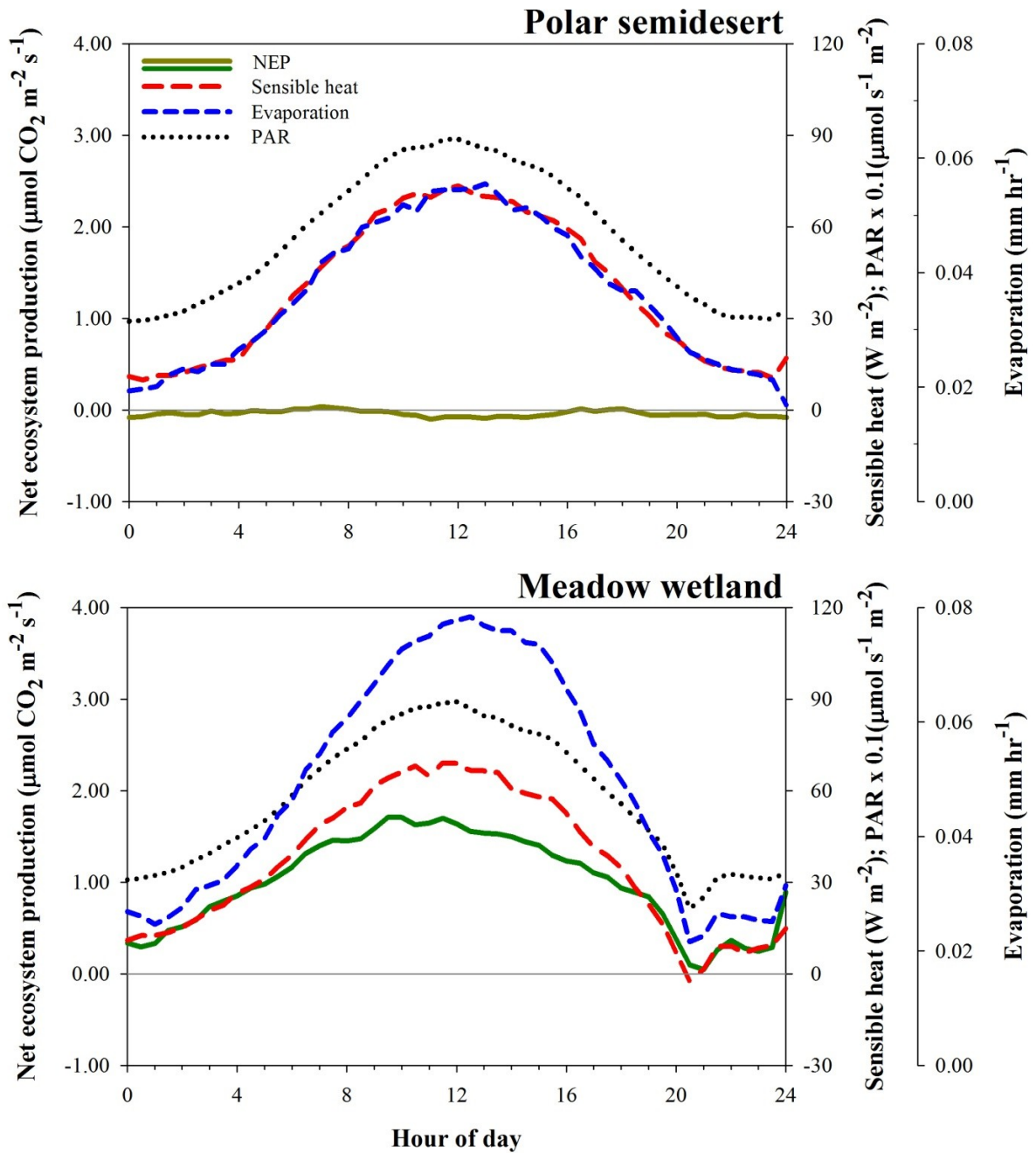
Figure 2.3 Gap-filled, half-hour diurnal net ecosystem production flux, sensible heat flux, total evaporation and photosynthetically active radiation during the growing season (June to September) at the polar semidesert and wetland sites from 2010-12.

from different collars because they enclosed comparable vegetation types and cover (Figure A1.3, A1.5c.). Modeled full growing season mean R_{ECO} fluxes at each site were similar to mid-summer mean chamber measurements (Figure 2.1). Low fluxes at the semidesert may have been partly the cause of poorer model (Eq. [2]) fit (RMSE=0.08; r^2=0.25) relative to the larger fluxes at the wetland and the better model fit at that site (RMSE=0.36; r^2=0.67).

GEP - Using daily NEP and R_{ECO} on days when chamber measurements were performed, we estimated mean daily GEP (Figure 2.1) of 0.69 g C m^{-2} d^{-1} (maximum 1.18 g C m^{-2} d^{-1}) at the semidesert and 6.05 g C m^{-2} d^{-1} (maximum 8.24 g C m^{-2} d^{-1}) at the wetland. Peak season biomass clipping of vegetation in plots across transects at each site in mid-July 2011 found a similar ratio between sites for green leaf biomass (Figure A1.7).

NEP in response to changing environmental conditions

During the growing season (2010-12), the coldest 5% of semidesert soils (<2.1ºC) net released CO_2 to the atmosphere (-0.4 g C m^{-2} d^{-1}; Figure 2.4). When soils were warmer than 2.1ºC, changes in surface soil moisture (via the ET proxy), as well as temperature, coincided closely with changes in NEP. For example, when soils were relatively wet (ET>0.06 mm hr^{-1}) or were dry and cool (<10.8ºC), net heterotrophy occurred, but when soils were dry and warm (>10.8ºC), net autotrophy occurred on the landscape. When ignoring the first temperature split at 2.3ºC, which isolated only 5% of the data, ET accounted for 42% of the total model fit with NEP, compared to only 13% by the second soil temperature split. At the wetland, NEP was grouped primarily using soil temperature with net heterotrophy occurring when soils were cooler than 6.8ºC (Figure 2.4). When soils were warmer than 6.8ºC, lower R_N coincided with stronger NEP. Overall, soil temperature (62%) and R_N (27%) comprised most of the model variability.

Site and regional relationships of NEP

Semidesert tower area NDVI (via tower optical sensors) transitioned sharply from snow-covered conditions (mean 0.047±0.003) to growing season conditions (mean 0.158±0.000). NDVI was highest just after snowmelt and again at the end of July during wet conditions. NDVI dipped slightly towards midseason, marked by drier soils. Satellite NDVI (via MODIS) in 2009, and in 2011-12, also detected strong transitions in semidesert NDVI between pre- and post-
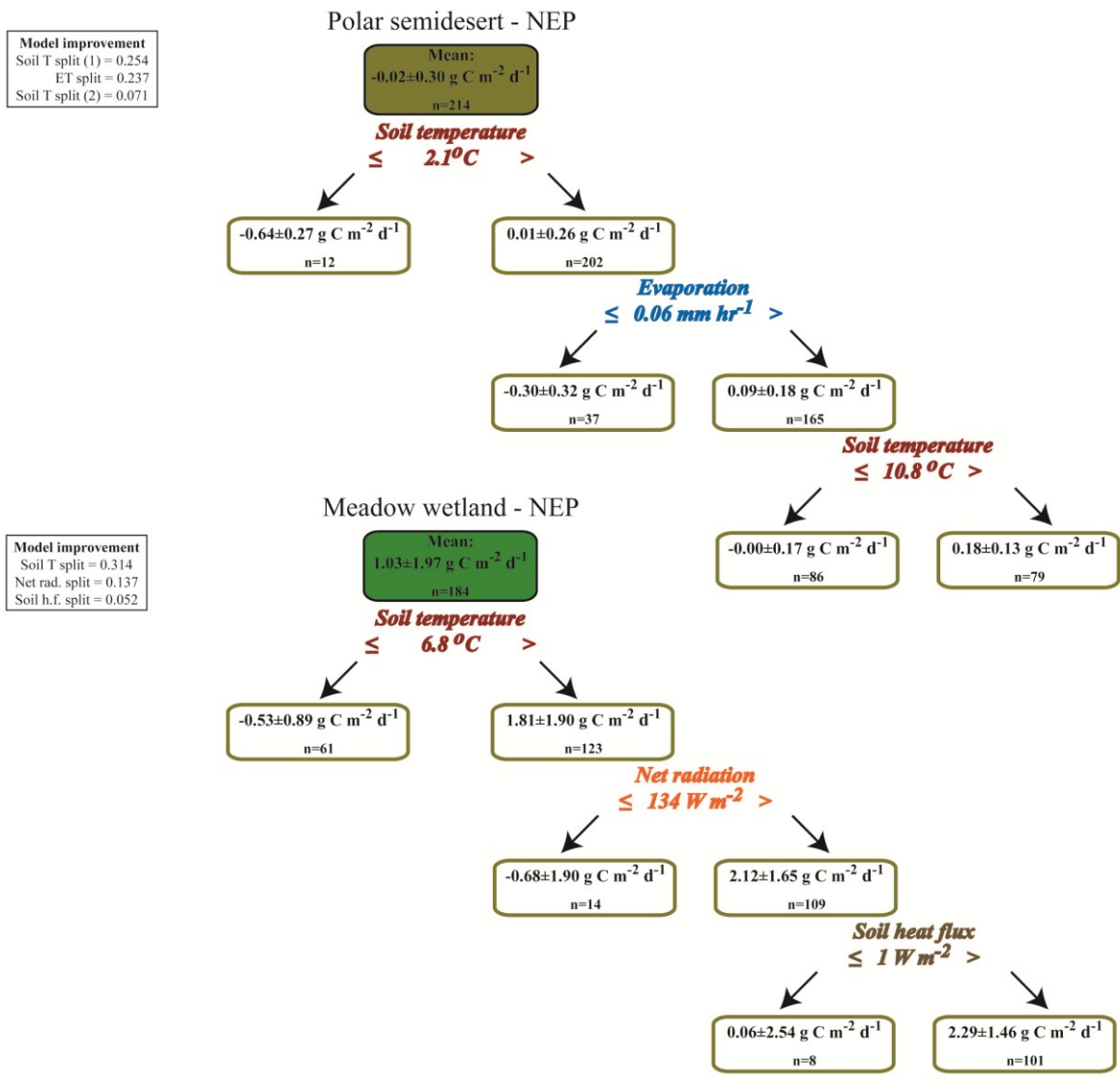
Figure 2.4 Regression tree of daily net ecosystem production fluxes for the growing season at the polar semidesert and meadow wetland between 2010 and 2012. Note: inset shows model improvement statistics.

snow-cover, but with only minor fluctuations through the growing season (Figure 2.5a.). Satellite NDVI at the wetland also clearly detected the rapid change from snow-covered to growing season conditions in 2011 and 2012. However, unlike the semidesert site where NDVI dipped towards mid-summer , a distinct mid-summer peak of NDVI occurred each year at the wetland site (mean 0.43).
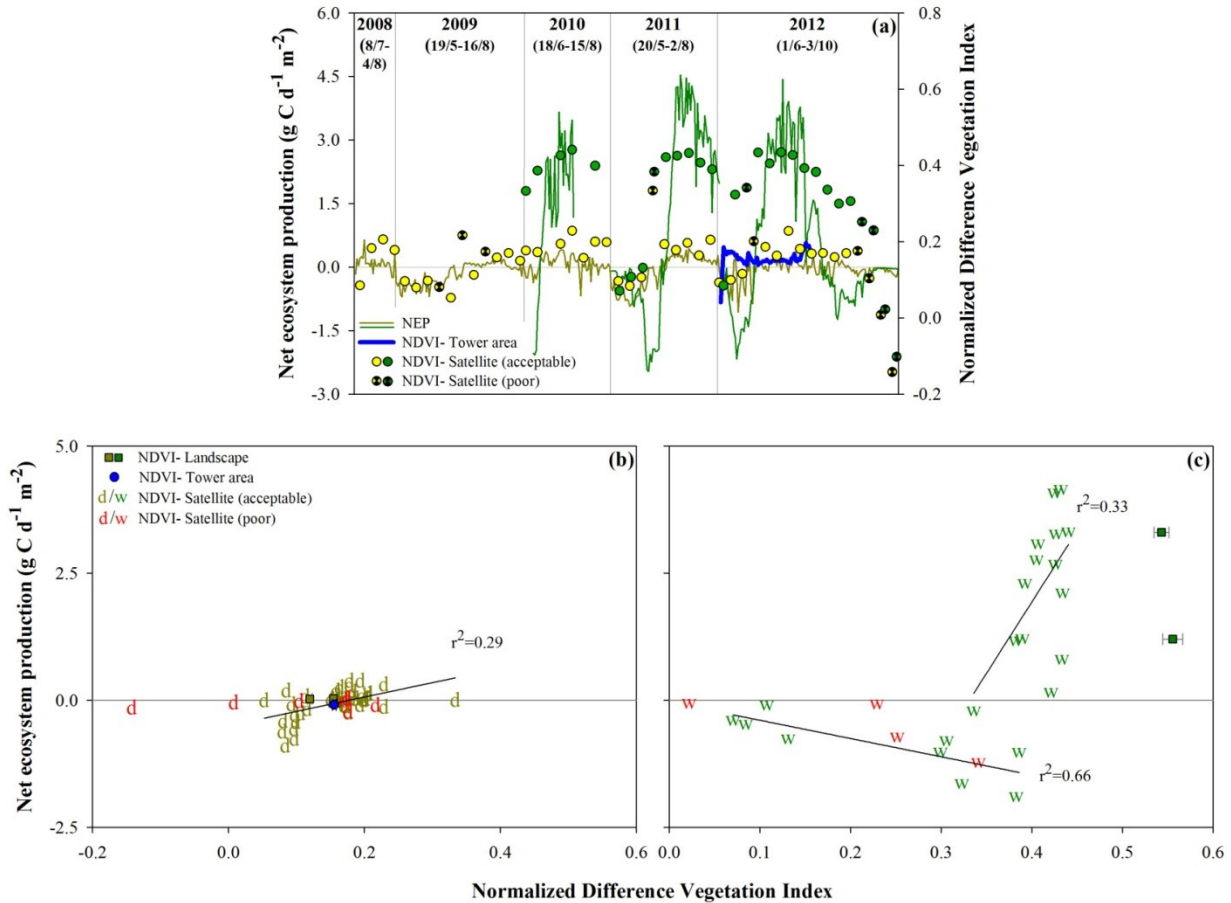
Figure 2.5 Seasonal (a.) and regressed (b.-c.) comparison of multiple ground-level measurements of mean daily net ecosystem productivity (2008-12), ground-measured Normalized Difference Vegetation Index (NDVI) and composite 16-day measurements (shown at day of collection) of NDVI by satellite-based MODIS Aqua and Terra sensors at the polar semidesert (yellow) and meadow wetland (green) sites.

In the semidesert area, mean tower NDVI matched well with mean satellite NDVI during the growing season (Table 2.2a.), and NDVI measurements of the tower area using optical sensors and the spectrometer were within 5% (Table 2.2b.). Semidesert landscape NDVI (via spectrometer) measured twice during the growing season was within 2-12% of tower area measurements (Table 2.2c.) Satellite NDVI recorded 1-3 days later was slightly higher, but matched reasonably well with ground-level measurements (<8-26% difference). Wetland landscape NDVI, however, was ~21-31% higher than satellite NDVI in 2012, due to the mismatch of the wetland area with the larger satellite pixel area (Table 2.2c., d.).

26

Table 2.2 Comparison of similar Normalized Difference Vegetation Index (NDVI) measurements using ground (optical tower, spectrometer) and satellite measurements (MODIS) during the 2012 growing season at the polar semidesert and meadow wetland.

		Scale	Measurement	NDVI
Polar semidesert	**a.**	**Seasonal comparison (June-August)**		
		Tower area	Proxy NDVI sensors[α]	0.157±0.000
		Satellite	MODIS[β]	0.161±0.012
	b.	**Tower area comparison (03 August)**		
		Tower area	Proxy NDVI sensors	0.157±0.000
		Tower area	Spectrometer	0.155±0.016
	c.	**Spatial comparison (08-11 July)**		
		08-11 July		
		Tower area	Proxy NDVI sensors	0.136±0.000
		Landscape	Spectrometer[θ]	0.120±0.004
		Satellite	MODIS	0.163±0.004
		03-04 August		
		Tower area	Proxy NDVI sensors	0.158±0.001
		Landscape	Spectrometer	0.155±0.005
		Satellite	MODIS	0.168±0.005
Meadow wetland	**d.**	**Spatial comparison (19-20 July)**		
		19-20 July		
		Landscape	Spectrometer	0.543±0.008
		Satellite	MODIS	0.427±0.008
		03-04 August		
		Landscape	Spectrometer	0.555±0.011
		Satellite	MODIS	0.382±0.011

Notes:
[α]300-1100 nm (pyranometer: ρ_{NIR}) and 400-700 nm (PAR sensor: ρ_{VIS})
[β]800 nm (ρ_{NIR}) and 680 nm (ρ_{VIS})
[θ]841-876 nm (ρ_{NIR}) and 620-670 nm (ρ_{VIS})

Despite decent correspondence between NDVI measurements of the semidesert, correlations of NEP fluxes measured by the EC tower with satellite NDVI (r^2=0.29) fit only moderately well and were driven mostly by the transition between pre- and post-leaf conditions. NEP correlated poorly with tower area NDVI through the season (r^2=<0.01; Figure 2.5b.). At the wetland, correlations between satellite NDVI and NEP showed a two-phase structure. During periods of net heterotrophy, NEP correlated negatively with satellite NDVI (r^2=0.66). However, when stronger plant growth occurred, NEP correlated positively (r^2=0.33) with satellite NDVI (Figure 2.5c.).

Discussion

Growing season NEP

Polar semideserts are among the least productive landscapes globally, where vegetation and decomposition are limited by low summer air temperatures, water limitation, heterogeneous soil OC distribution, and poor nutrient availability (Tarnocai *et al.*, 2001). In contrast, high Arctic wetlands typically exchange much more CO_2 than semideserts because of stronger plant growth and decomposition resulting from a wetter environment (Christensen *et al.*, 2000; Laurila *et al.*, 2001; Kutzbach *et al.*, 2007; Groendahl *et al.*, 2007; Lund *et al.*, 2010). This resulted in NEP fluxes consistently near zero at the QNP semidesert with only weak seasonality at snowmelt and mid-summer, and a near-flat diurnal trend typical of barren ground. Diurnal and seasonal NEP patterns at the QNP wetland were typical of vegetated landscapes, with highest NEP fluxes when PAR and air temperatures were optimal. The more productive wetland also showed strong pre-leaf spring net emission of CO_2 to the atmosphere due to microbial processing of fresh OC deposited the previous autumn (Elberling and Brandt, 2003), and a rapid plant growth signal.

These obviously contrasting conditions resulted in a weak, near-zero, semidesert growing season release of -4.1±11.8 g C m^{-2} to the atmosphere, which was less than a more lush heath in Greenland (+7 g C m^{-2} July-August; Soegaard *et al.*, 2000), comparable to a sparsely vegetated landscape at Svalbard (-4 to 5 g C m^{-2} June-August; Lloyd, 2001; Lüers *et al.*, 2014), but much smaller than low Arctic tundra (-117 to 203 g C m^{-2}; Heikkinen *et al.*, 2002; Kutzbach *et al.*, 2007; Humphreys and Lafleur, 2011; Marushchak *et al.*, 2013). Conditions at the wetland, driven by greater water availability, resulted in growing season NEP fluxes over 16 times higher than at the semidesert (58.1±20.5 g C m^{-2}). Surprisingly, growing season mean, peak and total NEP were comparable to wetlands across the Arctic, including those further south (mean 96±60 g C m^{-2}; Corradi *et al.*, 2005; Kutzbach *et al.*, 2007; Humphreys and Lafleur, 2011). These perhaps unexpected similarities may be due to conditions unique to the high Arctic. At QNP, cool temperatures and shallow thaw depths (< 30 cm) likely suppress decomposition while 24-hour daylight and PAR consistently above 300 μmol s^{-1} m^{-2} allows for 24-hour CO_2 uptake in June and July, whereas locations south of 80ºN have fewer hours for photosynthesis to occur. For example, a sedge fen at a Canadian low Arctic site had a maximum mean daytime uptake of ~3.5

μmol CO_2 m^{-2} s^{-1} in July that was offset by losses during six overnight hours (Lafleur *et al.*, 2012). At the QNP wetland, maximum mean full-day uptake was 4.4 μmol CO_2 m^{-2} s^{-1} and supported by possibly the clearest skies and warmest monthly mean temperatures in the high Arctic (Thompson, 1994).

Though prolonged dark and frozen conditions occur at Lake Hazen, soil respiration has been found to continue in similar harsh conditions elsewhere (Elberling and Brandt, 2003) and can reduce growing season NEP by 14-22% (Welker *et al.*, 2004; Eberling, 2007). In our study, we could obtain only shoulder season NEP measurements of weak CO_2 emission, which were likely stronger than rates during winter when air temperatures can fall below -40ºC. Therefore, our winter total carbon estimates were likely overestimated losses (4 to 6 g C m^{-2} d^{-1}) at both sites. Though error about this estimate is likely high, it is reasonable to suggest that the semidesert was still a near-zero, annual weak CO_2 source, and the wetland a reliable CO_2 sink, relative to the atmosphere.

NEP in response to changing environmental conditions

Heating and wetting of landscapes are two fundamental processes supporting microbial and plant life in soils, and each affects soil carbon exchange with the atmosphere (Rustad *et al.*, 2001; Davidson *et al.*, 2006; Hill and Henry, 2011). Our CART results found that soil temperature drove the first split in our NEP fluxes at both sites, though the split was more important at the wetland site. At the semidesert, soils colder than 2.3ºC (5% of data) were net emitters of CO_2 to the atmosphere, possibly indicative of a threshold temperature above which cryptogam and vascular plant species can photosynthesize, even under snow-cover (Lloyd, 2001). We also observed strong net heterotrophy when wetland soils were cooler (33% of data), with the higher threshold temperature (6.8ºC) likely due to a 1-2 week delay in plant emergence post-thaw.

As soils warmed above 2.3ºC at the semidesert, net heterotrophy corresponded strongly with increasing surface moisture (ET proxy), something we observed independently in our dark chambers after snowmelt or sporadic rainfalls (Figure A1.4), as have other studies (e.g., Elberling, 2003). When soils were drier and warmer (>10.8ºC) during mid-summer, net autotrophy occurred, however this was more a result of decreasing soil respiration, rather than

29

increased plant growth (Figure 2.1). This suggested that water stress was a minor issue for plants, likely because of adaptations to conserve water (Welker *et al.*, 1993), and that water limitation of heterotrophs was possibly occurring and affecting net carbon exchange at our site. Because R_{ECO} was mostly from ground uncovered by vascular plants, and cryptogam productivity can be sporadic, it is plausible that carbon exchange on this barren landscape is primarily controlled by heterotrophic access to OC and suitable environmental conditions, similar to findings from Svalbard (Lloyd, 2001). Further, this may also indicate that semidesert soils were too dry with poor water retention capacity to support stronger plant growth observed at other wetter high Arctic sites including coastal or lowland valley tundra (Welker *et al.*, 2004; Groendahl *et al.*, 2007; Lund *et al.*, 2012; Lafleur *et al.*, 2012; Lupascu *et al.*, 2014). Alternatively, dry region weathering and dissolution chemistry of carbonate rock (ubiquitous in the Lake Hazen watershed) has been shown to release CO_2 to the atmosphere as soils dry, and therefore integrate into NEP measurements by EC towers (Serrano-Ortiz *et al.*, 2010). This may have particularly contributed to post-snowmelt emission of CO_2 at the semidesert as soils were drying and calcium carbonate was potentially precipitating out of solution, releasing free gaseous CO_2 to the atmosphere. Regardless, carbon exchange of dry inland soils, which are of considerable area but underrepresented in high Arctic studies, appear to be most affected by the state of the soil moisture regime, rather than heating.

When soils warmed above 6.8ºC at the wetland, R_N coincided most strongly, but negatively with NEP because most intense R_N occurred near the summer solstice, which was just at the start of plant emergence. Therefore, heterotrophic processes were benefiting from increased radiative heating. At lower R_N values, increasing soil heat flux corresponded with stronger NEP. Considering temperature and heat fluxes together (73% of model fit), increased soil heating resulted in stronger NEP, something clearly shown in other high Arctic CO_2 exchange (Soegaard and Nordstroem, 1999; Soegaard *et al.*, 2000; Rennermalm *et al.*, 2005) and plant phenology (Wookey *et al.*, 1993; Welker *et al.*, 2004; Elmendorf *et al.*, 2012) studies. Moisture was a secondary factor affecting NEP as we observed lower fluxes at the wetland in 2012 when streamflow ceased for several weeks. However, the shallow permafrost table in the wetland likely meant that water was still available in the rhizosphere of the wetland plants.

Site and regional relationships of NEP

Extrapolating measurements at the ground-level to broader regions is critical for global carbon budgeting. Previous studies have reported climate-related increases in Arctic vegetation growth, biomass and cover using ground and remote-sensing approaches (Stow *et al.*, 2004; Tape *et al.*, 2006; Sitch *et al.*, 2007). However, a more recent study illustrating variation between satellite Arctic NDVI trends calls into question the unambiguous interpretation of the satellite record for this region (Guay *et al.* 2014). Detecting remotely-sensed ecosystem productivity of northern landscapes is particularly troublesome at high Arctic locations because of few ground based calibration studies (e.g., Hudson and Henry, 2009; Tagesson *et al.*, 2013) and generally poor optical conditions for orbiting satellites due to clouds, low sun-angle and patchy landscapes (Boelman *et al.*, 2003).

In some respects, the Lake Hazen watershed provides an excellent high Arctic landscape to evaluate ecosystem productivity by satellite because of relatively clear conditions and modest plant growth compared to other Arctic locations (Gamon *et al.*, 2013). Our satellite and tower area NDVI measurements clearly detected the transition between pre- and post-snow cover in the watershed and were robust tools for delineating growing season length and integrated seasonal NDVI. Mean absolute NDVI measured concurrently at the semidesert tower area, at the landscape scale, and by satellites was also similar, indicating that remotely-sensed NDVI well characterized a snap-shot of mean productivity on the ground. However, the relatively flat NDVI trends at this site (Figure 2.5a) suggested that plant growth and coverage at the semidesert was too faint to delineate seasonal changes in NEP, which were driven more by subtle changes in carbon balance than by substantial plant growth. This was also apparent with the weak correlations between NEP and NDVI, which would be expected with sensors measuring near detection limits. Moisture, more than plant growth or NEP, appeared to influence the proximal NDVI patterns, and this was evident in the increased NDVI at the tower area during wet conditions after snowmelt and later July 2012. It is likely that bryophytes or other cryptogams present at this site responded to moisture by greening, resulting in slightly enhanced tower NDVI during moist periods. Though water on the landscape, as well as plant growth, can influence NDVI, our results suggested wet conditions support stronger net heterotrophy at the semidesert, rather than autotrophy, as found in other studies (Lloyd, 2001). This suggests that direct

measurements of NEP time series at barren, low vegetation cover, high Arctic locations may not be directly comparable to seasonal NDVI time trends due to their different proximal drivers of these two measurements. In particular, because NEP balances both respiration and photosynthesis processes, clear connections between NEP and NDVI were not always evident for this high Arctic site. This was further highlighted by our wetland NDVI results showing an abrupt switch in the NEP-NDVI relationship depending on the timing of plant growth (Figure 2.5c.).

These findings suggest challenges for detecting changing productivity with satellite measurements alone. Overall, our data suggested that incremental, weak greening of the broader, less-productive semidesert may be hard to detect using NDVI, and may only occur when vegetation cover increases substantially. Other factors, including surface moisture, snow, and ice can further confound NDVI signals in the Arctic (Stow *et al.*, 2004; Gamon *et al.*, 2013). Wetlands appear more suitable to remotely-sense productivity, however their extent is often limited by topography to small areas that may be difficult to resolve with larger satellite pixels. Future remote-sensing work in the high Arctic may benefit from more consistent measurements of GEP, which may correspond more suitably with NDVI on semidesert landscapes.

High Arctic landscapes and future change

The QNP semidesert is a cold, dry and sparsely vegetated location, and among the least productive landscapes on Earth. Surface moisture , heterotrophic activity or carbonate weathering at the semidesert currently control NEP, while greater access to water produces remarkable productivity in meadow wetlands and greater influence of heating on NEP changes. Air temperatures are increasing across high Arctic landscapes as evidenced by rising annual air temperatures over the past three decades (Hill and Henry, 2011), but it is unclear how landscape moisture may respond. Other studies from polar semideserts have shown substantial increases in NEP with the application of considerable amounts of water, and moderate NEP increases with temperature (Lupascu *et al.*, 2014), while heating generally favors greater productivity at wetlands (Soegaard and Nordstroem, 1999). At QNP, heating alone will likely take much time to increase productivity as water retention is poor in semidesert soils. Rather, heating and substantial, consistent precipitation may be needed to support greater plant growth, OC

accumulation and nutrient availability to improve water retention and jump start true high Arctic "greening", which may be a very long process (Wookey et al., 1995). However, increased heating should support more robust plant growth at wetlands, though potential for more widespread expansion of wetlands is likely small due to topography limitations of these ecosystems. Therefore, it seems plausible that these landscapes have considerable inertia against changes in NEP, which presents challenges for our ability to detect biome-level changes with current remote sensing technology.

References

AMAP (1998) AMAP Assessment Report: Arctic Pollution Issues. Arctic Monitoring and Assessment Programme (AMAP), Oslo, Norway. xii+859 pp.

Arneth A, Harrison SP, Zaehle S et al. (2010) Terrestrial biogeochemical feedbakcs in the climate system. Nature Geoscience, 3, 525-532.

Baldocchi DD (2003) Assessing the eddy covariance technique for evaluating carbon dioxide exchange rates of ecosystems: past, present and future. Global Change Biology, 9, 479-492.

Barichivich J, Briffa KR, Myneni RB et al. (2013) Large-scale variations in the vegetation growing season and annual cycle of atmospheric CO_2 at high northern latitudes from 1950 to 2011. Global Change Biology, 19, 3167-3183.

Bintanja R, Selten FM (2014) Future increases in Arctic precipitation linked to local evaporation and sea-ice retreat. Nature, 509, 479-482.

Boelman NT, Stieglitz M, Rueth HM, Sommerkorn M, Griffin KL, Shaver GR, Gamon JA (2003) Response of NDVI, biomass, and ecosystem gas exchange to long-term warming and fertilization in wet sedge tundra. Oecologia, 135, 414-421.

Brummell ME, Farrell RE, Siciliano SD (2012) Greenhouse gas soil production and surface fluxes at a high arctic polar oasis. Soil Biology & Biochemistry, 52, 1-12.

Burba GG, McDermitt DK, Grelle A, Anderson DJ, Xu L (2008) Addressing the influence of instrument surface heat exchange on the measurements of CO_2 flux from open-path gas analyzers. Global Change Biology, 14, 1854-1876.

Callaghan TV, Johansson M, Key J, Prowse T, Ananicheva M, Klepikov A (2011) Feedbacks and interactions: From the Arctic cryosphere to the climate system. Ambio, 40, 75-86.

Cheng Y, Gamon JA, Fuentes DA et al. (2006) A multi-scale analysis of dynamic optical signals in a Southern California chaparral ecosystem: A comparison of field, AVIRIS and MODIS data. Remote Sensing of Environment, 103, 369-378.

Christensen TR, Friborg T, Sommerkorn M et al. (2000) Trace gas exchange in a high Arctic valley 1. Variations in CO2 and CH4 flux between tundra vegetation types. Global Biogeochemical Cycles, 14, 701-713.

Corradi C, Kolle O, Walter K, Zimov SA, Schulze ED (2005) Carbon dioxide and methane exchange of a north-east Siberian tussock tundra. Global Change Biology, 11, 1910-1925.

Davidson EA, Janssens IA, Luo YQ (2006) On the variability of respiration in terrestrial ecosystems: moving beyond Q(10). Global Change Biology, 12, 154-164.

Edlund SA (1994) Vegetation. In: *Resource description and analysis - Ellesmere Island National Park Reserve*, pp.1-57, Department of Canadian Heritage, Winnipeg, Canada.

Elberling B (2003) Seasonal trends of soil CO2 dynamics in a soil subject to freezing. Journal of Hydrology, 276, 159-175.

Elberling B, Brandt KK (2003) Uncoupling of microbial CO2 production and release in frozen soil and its implications for field studies of Arctic C cycling. Soil Biology & Biochemistry, 35, 263-272.

Elberling B (2007) Annual soil CO_2 effluxes in the high Arctic: the role of snow thickness and vegetation type. Soil Biology & Biochemistry, 39, 646-654.

Elmendorf SC, Henry GHR, Hollister RD *et al.* (2012) Plot-scale evidence of tundra vegetation change and links to recent summer warming. Nature Climate Change, 2, 453-457.

Finkelstein PL, Sims PF (2001) Sampling error in eddy correlation flux measurements. Journal of Geophysical Research-Atmospheres, 106, 3503-3509.

France RL (1993) The Lake Hazen trough - a late winter oasis in a polar desert. Biological Conservation, 63, 149-151.

Gamon JA, Coburn C, Flanagan L *et al.* (2010) SpecNet revisited: bridging flux and remote sensing communities. Canadian Journal of Remote Sensing, 36, S376-S390.

Gamon JA, Huemmrich KF, Stone RS, Tweedie CE (2013) Spatial and temporal variation in primary productivity (NVDI) of coastal Alaskan tundra: decreased vegetation growth following earlier snowmelt. Remote Sensing of Environment, 129, 144-153.

Gaumont-Guay D, Black TA, Griffis TJ, Barr AG, Jassal RS, Nesic Z (2006) Interpreting the dependence of soil respiration on soil temperature and water content in a boreal aspen stand. Agricultural and Forest Meteorology, 140, 220-235.

Groendahl L, Friborg T, Soegaard H (2007) Temperature and snow-melt controls on interannual variability in carbon exchange in the high Arctic. Theoretical and Applied Climatology, 88, 111-125.

Guay KC, Beck PSA, Berner LT, Goetz SJ, Baccini A, Buermann W (2014) Vegetation productivity patterns at high northern latitudes: a multi-sensor satellite data assessment. Global Change Biology, 20, 3147-3158.

Heikkinen JEP, Elsakov V, Martikainen PJ (2002) Carbon dioxide and methane dynamics and annual carbon balance in tundra wetland in NE Europe, Russia. Global Biogeochemical Cycles, 16, 1115.

Hill GB, Henry GHR (2011) Responses of high Arctic wet sedge tundra to climate warming since 1980. Global Change Biology, 17, 276-287.

Hudson JMG, Henry GHR (2009) Increased plant biomass in a high arctic heath community from 1981 to 2008. Ecology, 90, 2657-2663.

Huemmrich KF, Black TA, Jarvis PG, McCaughey JH, Hall FG (1999) High temporal resolution NDVI phenology from micrometeorological radiation sensors. Journal of Geophysical Research, 104, 27,935-27,944.

Huemmrich KF, Gamon JA, Tweedie CE *et al.* (2010) Remote sensing of tundra gross ecosystem productivity and light use efficiency under varying temperature and moisture conditions. Remote Sensing of Environment. 114, 481-489.

Humprheys ER, Lafleur PM (2011) Does earlier snowmelt lead to greater CO2 sequestration in two low Arctic tundra systems? Geophysical Research Letters, 38, L09703.

Kutzbach L, Wille C, Pfeiffer EM (2007) The exchange of carbon dioxide between wet Arctic

tundra and the atmosphere at the Lena River Delta, Northern Siberia. Biogeosciences, 4, 869-890.

Lafleur PM, Humphreys ER, St Louis VL *et al.* (2012) Variation in peak growing season net ecosystem production across the Canadian Arctic. Environmental Science & Technology, 46, 7971-7977.

Laurila T, Soegaard H, Lloyd CR, Aurela M, Tuovinen JP, Nordstroem C (2001) Seasonal variations of net CO2 exchange in European Arctic ecosystems. Theoretical and Applied Climatology, 70, 183-201.

Lloyd J, Taylor JA (1994) On the temperature dependence of soil respiration Functional Ecology, 8, 315-323.

Lloyd CR (2001) The measurement and modelling of the carbon dioxide exchange at a high Arctic site in Svalbard. Global Change Biology, 7, 405-426.

Lüers J, Westermann S, Piel K, Boike J (2014) Annual CO_2 budget and seasonal CO_2 exchange signals at a high Arctic permafrost site on Spitsbergen, Svalbard archipelago. Biogeosciences, 11, 6307-6322.

Lund M, Lafleur PM, Roulet NT *et al.* (2010) Variability in exchange of CO_2 across 12 northern peatland and tundra sites. Global Change Biology, 16, 2436-2448.

Lund M, Falk JM, Friborg T, Mbufong HN, Sigsgaard C, Soegaard H, Tamstorf MP (2012) Trends in CO2 exchange in a high Arctic tundra heath, 2000-2010. Journal of Geophysical Research-Biogeosciences, 117,

Lupascu M, Welker JM, Seibt U, Maseyk K, Xu X, Czimczik CI (2014) High Arctic wetting reduces permafrost carbon feedbacks to climate warming. Nature Climate Change, 4, 51-55.

Mack MC, Schuur EAG, Bret-Harte MS, Shaver GR, Chapin FS (2004) Ecosystem carbon storage in Arctic tundra reduced by long-term nutrient fertilization. Nature, 431, 440-443.

Marushchak ME, Kiepe I, Biasi C *et al.* (2013) Carbon dioxide balance of subarctic tundra from plot to regional scales. Biogeosciences, 10, 437-452.

Oechel WC, Hastings SJ, Vourlitis G, Jenkins M, Riechers G, Grulke N (1993) Recent change of Arctic tundra ecosystems from a net carbon-dioxide sink to a source. Nature, 361, 520-523.

Oechel WC, Vourlitis GL, Hastings SJ, Zulueta RC, Hinzman L, Kane D (2000) Acclimation of ecosystem CO2 exchange in the Alaskan Arctic in response to decadal climate warming. Nature, 406, 978-981.

Parmentier F-JW, Christensen TR, Sorensen LL, Rysgaard S, McGuire AD, Miller PA, Walker DA (2013) The impact of lower sea-ice extent on Arctic greenhouse-gas exchange. Nature Climate Change, 3, 195-202.

Pearson RG, Phillips SJ, Loranty MM, Beck PSA, Damoulas T, Knight SJ, Goetz SJ (2013) Shifts in Arctic vegetation and associated feedbacks under climate change. Nature Climate Change, 3, 673-677.

Post E, Forchhammer MC, Bret-Harte MS *et al.* (2009) Ecological dynamics across the Arctic associated with recent climate change. Science, 325, 1355-1358.

Reichstein M, Stoy PC, Desai AR, Lasslop G, Richardson AD (2012) Partitioning of net fluxes. In: *Eddy covariance: A practical guide to measurement and data analysis* (eds Aubinet M, Vesala T, Papale D), pp. 263-289, Springer, Dordrecht, The Netherlands.

Rennermalm AK, Soegaard H, Nordstroem C (2005) Interannual variability in carbon dioxide exchange from a high arctic fen estimated by measurements and modeling. Arctic, Antarctic, and Alpine Research, 37, 545-556.

Rustad LE, Campbell JL, Marion GM *et al.* (2001) A meta-analysis of the response of soil respiration, net nitrogen mineralization, and aboveground plant growth to experimental ecosystem warming. Oecologia, 126, 543-562.

Sala OE, Chapin FS, Armesto JJ *et al.* (2000) Biodiversity - Global biodiversity scenarios for the year 2100. Science, 287, 1770-1774.

Serrano-Ortiz P, Roland M, Sanchez-Moral S, Janssens IA, Domingo F, Godderis Y, Kowalski AS (2010) Hidden, abiotic CO_2 flows and gaseous reservoirs in the terrestrial carbon cycle: Review and perspectives. Agricultural and Forest Meteorology, 150, 321-329.

Serreze MC, Walsh JE, Chapin FS *et al.* (2000) Observational evidence of recent change in the northern high-latitude environment. Climatic Change, 46, 159-207.

Sitch S, McGuire AD, Kimball J *et al.* (2007) Assessing the carbon balance of circumpolar arctic tundra using remote sensing and process modeling. Ecological Applications, 17, 213-234.

Soegaard H, Nordstroem C (1999) Carbon dioxide exchange in a high-arctic fen estimated by eddy covariance measurements and modelling. Global Change Biology, 5, 547-562.

Soegaard H, Nordstroem C, Friborg T, Hansen BU, Christensen TR, Bay C (2000) Trace gas exchange in a high Arctic valley 3. Integrating and scaling CO_2 fluxes from canopy to landscape using flux data, footprint modeling, and remote sensing. Global Biogeochemical Cycles, 14, 725-744.

Spielhagen RF, Werner K, Sorensen SA *et al.* (2011) Enhanced modern heat transfer to the Arctic by warm Atlantic water. Science, 331, 450-453.

Stow DA, Hope A, McGuire D *et al.* (2004) Remote sensing of vegetation and land-cover change in Arctic tundra ecosystems. Remote Sensing of Environment, 89, 281-308.

Street LE, Shaver GR, Williams M, Van Wijk MT (2007) What is the relationship between changes in canopy leaf area and changes in photosynthetic CO2 flux in arctic ecosystems. Journal of Ecology, 95, 139-150.

Tagesson T, Mastepanov M, Molder M *et al.* (2013) Modelling of growing season methane fluxes in a high-arctic wet tundra ecosystem 1997-2010 using in situ and high-resolution satellite data. Tellus B, 65, 19722.

Tape K, Sturm M, Racine C (2006) The evidence for shrub expansion in Northern Alaska and the pan Arctic. Global Change Biology, 12, 686-702.

Tarnocai C, Gould J, Broll G, Achuff P (2001) Ecosystem and trafficability monitoring for Quttinirpaaq National Park (11-year evaluation), pp.1-169, Agriculture and Agri-Food Canada, Ottawa, Canada.

Tarnocai C, Canadell JG, Schuur EAG, Kuhry P, Mazhitova G, Zimov S (2009) Soil organic carbon pools in the northern circumpolar permafrost region. Global Biogeochemical Cycles, 23, GB2023.

Thompson B (1994) Climate. In: *Resource description and analysis - Ellesmere Island National Park Reserve*, pp.1-78, Department of Canadian Heritage, Winnipeg, Canada.

Walker DA, Raynolds MK, Daniels FJA *et al.* (2005) The circumpolar Arctic vegetation map. Journal of Vegetation Science, 16, 267-282.

Welker JM, Wookey PA, Parsons AN, Press MC, Callaghan TV, Lee JA (1993) Leaf carbon isotope discrimination and vegetative responses of Dryas octopetala to temperature and water manipulations in a high Arctic polar semi-desert, Svalbard. Oecologia, 95, 463-469.

Welker JM, Fahnestock JT, Henry GHR, O'Dea KW, Chimner RA (2004) CO_2 exchange in three Canadian High Arctic ecosystems: response to long-term experimental warming. Global

Change Biology, 10, 1981-1995.

Wookey PA, Parsons AN, Welker JM, Potter JA, Callaghan TV, Lee JA, Press MC (1993) Comparative responses of phenology and reproductive development to simulated environmental-change in sub Arctic and high Arctic plants. Oikos, 67, 490-502.

Wookey PA, Robinson CH, Parsons AN, Welker JM, Press MC, Callaghan TV, Lee JA (1995) Environmental constraints on the growth, photosynthesis and reproductive development of Dryas-Octopetala at a high Arctic polar semidesert, Svalbard. Oecologia, 102, 478-489.

Zhang X, He J, Zhang J, Polyakov I, Gerdes R, Inoue J, Wu P (2012) Enhanced poleward moisture transport and amplified northern high-latitude wetting trend. Nature Climate Change, 3, 47-51.

Chapter 3.   The net exchange of methane with high Arctic landscapes during the summer growing season

Introduction

Rapid warming is altering polar regions at unprecedented rates (AMAP, 2012). Recent climate models suggest that Arctic mean annual temperatures will rise 2.5–7°C by the end of the 21st century (Overland *et al.*, 2011) but up to 9°C in local regions such as the Canadian Arctic Archipelago (ACIA, 2005). Mean annual precipitation is also projected to increase throughout the Arctic resulting from the capability of a warmer Arctic atmosphere to transport more water from low to high latitudes (Manabe and Stouffer, 1994). Warming and wetting of the Arctic has resulted in several environmental responses including permafrost thaw (Froese *et al.*, 2008), glacial and sea ice melt (Pfeffer *et al.*, 2008), increased surface runoff (Peterson *et al.*, 2002), increased primary productivity and vegetation cover (Walker *et al.*, 2006), and enhanced cycling of greenhouse gases (GHGs), including the powerful GHG methane (CH_4; O'Connor *et al.*, 2010), between the atmosphere and changing landscapes.

Both CH_4 production (methanogenesis) and consumption (CH_4 oxidation, or methanotrophy) occur in Arctic terrestrial, freshwater and marine ecosystems. Methanogenesis is carried out by obligate anaerobic microorganisms (except in ocean surface waters), whereas methanotrophy occurs primarily in oxic environments. In the low and high Arctic (as defined by *AMAP*, 1998), there are numerous sources of CH_4 to the atmosphere, most of which are predicted to strengthen in a warming and increasingly ice-free environment. These sources include thermokarst lakes, peatlands, lake sediments, thawing permafrost, subglacial environments, CH_4 hydrates in marine sediments and CH_4 production in ocean surface waters (Roulet *et al.*, 1994, *O'Connor et al.*, 2010, *Kort et al.*, 2012, *Wadham et al.*, 2012). Far more attention has been bestowed on these sources of CH_4 to the atmosphere, with proportionally less attention given to numerous sinks of CH_4 in polar regions. Sinks of CH_4 include the oxic layer above the saturated zone in peatlands where CH_4 is produced, in oxygenated water columns of lakes and oceans, and in dry, desert tundra soils that make up a large portion of the high Arctic landscape (Whalen and Reeburgh, 1990). These sinks are equally important to understand and quantify because they can both prevent CH_4 from entering the atmosphere and directly consume atmospheric CH_4.

Currently, the average atmospheric concentration of CH_4 is just over 1 800 parts per billion (ppb) in the northern hemisphere, compared to a background concentration of ~600 ppb for the majority of past 600,000 years (Kirschke *et al.*, 2013). Although monitoring the rise of atmospheric CH_4 concentrations is extremely important for understanding net emissions of this powerful GHG, it is equally important to quantify how CH_4 is interacting with landscapes to understand processes driving concentration changes. For example, the flux of CH_4 (F_{CH4}) between landscapes and the atmosphere is the balance between methanogenesis and CH_4 oxidation (consumption). When F_{CH4} is negative, the system is in a phase of net CH_4 consumption (or methanotrophy), and CH_4 is being removed from the atmosphere. When positive, the system is in a phase of net methanogenesis, and CH_4 is being added to the atmosphere. Thus, as climate changes, the state of F_{CH4} in any ecosystem can have a positive or negative feedback on the atmospheric pool of CH_4. Currently, there is a paucity of F_{CH4} measurements in high Arctic ecosystems (Olefeldt *et al.*, 2013) and little is known about how its direction and magnitude will respond as climate and landscapes change in the future.

The goal of this research was to quantify F_{CH4} for remote high Arctic landscapes where very little is known regarding carbon cycling in general and CH_4 fluxes in particular. Between 2008 and 2012, we measured F_{CH4} near Lake Hazen in Quttinirpaaq National Park, Ellesmere Island, Canada (81.8°N, 71.4°W). Using static chamber measurements, eddy covariance (EC) measurements and a mass budget analysis, we examined spatial and temporal variations in F_{CH4} over this high Arctic landscape. We hypothesized that dry, unproductive polar desert landscapes would act as a CH_4 sink while wet, productive meadow wetlands would be a CH_4 source to the atmosphere. As elsewhere, soil moisture, and air and soil temperature were expected to be important drivers of F_{CH4}. However the high Arctic land area is substantial and represents the extremes of environmental conditions which are changing rapidly, making it a key ecosystem to examine in the context of global CH_4 cycling. To our knowledge, this study represents one of the longest records of F_{CH4} in the high Arctic, and the highest northern latitude EC CH_4 measurements collected to date.

Methods

Research Site

We conducted our research out of the Lake Hazen base camp in Quttinirpaaq National Park, Canada's most northerly and remote national park, on northern Ellesmere Island, Nunavut (Figure 3.1). Fewer than 15 people typically visit the site each year. The lower reach of the lake's watershed is considered a high Arctic thermal oasis (France, 1993) because it is protected from coastal weather by the Grant Land Mountains and the Hazen Plateau adjacent to the lake. Much of the watershed is typical of the high Canadian Arctic, consisting of a dry, mineral soil landscape with intermittent meadow wetlands and ponds where water flows and collects. Following nine months of sub-$0°C$ temperatures, snowmelt commences in the watershed in early June and vegetation growth proceeds quickly to peak biomass in mid-July before senescence toward freezing conditions in September. Despite continuous daylight during the growing season, pronounced diurnal patterns in solar radiation exist.
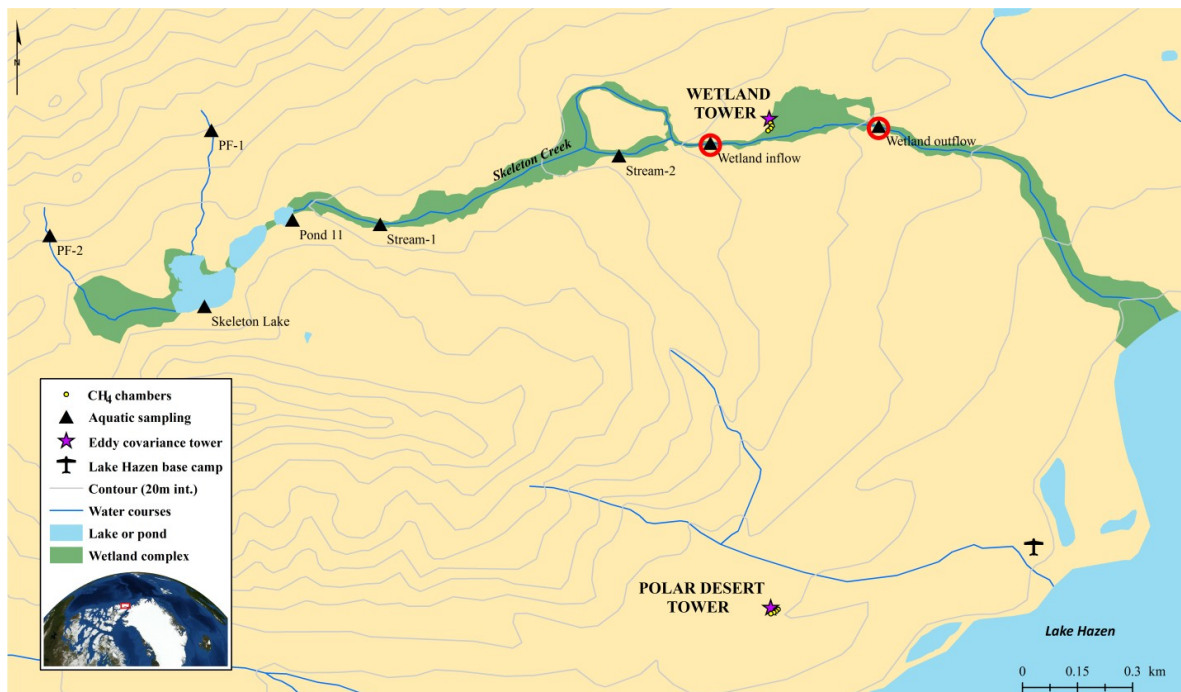
Figure 3.1 Lake Hazen base camp in Quttinirpaaq National Park, Nunavut, Canada (81.8°N, 71.4°W). Both the polar desert and meadow wetland study sites are shown with static chamber, eddy covariance and aquatic CH_4 sampling locations indicated. Emphasis added to aquatic sites upstream and downstream of the wetland. PF sites indicate permafrost seep streams and Stream sites indicate Skeleton Creek sites.

We focused our study on two common, contrasting landscape types in the high Arctic: a dry, unproductive polar desert (herein "desert") and a moist, productive meadow wetland (herein "wetland") (Figure 3.1). Ground cover at the desert (~188 m amsl) is classified as graminoid, prostrate dwarf-shrub forb tundra (Walker *et al.*, 2005) consisting of cryptogamic crust (56.1%), lichen (11.8%), *D. integrifolia* (4.8%), moss (1.9%), *Carex nardine/Kubresia myosuroides* (1.3%), *Salix archea* (0.6), litter (3.5%) and bare ground (20.5%, Tarnocai *et al.*, 2001). Ground cover at the wetland (~231m amsl; 2.9 ha) is classified as sedge/grass, moss meadow wetland (Walker *et al.*, 2005) consisting of *Carex*, *Eriophorum* and graminoids (Edlund, 1994). The wetland is part of the larger Skeleton Creek meadow wetland complex, consisting of permafrost seeps (PF sites), Skeleton Lake, shallow ponds (e.g., Pond 11) and a creek flowing through a wetland valley (Figure 3.1). During a typical growing season, the creek flows into the wetland, saturates soils and exits downstream towards Lake Hazen.

Quantifying F_{CH4}

Measurement overview: F_{CH4} has overwhelmingly been measured throughout the Arctic using static chambers because of their simplicity and convenience (Parmentier *et al.*, 2011). The EC technique (Baldocchi, 2003) for measuring F_{CH4} has only been used sporadically in the high Arctic (e.g., Friborg *et al.*, 2000) because tunable diode laser detectors or other closed path detectors require large quantities of power not readily available in remote high Arctic locations. Recently, a low power consuming open path CH_4 analyser (LI-7700; LI-COR, Lincoln, NE) has appeared on the market (McDermitt *et al.*, 2011). EC provides F_{CH4} near continuously over short temporal scales (30 min.) and large spatial scales (hectares) providing great potential to focus on ecosystem-scale exchanges with the atmosphere and the biotic and abiotic factors driving temporal variations across northern ecosystems. This study was part of a larger one in which we are quantifying the flux of the GHG carbon dioxide (F_{CO2}; the balance between CO_2 uptake via photosynthesis and the release of CO_2 via ecosystem respiration) between the atmosphere and desert (2008-12) and wetland (2010-12) landscapes using EC flux towers. Towers were equipped with Campbell Scientific Inc. (CSI; Logan, UT) CSAT3 sonic anemometers and LI-COR LI-7500 (open-path) and LI-7200 (enclosed-path) CO_2\water vapor (H_2O) infrared gas analyzers (Figure A2.1). In addition to F_{CH4} and F_{CO2}, these tower-based EC systems quantified H_2O and

energy fluxes and were equipped with sensors to measure soil temperature and moisture at 5 cm depth (CS107B, CS616, CSI; 30 min. mean each tower, each growing season), and other meteorological parameters (Table A2.1). Signals from all sensors were recorded as half-hour means on CSI CR3000-XT dataloggers. Thaw depth was monitored weekly at ten points along a transect at each site using a steel probe.

Chamber measurements: Static, non-steady state chambers were used to quantify F_{CH4} at the desert and wetland sites (Figure 3.1). At the start of each season, we set four 25 cm diameter white PVC collars 10–15 cm into the soil within 20 m of each tower (the same locations each year), where they remained for the rest of the field season. Two desert collars enclosed bare soil and two other collars enclosed >50% vegetation cover consisting mostly of *Dryas* (Figure 3.1, A2.1). At the wetland, four collars were placed along its margin because a boardwalk was not permitted in the National Park to access the centre of the wetland (Figure 3.1, A2.1). Each collar enclosed vegetation of similar type and cover as the rest of the wetland. Chambers were deployed at each site every five to seven days between June and August. On sampling days, between 10:00–16:00, foil-covered 18 L plastic chambers with sampling lines were placed into a water-filled groove on the collars. At 0, 20, 40 and 60 minutes after deployment, air inside each chamber was mixed by syringe before chamber air was collected into an evacuated 35 mL Wheaton glass bottle. Ambient air pressure and temperature were recorded. All samples were stored in the dark at 4°C until analysis at the University of Alberta. We used a Varian 3800 gas chromatograph (GC) with a flame-ionizing detector to measure the CH_4 concentration (in parts-per-million; ppm) of each gas sample from each chamber. Three standard-grade gases (0, 1, 54 ppm-CH_4) were used to calibrate the GC, and all samples were analysed in duplicate. We then used the CH_4 concentration, the ideal gas law, chamber metrics, ambient pressure and temperature, and the gas constant to quantify the mass of CH_4 enclosed by each chamber at each sampling time. Linear regressions were used to fit relationships between sample times and total masses of CH_4 for each chamber and root mean squared errors (RMSEs) were used to assess regression performance (Kutzbach *et al.*, 2011). Regression estimates typically fit well to observed CH_4 masses in both desert (mean measured±RMSE; 11.19±0.45 μg; n=101) and wetland (13.23±0.47 μg CH_4; n=66) chambers. The slope of the regression line determined F_{CH4} (mg CH_4 m^{-2} hr^{-1}) for each chamber. Fluxes from the four chambers were averaged to determine

site daily means (mg CH_4 m^{-2} d^{-1}) with the assumption that there would be little diurnal variation in F_{CH4} (supported by EC measurements; see section 3.2).

Eddy covariance measurements: As described above, although EC technology is not new, only recently has a low-power, robust CH_4 analyzer become available. We had the opportunity during the 2012 growing season to deploy an LI-7700 open-path CH_4 gas analyzer on one of our two EC towers. Because we could not obtain chamber measurements in the centre of the wetland, we deployed the LI-7700 on the wetland EC tower to attain more representative CH_4 fluxes from that ecosystem than provided by the chambers on the wetland's periphery. The wetland EC tower was positioned just outside the western margin of the wetland, leeward of the prevailing wind. Winds originated from the prevailing direction 82% of all half-hour measurements, and 90% of all fluxes originated from within the wetland footprint using the Kljun *et al.* (2004) model. The LI-7700 was laterally positioned 25 cm from the sonic anemometer and 1.9 m above the vegetation canopy height. Measurements of CH_4 molar density, wind velocity in three coordinates, sonic temperature, ambient pressure, and CO_2 and H_2O mixing ratios (LI-7200) were collected at 10 Hz and logged on a LI-COR LI-7550 interface unit.

We used EddyPro (LI-COR, v. 4.1) to calculate CH_4, CO_2 and H_2O fluxes and to QA/QC data and remove outliers. Gas fluxes were calculated at half-hour intervals using a block averaging approach. To correct for anemometer tilt, a double rotation was performed to force mean vertical and lateral wind components to zero. F_{CH4} data were de-spiked and corrected for time lag between the anemometer and the gas analyzer measurements using a covariance maximization approach. Because the LI-7700 is an open-path analyzer, density fluctuations were corrected for using the Webb *et al.* (1980) approach. We used spectral corrections to adjust for flux loss at high and low frequencies (after Ibrom *et al.*, 2007) and to correct for the spectroscopic effects of H_2O (LI-COR, 2011). We removed half-hour fluxes when EC sensors malfunctioned, returned poor diagnostic values (e.g., during rare rain events), when wind did not pass over the wetland (17.8% of all half-hour fluxes), and when the friction velocity fell below 0.1 m s^{-1}, similar to other studies (Wille *et al.*, 2008). We also applied turbulence tests after Mauder and Foken (2006) to remove the poorest-quality fluxes (level 2) when they did occur. Half-hour fluxes that were beyond ±3 SD of the growing season mean were also removed. These

corrections resulted in removal of 43.8% of total collected flux data. Measurement gaps occurred between 22-Jun. and 01-Jul. and between 31-Jul. and 01-Aug. when solar charging could not match power requirements. For both chamber and EC F_{CH4} measurements, positive values represented CH_4 emission to the atmosphere, whereas negative values represented CH_4 consumption in soils.

Wetland aquatic chemistry

We determined if there were significant dissolved CH_4 inputs by Skeleton Creek into the wetland so we could examine the potential for methanogenesis within the wetland soils. These measurements, in combination with EC flux tower measurements, would also allow us to construct a general CH_4 mass budget for the wetland. We collected surface water upstream and downstream of the wetland every two to five days during the 2012 growing season (Figure 3.1). We measured the partial pressure of dissolved CH_4 by collecting surface water at each site into evacuated 160 mL Wheaton glass serum bottles with butyl rubber stoppers (after Kling *et al.*, 1991). Each bottle contained 8.9 g of potassium chloride preservative, and 10 mL of ultra high-purity N_2 headspace. Samples were analysed on the same GC used to analyze the chamber samples, but using 0, 50, 350, and 900 ppm CH_4 standard gases. All samples were placed in a wrist-action shaker for 20 minutes to equilibrate headspace gas with the sample. 500 uL of headspace gas was extracted from each sample for analysis using a gas-tight syringe. Duplicate analyses were performed on all samples. We used the headspace CH_4 gas concentrations from each sample, ambient and laboratory temperature and pressure, and Henry's Law to determine the dissolved CH_4 concentration in the collected water sample. Water was also collected at each site for analyses of general water chemistry parameters including concentrations of particulate and dissolved nutrients, ions, chlorophyll-*a* and dissolved organic carbon. All samples were initially processed and preserved on-site in the Lake Hazen/Quttinirpaaq Polar Laboratory and subsequently analysed using standard methods at the University of Alberta's Biological Analytical Services Laboratory. In-situ measurements including pH, dissolved oxygen, water temperature, oxidation-reduction potential and specific conductivity were also taken at each site at time of sampling using a YSI (YSI Environmental, Yellow Springs, OH) 556 MPS multi probe system. Water flow at each site was measured every two to three days using a Pygmy

current meter. At each site, we chose a channelized section of stream and measured the water velocity at half-depth across 5 cm segments of stream. We then took the product of stream cross sectional area and mean velocity in each segment and summed all segments to quantify total stream flow.

Results

Chamber measurements

Over several growing seasons, soils at the desert site consumed atmospheric CH_4 at a mean rate (±1SE) of −1.37±0.06 mg CH_4 m^{-2} d^{-1} (n=4, mean of 4 independent collars measured 27 times each between 2008 and 2012), whereas the wetland site emitted fluxes of CH_4 (0.22±0.14 mg CH_4 m^{-2} d^{-1}; n=4, mean of 4 independent collars measured 18 times each between 2010 and 2012). Desert soils consistently consumed atmospheric CH_4 throughout the growing season, whereas wetland soils typically consumed atmospheric CH_4 during the first two weeks of July (0.40±0.12 mg CH_4 m^{-2} d^{-1}) before transitioning to a source of CH_4 to the atmosphere (0.72±0.22 mg CH_4 m^{-2} d^{-1}) (Figure 3.2). When comparing paired sampling dates from each site from 2010 to 2012, we found that the desert landscape consumed significantly more atmospheric CH_4 than the wetland (Repeated-measures ANOVA; $F_{(1,17)}$=92, $p<0.001$; Figure 3.3). These site differences in F_{CH4} were related to the large differences in soil moisture and soil temperature (Figure 3.3). Daily mean soil moisture at 5 cm depth of the desert soils was consistently near 15.1±1.0% v/v during the measurement period, except during short rain events. Wetland soil moisture at the same depth was considerably higher (75.1±3.2%) than at the desert. Because the wetland was bowl-shaped, snow melt and creek water saturated the centre of the wetland first before wetting the margins where the chamber collars were located. In 2012, the wetland gradually dried after snowmelt because creek flow ceased due to low water levels in ponds upstream. Once ponds returned to maximum storage, creek flow resumed on 16-Jul-12 and eventually re-saturated the wetland margin soils to levels similar to other years. Throughout the chamber measurement period, the desert site, relative to the wetland, had higher 5 cm depth soil temperature (14.4±0.5 °C-desert vs. 10.4±0.5 °C-wetland), higher soil heat flux at 5 cm depth (52.3±4.2 W m^{-2}-desert vs. 15.8±1.5 W m^{-2}-wetland) and deeper thaw depths (0.88±0.03 m-desert vs. 0.29±0.01m-wetland; Figure 3.3).
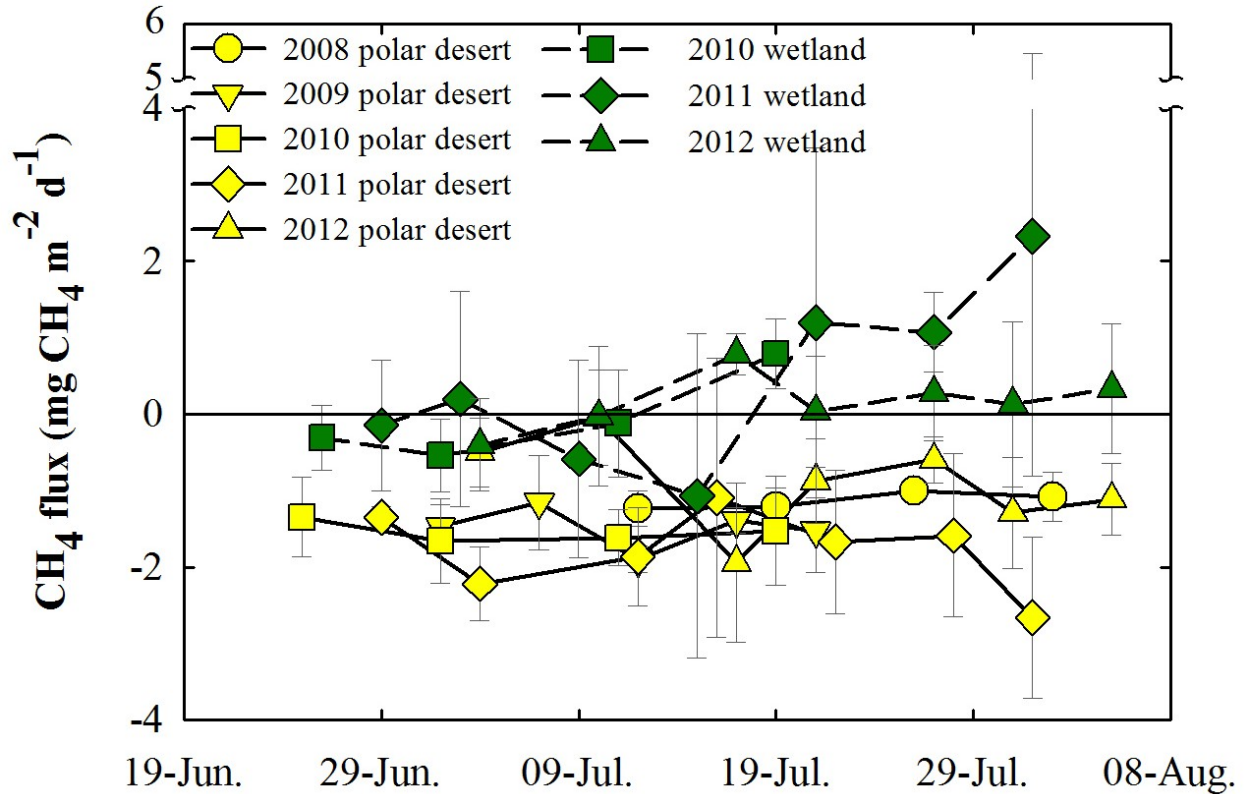
Figure 3.2 Mean CH$_4$ fluxes (F$_{CH4}$; ±1SD) from four polar desert and four wetland static chambers during the 2008 to 2012 growing seasons.

Between 2008 and 2012 at the desert site, mean growing season F$_{CH4}$ ranged between –0.91 and –1.78 mg CH$_4$ m^{-2} d^{-1} (Table 3.1, Figure 3.2). CH$_4$ consumption rates were positively correlated with soil temperatures between years (r^2=0.99; n=5; simple correlation) but not influenced by changes in soil moisture (r^2=0.03). Consumption rates of CH$_4$ were not significantly different in chambers with or without vegetation (RM-ANOVA; F$_{(1,26)}$=0.15, p=0.76). Associations between within-season F$_{CH4}$ and environmental factors were generally weak (–0.28<ρ<0.07; Spearman Rank Correlation; Table A2.2-A.). From 2010 to 2012 at the wetland site, mean growing season F$_{CH4}$ ranged between -0.05 and +0.43 mg CH$_4$ m^{-2} d^{-1} (Table 3.1, Figure 3.2). With only three years of data, trends between mean growing season F$_{CH4}$ at the wetland site and explanatory variables were not meaningful. However, we do note that years with fairer weather (air pressure r^2=0.95) and warmer conditions (thaw depth r^2=0.81; soil heat flux at 5 cm depth r^2=0.67) seemed to be associated with greatest emissions at the wetland.
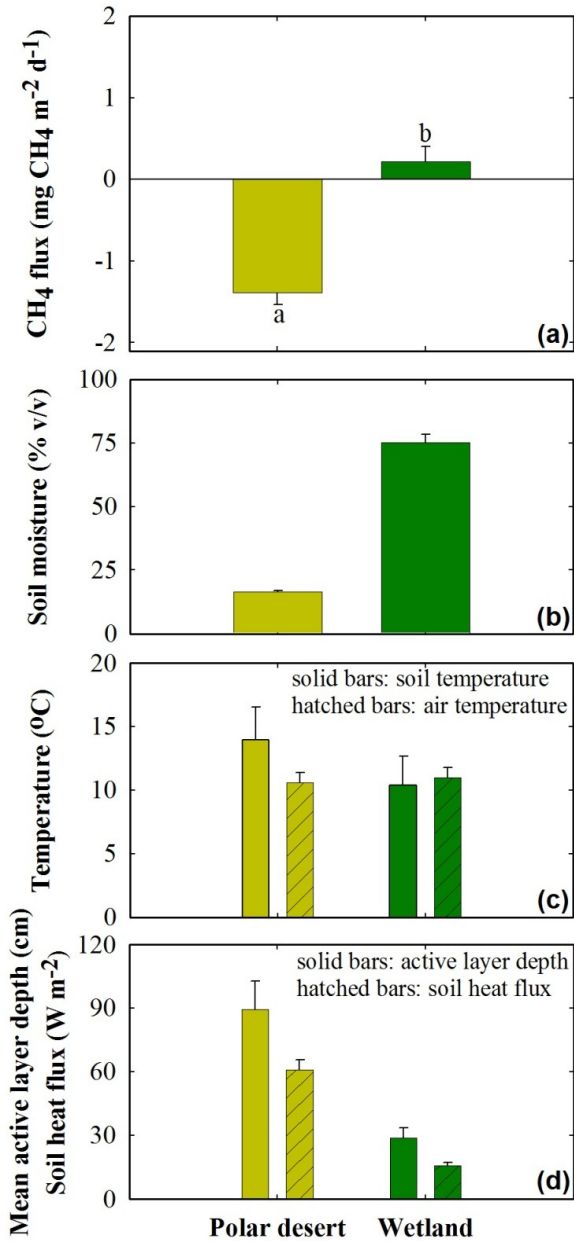
Figure 3.3 Comparison of 2010-12 growing season mean CH_4 fluxes (F_{CH4}; ±1SE) measured in chambers (a) and other environmental variables (b-d), paired by site. The sampling period represented by each bar spans approximately late June to early August. Letters indicate if there were statistically significant differences of F_{CH4} between sites using a repeated-measures ANOVA.

Within-season wetland F_{CH4} was positively correlated with mean daily stream flow in Skeleton Creek ($\rho=0.72$; Table A2.2-B.).

Eddy covariance measurements

F_{CH4}, measured using the EC flux tower in 2012, was between –0.84 and +2.73 mg CH_4 m^{-2} d^{-1} with a mean daily F_{CH4} (±1SE) of 1.27±0.18 mg CH_4 m^{-2} d^{-1} at the wetland (Figure 3.4a.) with no discernible diurnal patterns (Figure A2.2). On days when net CH_4 consumption occurred, mean F_{CH4} was –0.33±0.07 mg CH_4 m^{-2} d^{-1} (n=9) compared to +1.76±0.14 mg CH_4 m^{-2} d^{-1} (n=29) when net CH_4 emission was occurring. Net uptake of CH_4 quickly changed to net emission just after wetland soils rapidly thawed. Soil temperature warmed from freezing conditions (–1.3°C) to above 7°C during the first seven days of measurements (Figure 3.4b.). During that time, frozen moisture within soils and in snow covering the wetland, thawed and saturated the wetland landscape (Figure 3. 4c). The increase in evaporative fluxes preceded the saturation of the 5 cm depth of the wetland margin while F_{CO2}

Table 3.1 Mean (±1SE) daily CH$_4$ flux (F$_{CH4}$) and environmental variables during the chamber measurement period of several growing seasons at the desert and wetland sites.

	F$_{CH4}$ (mg CH$_4$ m^{-2} d^{-1})	n (#)	Air$_T$ (°C)	PAR (µmol m^{-2}s^{-1})	SHF (W m^{-2})	Soil$_M$ (% v/v)	Soil$_T$ (°C)	n (daily)
Desert								
2008	−1.13±0.05	4	7.3±0.6	520±22	14.6±2.7	17.0±2.2	11.4±0.4	24
2009	−1.49±0.12	5	10.0±0.7	678± 20	26.9±1.1	9.4±0.1	12.9±0.5	20
2010	−1.54±0.07	4	9.8±0.6	685±26	28.8±1.9	17.5±0.2	12.7±0.5	25
2011	−1.78±0.20	7	9.5±0.3	678±22	32.1±1.4	16.9±0.1	13.7±0.3	34
2012	−0.91±0.23	7	8.1±0.4	520±32	26.5±2.0	15.4±0.1	11.1±0.4	33
Wetland								
2010	−0.05±0.29	4	11.0±0.8	652±24	7.8±0.8	79.0±1.3	10.6±0.4	22
2011	0.43±0.44	7	10.7±0.4	657±21	6.4±0.6	80.6±0.6	10.8±0.2	34
2012	0.16±0.14	7	9.1±0.5	507±31	8.1±0.4	58.2±1.3	8.2±0.1	33

Air$_T$: air temperature; PAR: photosynthetically active radiation; SHF: soil heat flux at 5 cm depth; Soil$_M$: volumetric soil moisture; Soil$_T$: soil temperature; n indicates the number of landscape mean measurements (of four chambers) taken during each growing season (also see Figure 3.2).

remained positive (net CO$_2$ emission) for another week after this initial thaw period (Figure 3.4d.). CH$_4$ emissions peaked during the first 2 weeks of July, similar to when net CO$_2$ uptake peaked. We did not observe significant changes in whole-wetland CH$_4$ emission rates when Skeleton Creek flow resumed during the third week of July and soil moisture in the wetland margin returned to values similar to the post-thaw period (Figure 3.4a.,c.). In contrast, F$_{CH4}$ measured by static chambers increased through the summer with peak CH$_4$ emissions at the end of the season when Skeleton Creek flow was greatest. However, chamber-based F$_{CH4}$ on the wetland margin was always lower than the fluxes measured by the EC technique including a period in early July where average F$_{CH4}$ indicated net CH$_4$ uptake (Figure 3.4a.). Overall, seasonal variations in F$_{CH4}$ measured by EC associated strongest with F$_{CO2}$ and soil temperature (Table A2.3).

Wetland aquatic chemistry

Flow-weighted mean dissolved CH$_4$ concentrations (±1weighted SD) in Skeleton Creek water (Table 3.2) decreased from 0.005±0.004 µmol L^{-1} upstream of the wetland to 0.001±0.005 µmol L^{-1} downstream of the wetland between 03-Jul. and 05-Aug., a decrease of 70%. Ammonium concentrations increased downstream while nitrate concentrations were below the
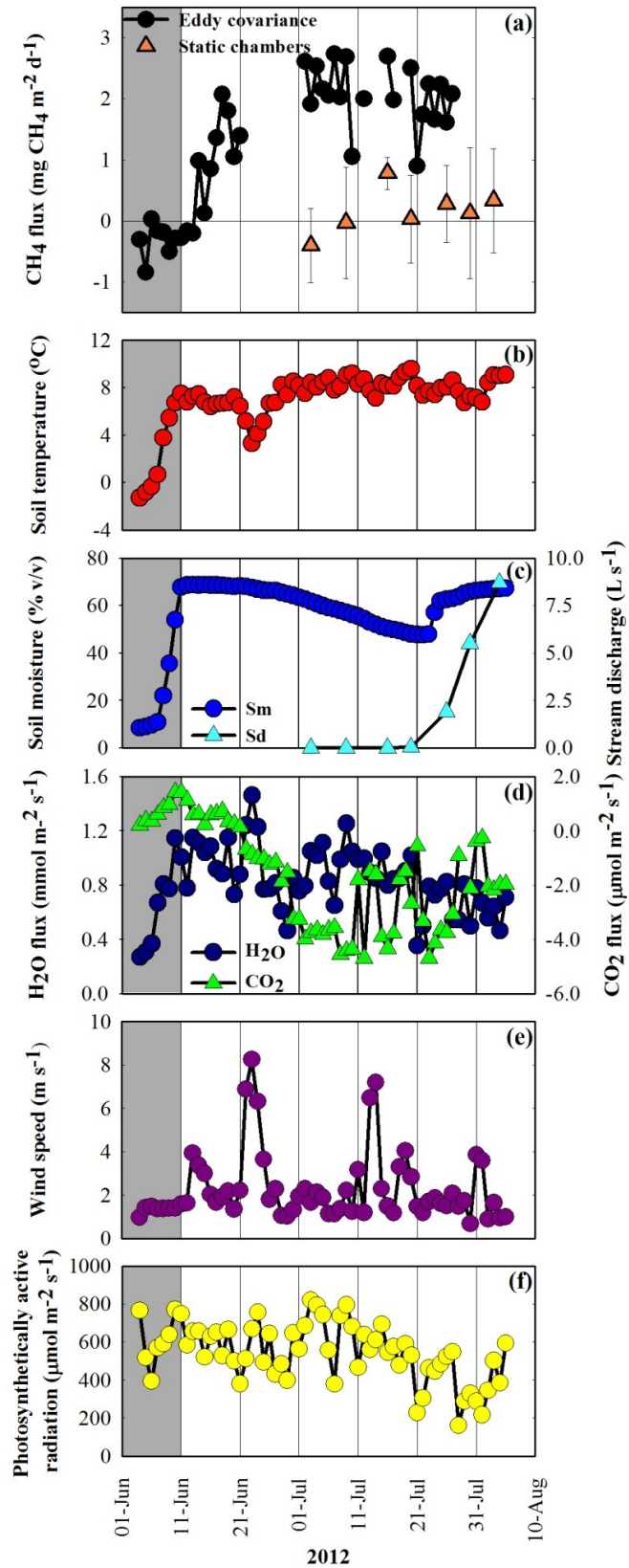
Figure 3.4 Comparison of mean daily eddy covariance and static chamber CH_4 fluxes (a) at the wetland and several mean daily environmental variables (b-f) during the 2012 growing season. Shaded bars highlight the period of rapid soil thaw.

Table 3.2 Flow-weighted mean concentrations (±1wSD) of several chemicals in Skeleton Creek water upstream and downstream of the wetland during the 2011 and 2012 growing seasons. All chemicals are reported in μmol L^{-1} except for water temperature (°C) and oxidation-reduction potential (mV).

Parameter	2011			2012		
	Wetland Inflow	Wetland Outflow	% change	Wetland Inflow	Wetland Outflow	% change
Dissolved CH_4	0.029±0.018	0.002±0.002	-94%	0.005±0.004	0.001±0.005	-70%
Dissolved CO_2	52±17	61±16	17%	72±29	65±10	-9%
NO_3^-	0.10±0.07	0.06±0.03	-42%	0.04±0.00	0.04±0.00	0%
NH_4^+	0.99±0.25	1.01±0.26	1%	0.53±0.13	0.76±0.07	42%
DON	17.5±0.5	20.6±1.3	17%	19.4±1.0	22.0±0.5	13%
TDN	18.5±0.7	21.7±1.3	17%	20.0±0.9	22.8±0.5	14%
DOC	421±21	479±27	14%	497±28	549±19	10%
Particles (PN)	0.41±0.09	1.07±0.68	160%	n/a	n/a	n/a
Water $_T$	10.8±0.9	11.2±0.9	3%	8.1±1.6	7.8±1.4	-4%
ORP	n/a	n/a	n/a	53±57	21±17	-60%

NO_3^-: dissolved nitrate; NH_4^+: dissolved ammonium; DON: dissolved organic nitrogen; TDN: total dissolved nitrogen; DOC: dissolved organic carbon; PN: particle-bound nitrogen; Water $_T$: water temperature; ORP: oxidation-reduction potential.

analytical detection limit at both sites. Concentrations of dissolved organic nitrogen and carbon were higher in the wetland outflow than inflow (Table 3.2). If we assume no net storage of CH_4 in the wetland over a growing season when stream flow was occurring (~late June to early August), we can calculate the *net* production of CH_4 (production-oxidation losses) in wetland soils using the following equation:

$$\Sigma(I_{CH4} + NP_{CH4})_{daily} = \Sigma(F_{CH4} + O_{CH4})_{daily} \tag{1}$$

where I_{CH4} and O_{CH4} are the daily masses of dissolved CH_4 entering and exiting the wetland, NP_{CH4} is the daily net production of CH_4 in soils scaled to 2.9 ha of the wetland, and F_{CH4} is the daily flux of CH_4 from the wetland surface (2.9 ha) as measured by the EC tower. Net storage of CH_4 in wetland soils during the growing season was clearly shown via burst events in site (unpublished data), which is often coincident with CH_4 burst events (Mastepanov *et al.*, 2013). I_{CH4} and O_{CH4} were calculated using:

$$I_{CH4} \text{ or } O_{CH4} \text{ (g)} = (([CH4_{t1}]+[CH4_{t2}]) / 2) *V \tag{2}$$

where $[CH4_{t1}]$ and $[CH4_{t2}]$ were mean concentrations of dissolved CH_4 at two consecutive sampling times and V was the total volume of water that flowed through each station between those times. Solving for NP_{CH4} in Equation (1), we estimated that the net production of CH_4 in

Table 3.3 Wetland mass balance (Eq. 2) of CH_4 for the 2012 growing season (03-Jul. to 05-Aug.), including stream input (I_{CH4}) and output (O_{CH4}), flux of CH_4 (F_{CH4}) from the EC tower, and estimate of net CH_4 production within wetland soil (NP_{CH4}).

	Stream flow (m^3)	n (#)	CH_4 transfer (g)
I_{CH4}	6 578	8	0.5
O_{CH4}	5 451	6	0.1
F_{CH4}	-	34	2 002
NP_{CH4}	-	-	2 002

wetland soils was 2 002 g CH_4 (2.0 mg CH_4 m^{-2} d^{-1}; Table 3.2). We also found that even if dissolved CH_4 in Skeleton Creek was entirely evaded to the atmosphere in the wetland (i.e., not oxidized within soils), it was still a very small component (<1%) of F_{CH4} compared to net production in soils (Table 3.2).

Discussion

Factors driving CH4 consumption within polar desert soils

The range in mean growing season F_{CH4} at our desert site during five growing seasons (–0.9 to –1.8 mg CH_4 m^{-2} d^{-1}) was similar to F_{CH4} measured at other dry soils in Arctic and temperate ecosystems (~0 to –3.5 mg CH_4 m^{-2} d^{-1}; Table A2.4; *King et al.*, 1997; Smith *et al.*, 2000; Olefeldt *et al.*, 2013). Methanotrophs use CH_4 as their primary carbon and energy source for metabolism and in dry soils, rates of methanotrophy are controlled by factors that: 1) deliver CH_4 and oxygen into soils (Benstead and King, 1997; Flessa *et al.*, 2008); 2) allow passage and replenishment of these gases where methanotrophs reside (Moosavi and Crill, 1998); and 3) facilitate heat transfer and increase soil temperatures where methanotrophs reside (Christensen *et al.*, 1999).

The bulk density and gas diffusivity of upper soil horizons affect diffusion rates of atmospheric gases into soils (Smith *et al.*, 2000). No vegetation canopy, high wind speeds and surface roughness promote the exchange of gases between the soil surface and the atmosphere by increasing the concentration gradient for CH_4 and oxygen from the soil to the atmosphere. The barren and flat terrain with large fetch and some surface roughness (1.5 cm) at the polar desert site would have promoted sustained gas exchange in this way.

Soil moisture is also a crucial factor influencing methanotrophy within dry soils. As water content increases, it replaces gas-filled pore spaces leading to reduced diffusivity thereby restricting oxygen (and CH_4) replenishment required for microbial metabolism. Whalen and Reeburgh (1996) found that methanotrophic rates peaked near 20% soil moisture (v/v) in boreal soils before decreasing substantially towards saturation. At our desert site, soils were sandy, well-drained, and typically between 9-16% v/v at 5 cm below the surface. We found little association between within-season F_{CH4} rates and soil moisture, suggesting that desert soil moisture content was well below a threshold where moisture restricted gas availability for methanotrophs and above the threshold where desiccation restricted microbial activity. This conclusion was further supported by the chamber results where F_{CH4} was similar in chambers with and without vascular vegetation suggesting that the moister vegetated soils were still within a moisture range that sustained methanotrophs without restricting gas transport.

The significant CH_4 consumption rates at the desert through the measurement period in each year (Figure 3.2) were also a function of relatively warm soil temperatures (Table 3.1) since methanotrophy is a microbial metabolic process. Despite the high latitude of our site, near surface soils were warm with little variation through the measurement period (Figure A2.3). This region experiences low cloud cover relative to much of the high Arctic (Thompson, 1994) resulting in high daily isolation (Figure 3.4). The deep, narrow valley structure of the watershed also retains heat more efficiently than other Arctic locales (Thompson, 1994).

Factors driving CH$_4$ emission from meadow wetland soils

F_{CH4} measured in our wetland margin chambers (–0.12 to +0.43 mg CH_4 m^{-2} d^{-1}) and using the EC technique (–0.84 to +2.73 mg CH_4 m^{-2}d^{-1}) were considerably lower than other low Arctic and sub Arctic wetlands (Olefeldt *et al.*, 2013; Table A2.4). CH_4 is produced by methanogenic bacteria as a by-product of carbon metabolism in anaerobic soil environments and several factors control its production and release to the atmosphere including: 1) soil moisture/water table position (Moosavi and Crill, 1997; Christensen *et al.*, 2000); 2) soil temperature (Christensen *et al.*, 1995; Nakano *et al.*, 2000; Ström *et al.*, 2012); 3) vegetation species composition and primary productivity rates (Christensen *et al.*, 1999; Ström *et al.*, 2012); and 4) substrate availability (Ström *et al.*, 2012).

Saturated, poorly-draining soils may sustain anaerobic conditions crucial for methanogens and also reduce habitat for CH_4 consuming methanotrophs above water tables. Soils in our wetland margin collars switched abruptly from net CH_4 consumption to net CH_4 emission when Skeleton Creek water saturated the previously dry organic soils. However, the EC flux tower measurement (near constant CH_4 emission) integrated the full wetland area suggesting that a significant portion of the wetland within the flux footprint was constantly near or at saturation following the rapid thaw period. This also may explain the lack of correlation between the soil moisture measured at the wetland margin and tower F_{CH4}. Other studies have shown that F_{CH4} may cease to relate to soil moisture once saturation occurs (Heikkinen *et al.*, 2002a), and we suspect that was the case at our site.

Temperature influences CH_4 production and emission from wetlands in cold environments (van Huissteden *et al.*, 2005). Soil temperature was strongly associated with F_{CH4} measured by the EC tower primarily as a consequence of the switch from CH_4 uptake to loss during soil thaw. After this period, soil temperatures were relatively stable as discussed above. Without more variation in soil temperature during the growing season, it is difficult to assess the sensitivity of F_{CH4} at these higher soil temperatures (>8-12 °C). Although soil temperatures at our wetland were generally lower than at wetlands which emit large amounts of CH_4 in low Arctic regions (e.g., Parmentier *et al.*, 2011), we found that other high Arctic wetlands with similar soil temperatures still emitted significantly more CH_4 to the atmosphere (Christensen *et al.*, 1995; Friborg *et al.*, 2000; Tagesson *et al.*, 2012) than at our site. Soil temperatures, therefore, did not appear to fully explain the low CH_4 fluxes at our wetland.

Several Arctic studies have demonstrated the importance of plant structures and root exudates to the emission of CH_4 from wetlands (e.g., Ström *et al.*, 2012). Certain aerenchymous plants are known to be important conduits of CH_4 to the atmosphere (e.g., *Eriophorum, Carex*; Ström *et al.*, 2003). Plants also release carbon and nutrient-rich exudates from roots during growth, supplying methanogenic communities with key substrates. At our wetland site, vegetation cover included a substantial portion of *Eriophorum* and *Carex* species (Edlund, 1994) similar to other high Arctic wetlands (e.g., Ström *et al.*, 2003). Since F_{CH4} measured by the EC tower correlated best with F_{CO2} during thaw and through the growing season (Figure 3.4, Table

A2.3), this suggests either plant productivity and/or plant mediated transport of CH_4 may have been important in driving the seasonal variations in F_{CH4} at the wetland. However, F_{CO2} rates at our wetland were comparable to other high Arctic wetlands (Friborg *et al.*, 1997; *Tagesson et al.*, 2012) and others much further south (e.g., Lafleur *et al.*, 2012, Humphreys and Lafleur, 2011), suggesting that plant productivity cannot explain low rates of CH_4 emission from our wetland.

Substrate quantity and quality are key factors supporting microbial viability in soils. Peat accumulates in cold wetland environments because cold temperatures restrict microbial decomposition of fresh litter while saturation limits more efficient aerobic degradation pathways. Peat can be a high-quality carbon source for microbes in Arctic wetlands because of its high labile carbon content (Updegraff *et al.*, 1995). At Zackenburg, GR (74°N, 20°W), where soil temperatures and CO_2 fluxes were similar to our site, peat depths extended to over 30 cm encompassing most of the active layer during the growing season (Christensen *et al.*, 2000). At the centre of our wetland, the organic layer was only 7 cm thick with a sharp transition to mineral soil (Figure A2.4). Therefore, approximately one-quarter to two-thirds of the wetland active layer was comprised of organic-poor mineral soils likely not ideal for substantial microbial activity. Further, the shallow mineral soils and flow-through nature of our wetland may have made strong oxidizing species more available for microbial communities and thus restricting methanogen activity (Lipson *et al.*, 2012). Therefore, this wetland site, and presumably its low CH_4 emissions, was distinguished from other high Arctic wetlands. The reason for a roughly 7-10 cm deep accumulation of organic materials at the centre of this wetland, despite CO_2 uptake rates comparable to other high Arctic wetlands, may be due to its young age or could be due to other factors, such as redox conditions, that limit carbon accumulation and do not support methanogenesis.

CH$_4$ transport and transformations through a high Arctic wetland

The Skeleton Creek wetland complex is a typical meadow wetland within the Lake Hazen watershed and includes soils and productive lakes which are potentially important CH_4 emission sources to the atmosphere. Chemistry sampling of six aquatic sites upstream of the wetland (Figure 3.1) showed significant changes in dissolved CH_4 concentrations (Table A2.5). Low CH_4 concentrations occurred in permafrost melt water (PF sites), high concentrations and

emission rates were observed in productive lakes (Skeleton Lake, Pond 11; unpublished data), and concentrations declined downstream in the creek (stream sites) and wetland areas (wetland inflow, outflow) due to a combination of evasion and/or oxidation. These results suggest that wetland complexes in the watershed are comprised of potential "hot-spots" of CH_4 production and emission with very little lateral transfer of CH_4 between these systems and to Lake Hazen. This model of CH_4 flow differs from similar studies in the south which showed greater importance of lateral CH_4 transport in streams (e.g., Dinsmore *et al.*, 2010).

One of these "hot-spots" of CH_4 production and emission was at our wetland site. Because Skeleton Creek delivered only small amounts of CH_4 to the wetland (despite high CH_4 concentrations draining from Skeleton Lake), we found that the majority of CH_4 emitted by the wetland was from CH_4 produced within its soils (Table 3.2). Although we did not measure pore water CH_4 within the wetland, these results suggest that CH_4 emissions in the wetland were due to in-situ production exceeding oxidation even if we assume all creek CH_4 was evaded and included in F_{CH4} measurements. Bacterial production of CH_4 in wetland soils was further supported by chemistry results downstream of the wetland which showed signatures of anaerobic microbial activity in the form of: 1) increased $NH_4^+:NO_3^-$ ratios; 2) increases in dissolved organic matter; and 3) decreases in oxidation-reduction potential. However, it is unclear if fast stream flow velocity and short water residence times in the wetland affected ultimate concentrations and redox potentials measured in stream water exiting the wetland. For example, redox potential measurements in stream water exiting the wetland ($\sim$+20 mV) were generally higher than expected for CH_4-producing environments, possibly indicating that stream flow rates were too high to accumulate significant dissolved CH_4 and lower redox potentials.

CH_4 fluxes in the high Arctic and future climate
Most CH_4 studies on Arctic landscapes focus on emission sources to the atmosphere, such as peatlands and wetlands, because of their considerable coverage in the low- and sub Arctic, and their important role in global CH_4 budgets (O'Connor *et al.*, 2010, Kirschke *et al.*, 2013). Results from the Lake Hazen watershed suggest that CH_4 consumption, not emission, is the larger, more consistent pattern of F_{CH4} in the high Arctic because of limited wetland and pond coverage (Lehner and Döll, 2004). The CH_4 consumption rates at Lake Hazen and other

locations across the high Arctic (Flessa *et al.*, 2008; Lamb *et al.*, 2011) suggest that this region cannot be overlooked as an important consumer of atmospheric CH_4. For example, within Quttinirpaaq National Park, approximately 99% of the plant-habitable zone in the Park (22,672 km^2) is considered to have moderate- to well-drained soils (Edlund, 1994) compared to only 1% classified as saturated or poorly-drained soils. Considering the extensive area of dry, upland landscapes in the broader high Arctic, substantially more CH_4 measurements on dry soils are required to support more robust Arctic CH_4 models.

Future changes in soil temperature and moisture (ACIA, 2005) are expected to have landscape-level effects in the Arctic, with some models predicting 18% of polar desert regions being replaced with southern tundra species by 2080, relative to 1960 (Sitch *et al.*, 2003). Results from our contrasting high Arctic landscapes suggest that soil moisture, soil temperature, and substrate quantity are key factors determining the magnitude and direction of F_{CH4} for these landscapes. However future changes within each ecosystem will likely result in different F_{CH4} responses. Polar desert soils are mostly well-drained mineral soils with pockets of cryoturbated organic matter (Tarnocai *et al.*, 2001). We found that CH_4 consumption rates were affected by soil temperature, but not vegetation cover. Therefore, we may expect that warming temperatures and longer growing seasons may increase CH_4 consumption rates. Predicted increases in precipitation and permafrost melt water on the landscapes, at least in the short-term, will likely not affect CH_4 consumption rates substantially because of this coarse-textured soil's poor ability to retain water. Until the soils develop greater organic matter content capable of retaining more water (to the point of limiting diffusivity), these soils should continue to consume CH_4 in a warmer and wetter climate. In the wetland, our EC measurements and mass budget analysis indicated that CH_4 emission rates to the atmosphere were very low. Although warming air temperatures and permafrost thaw should support methanogenic activity in the future, until substantial organic carbon accumulation occurs in this system, methanogenesis and thus CH_4 emission to the atmosphere will likely continue to be limited in poorly-draining soils in the Lake Hazen watershed. The rate at which landscapes can change is an important unknown for the future cycling of GHGs at this high latitude.

References

ACIA: Arctic Climate Impact Assessment – Scientific Report, 1st edn., Cambridge University Press, New York, 2005.

AMAP: AMAP Assessment Report: Arctic Pollution Issues, Arctic Monitoring and Assessment Programme (AMAP), Oslo, Norway, xii+859 pp., 1998.

AMAP: Arctic Climate Issues 2011: Changes in Arctic Snow,Water, Ice and Permafrost, SWIPA 2011 Overview Report, Arctic Monitoring and Assessment Programme (AMAP), Oslo, xi+97 pp., 2012.

Baldocchi, D. D.: Assessing the eddy covariance technique for evaluating carbon dioxide exchange rates of ecosystems: past, present and future, Glob. Change Biol., 9, 479–492, 2003.

Benstead, J. and King, G. M.: Response of methanotrophic activity in forest soil to methane availability, FEMS Microbiol. Ecol., 23, 333–340, 1997.

Christensen, T. R., Jonasson, S., Callaghan, T. V., and Havstrom, M.: Spatial variation in high latitude methane flux along a transect across Siberian and European Tundra environments, J. Geophys. Res.-Atmos., 100, 21035–21045, 1995.

Christensen, T. R., Jonasson, S., Callaghan, T. V., Havstrom, M., and Livens, F. R.: Carbon cycling and methane exchange in Eurasian tundra ecosystems, Ambio, 28, 239–244, 1999.

Christensen, T. R., Friborg, T., Sommerkorn, M., Kaplan, J., Illeris, L., Soegaard, H., Nordstroem, C., and Jonasson, S.: Trace gas exchange in a high-arctic valley, 1. Variations in CO_2 and CH_4 flux between tundra vegetation types, Global Biogeochem. Cy., 14, 701–713, 2000.

Dinsmore, K. J., Billett, M. F., Skiba, U. M., Rees, R. M., Drewer, J., and Helfter, C.: Role of the aquatic pathway in the carbon and greenhouse gas budgets of a peatland catchment, Glob. Change Biol., 16, 2750–2762, 2010.

Edlund, S. A.: Vegetation, in: Resource Description and Analysis – Ellesmere Island National Park Reserve, Natural Resource Conservation Section, Prairie and Northern Region, Parks Canada, Department of Canadian Heritage, Winnipeg, Canada, 55 pp., 1994.

Flessa, H., Rodionov, A., Guggenberger, G., Fuchs, H., Magdon, P., Shibistova, O., Zrazhevskaya, G., Mikheyeva, N., Kasansky, O. A., and Blodau, C: Landscape controls of CH_4 fluxes in a catchment of the forest tundra ecotone in northern Siberia, Glob. Change Biol., 14, 2040–2056, 2008.

France, R. L.: The Lake Hazen trough – a late winter oasis in a Polar Desert, Biol. Conserv., 63, 149–151, 1993.

Friborg, T., Christensen, T. R., and Sogaard, H.: Rapid response of greenhouse gas emission to early spring thaw in a subarctic mire as shown by micrometeorological techniques, Geophys. Res. Lett., 24, 3061–3064, 1997.

Friborg, T., Christensen, T. R., Hansen, B. U., Nordstroem, C., and Soegaard, H.: Trace gas exchange in a high-arctic valley, 2. Landscape CH_4 fluxes measured and modeled using Eddy correlation data, Global Biogeochem. Cy., 14, 715–723, 2000.

Froese, D. G., Westgate, J. A., Reyes, A. V., Enkin, R. J., and Preece, S. J.: Ancient permafrost and a future, warmer arctic, Science, 321, 1648–1648, 2008.

Heikkinen, J. E. P., Elsakov, V., and Martikainen, P. J.: Carbon dioxide and methane dynamics and annual carbon balance in tundra wetland in NE Europe, Russia, Global Biogeochem. Cy., 16, 1115, doi:10.1029/2002GB001930, 2002.

Humphreys, E. R. and Lafleur, P. M.: Does earlier snowmelt lead to greater CO2 sequestration in two low Arctic tundra ecosystems?, Geophys. Res. Lett., 38, L09703, doi:10.1029/2011GL047339, 2011.

Ibrom, A., Dellwik, E., Flyvbjerg, H., Jensen, N. O., and Pilegaard, K.: Strong low-pass filtering effects on water vapour flux measurements with closed-path eddy correlation systems, Agr. Forest Meteorol., 147, 140–156, 2007.

King, G. M.: Responses of atmospheric methane consumption by soils to global climate change, Glob. Change Biol., 3, 351–362, 1997.

Kirschke, S, Bousquet, P., Ciais, P., Saunois, M., Canadell, J. G., Dlugokencky, E. J., Bergamaschi, P., Bergmann, D., Blake, D. R., Bruhwiler, L., Cameron-Smith, P., Castaldi, S., Chevallier, F., Feng, L., Fraser, A., Heimann, M., Hodson, E. L., Houweling, S., Josse, B., Fraser, P.J., Krummel, P. B., Lamarque, J.-F., Langenfeld, R. L., Le Quéré, C., Naik, V., O'Doherty, S., Palmer, P. I., Pison, I., Plummer, D., Poulter, B., Prinn, R. G., Rigby, M., Ringeval, B., Santini, M., Schmidt, M., Shindell, D. T., Simpson, I. J., Spahni, R., Steele, L. P., Strode, S. A., Sudo, K., Szopa, S., van der Werf, J. R., Voulgarakis, A., van Weele, M., Weiss, R. F., Williams, J. E., and Zeng, G.: Three decades of global methane sources and sinks, Nat. Geosci., 6, 813–823, 2013.

Kling, G. W., Kipphut, G. W., and Miller, M. C.: Arctic lakes and streams as gas conduits to the atmosphere – implications for Tundra carbon budgets, Science, 251, 298–301, 1991.

Kljun, N., Calanca, P., Rotach, M. W., and Schmid, H.P. A simple parameterisation for flux footprint predictions, Boundary-Layer Meteorology, 112, 503-523, 2004.

Kort, E. A., Wofsy, S. C., Daube, B. C., Diao, M., Elkins, J. W., Gao, R. S., Hintsa, E. J., Hurst, D.F., Jimenez, R., Moore, F. L., Spackman, J. R., and Zondlo, M. A.: Atmospheric observations of Arctic Ocean methane emissions up to 82º North, Nat. Geosci., 5, 318–321, 2012.

Kutzbach, L., Schneider, J., Sachs, T., Giebels, M., Nykanen, H., Shurpali, N.J., Martikainen, P.J., Alm, J., and Wilmking, M.: CO2 flux determination by closed-chamber methods can be seriously biased by inappropriate application of liner regression, Biogeosciences, 4, 1005-1025, 2007.

Lafleur, P. M., Humphreys, E. R., St Louis, V. L., Myklebust, M. C., Papakyriakou, T., Poissant, L., Barker, J. D., Pilote, M., and Swystun, K. A.: Variation in peak growing season net ecosystem production across the Canadian Arctic, Environ. Sci. Technol., 46, 7971–7977, 2012.

Lamb, E. G., Han, S., Lanoil, B. D., Henry, G. H. R., Brummell, M. E., Banerjee, S., and Siciliano, S. D.: A high Arctic soil ecosystem resists long-term environmental manipulations, Glob. Change Biol., 17, 3187–3194, 2011.

Lehner, B. and Doll, P.: Development and validation of a global database of lakes, reservoirs and wetlands, J. Hydrol., 296, 1–22, 2004.

LI-COR Biosciences: LI-7700 Open Path CH4 Analyzer Instruction Manual (v.2; 984-10751), Lincoln, USA, 2011.

Lipson, D.A., Zona, D., Raab, T.K., Bozzolo, F., Mauritz, M., and Oechel, W.C. Water-table height and microtopography control biogeochemical cycling in an Arctic coastal tundra ecosystem. Biogeosciences, 9, 577-591, 2012.

Manabe, S. and Stouffer, R. J.: Multiple-century response of a coupled ocean-atmosphere model to an increase of atmospheric carbon-dioxide, J. Climate, 7, 5–23, 1994.

Mastepanov, M., Sigsgaard, C., Dlugokencky, E.J., Houweling, S., Strom, L., Tamstorf, M.P., Christensen, T.R.: Large tundra methane burst during onset of freezing, Nature, 456, 628-631, 2008.

Mastepanov, M., Sigsgaard, C., Tagesson, T., Strom, L., Tamstorf, M.P., Lund, M., Christensen, T.R.: Revisiting factors controlling methane emissions from high-Arctic tundra, Biogeosciences, 10, 5139-5158, 2013.

Mauder, M. and Foken, T.: Impact of post-field data processing on eddy covariance flux estimates and energy balance closure, Meteorol. Z., 15, 597–609, 2006.

McDermitt, D., Burba, G., Xu, L., Anderson, T., Komissarov, A., Riensche, B., Schedlbauer, J., Starr, G., Zona, D., Oechel, W., Oberbauer, S., and Hastings, S.: A new low-power, open path instrument for measuring methane flux by eddy covariance, Appl. Phys. B-Lasers O., 102, 391–405, 2011.

Moosavi, S. C. and Crill, P. M.: Controls on CH4 and CO2 emissions along two moisture gradients in the Canadian boreal zone, J. Geophys. Res.-Atmos., 102, 29261–29277, 1997.

Moosavi, S. C. and Crill, P. M.: CH4 oxidation by tundra wetlands as measured by a selective inhibitor technique, J. Geophys. Res.-Atmos., 103, 29093–29106, 1998.

Nakano, T., Kuniyoshi, S., and Fukuda, M.: Temporal variation in methane emission from tundra wetlands in a permafrost area, northeastern Siberia, Atmos. Environ., 34, 1205–1213, 2000.

O'Connor, F. M., Boucher, O., Gedney, N., Jones, C. D., Folberth, G. A., Coppell, R., Friedling stein, P., Collins, W. J., Chappellaz, J., Ridley, J., and Johnson, C. E.: Possible role of wetlands, permafrost, and methane hydrates in the methane cycle under future climate change: a review, Rev. Geophys., 48, 2010RG000326, doi:10.1029/2010RG000326, 2010.

Olefeldt, D., Turetsky, M. R., Crill, P. M., and McGuire, A. D.: Environmental and physical controls on northern terrestrial methane emissions across permafrost zones, Glob. Change Biol., 19, 589–603, 2013.

Overland, J. E., Wang, M., Walsh, J. E., Christensen, J. H., Kattsov, V. M., and Chapman, W. L.: Climate model projections for the Arctic. In: Snow, water, ice and permafrost in the Arctic (SWIPA): climate change and the cryosphere, Arctic Monitoring and Assessment Programme (AMAP), Oslo, 18 pp., 2011.

Parmentier, F. J. W., van Huissteden, J., van der Molen, M. K., Schaepman-Strub, G., Karsanaev, S. A., Maximov, T. C., and Dolman, A. J.: Spatial and temporal dynamics in eddy covariance observations of methane fluxes at a tundra site in northeastern Siberia, J. Geophys. Res.-Biogeo., 116, G03016, doi:10.1029/2010JG001637, 2011.

Peterson, B. J., Holmes, R. M., McClelland, J. W., Vorosmarty, C. J., Lammers, R. B., Shiklomanov, A. I., Shiklomanov, I. A., and Rahmstorf, S.: Increasing river discharge to the Arctic Ocean, Science, 298, 2171–2173, 2002.

Pfeffer, W. T., Harper, J. T., and O'Neel, S.: Kinematic constraints on glacier contributions to 21st-century sea-level rise, Science, 321, 1340–1343, 2008.

Roulet, N. T., Jano, A., Kelly, C. A., Klinger, L. F., Moore, T. R., Protz, R., Ritter, J. A., and Rouse, W. R.: Role of the Hudson-Bay lowland as a source of atmospheric methane, J. Geophys. Res.-Atmos., 99, 1439–1454, 1994.

Sitch, S., Smith, B., Prentice, I. C., Arneth, A., Bondeau, A., Cramer,W., Kaplan, J. O., Levis, S., Lucht, W., Sykes, M. T., Thonicke, K., and Venevsky, S.: Evaluation of ecosystem dynamics, plant geography and terrestrial carbon cycling in the LPJ dynamic global vegetation model, Glob. Change Biol., 9, 161–185, 2003.

Smith, K. A., Dobbie, K. E., Ball, B. C., Bakken, L. R., Sitaula, B. K., Hansen, S., Brumme, R., Borken, W., Christensen, S., Priemé, A., Fowler, D., Macdonald, J.A., Skiba, U., Klemedtsson, L., Kasimir-Klemedtsson, A., Degórska, A., and Orlanski, P.: Oxidation of atmospheric methane in northern European soils, comparison with other ecosystems, and uncertainties in the global terrestrial sink, Glob. Change Biol., 6, 791–803, 2000.

Ström, L., Ekberg, A., Mastepanov, M., and Christensen, T. R.: The effect of vascular plants on carbon turnover and methane emissions from a tundra wetland, Glob. Change Biol., 9, 1185–1192, 2003.

Ström, L., Tagesson, T., Mastepanov, M., and Christensen, T. R.: Presence of Eriophorum scheuchzeri enhances substrate availability and methane emission in an Arctic wetland, Soil Biol. Biochem., 45, 61–70, 2012.

Tagesson, T., Molder, M., Mastepanov, M., Sigsgaard, C., Tamstorf, M. P., Lund, M., Falk, J. M., Lindroth, A., Christensen, T. R., and Strom, L.: Land-atmosphere exchange of methane from soil thawing to soil freezing in a high-Arctic wet tundra ecosystem, Glob. Change Biol., 18, 1928–1940, 2012.

Tarnocai, C., Gould, J., Broll, G., and Achuff, P.: Ecosystem and trafficability monitoring for Quttinirpaaq National Park (11-year evaluation), Research branch, Agriculature and Agri-Food Canada, Ottawa, Canada, 169 pp., 2001.

Thompson, B.: Climate, in: Resource Description and Analysis – Ellesmere Island National Park Reserve, Natural Resource Conservation Section, Prairie and Northern Region, Parks Canada, Department of Canadian Heritage, Winnipeg, Canada, 78 pp., 1994.

Updegraff, K., Pastor, J., Bridgham, S. D., and Johnston, C. A.: Environmental and substrate controls over carbon and nitrogen mineralization in northern wetlands, Ecol. Appl., 5, 151–163, 1995.

van Huissteden, J., Maximov, T. C., and Dolman, A. J.: High methane flux from an arctic floodplain (Indigirka lowlands, eastern Siberia), J. Geophys. Res.-Biogeo., 110, G02002, doi:10.1029/2005JG000010, 2005.

Wadham, J. L., Arndt, S., Tulaczyk, S., Stibal, M., Tranter, M., Telling, J., Lis, G. P., Lawson, E., Ridgwell, A., Dubnick, A., Sharp, M. J., Anesio, A. M., and Butler, C. E. H.: Potential methane reservoirs beneath Antarctica, Nature, 488, 633–637, 2012.

Walker, D. A., Raynolds, M. K., Daniels, F. J. A., Einarsson, E., Elvebakk, A., Gould, W. A., Katenin, A. E., Kholod, S. S., Markon, C. J., Melnikov, E. S., Moskalenko, N. G., Talbot, S. S., and Yurtsev, B. A.: The Circumpolar Arctic vegetation map, J. Veg. Sci., 16, 267–282, 2005.

Walker, M. D., Wahren, C. H., Hollister, R. D., Henry, G. H. R., Ahlquist, L. E., Alatalo, J. M., Bret-Harte, M. S., Calef, M. P., Callaghan, T. V., Carrol, A. B., Epstein, H. E., Jonsdottir, I. S., Klein, J. A., Magnusson, B., Molau, U., Oberbauer, S. F., Rewa, S. P., Robinson, C. H., Shaver, G. R., Suding, K. N., Thompson, C. C., Tolvanen, A., Totland, O., Turner, P. L.,

Tweedie, C. E., Webber, P. J., and Wookey, P. A.: Plant community responses to experimental warming across the tundra biome, P. Natl. Acad. Sci. USA, 103, 1342–1346, 2006.

Webb, E. K., Pearman, G. I., and Leuning, R.: Correction of flux measurements for density effects due to heat and water-vapor transfer, Q. J. Roy. Meteor. Soc., 106, 85–100, 1980.

Whalen, S. C. and Reeburgh, W. S.: Consumption of atmospheric methane by Tundra soils, Nature, 346, 160–162, 1990.

Whalen, S. C. and Reeburgh, W. S.: Moisture and temperature sensitivity of CH4 oxidation in boreal soils, Soil Biol. Biochem., 28, 1271–1281, 1996.

Wille, C., Kutzbach, L., Sachs, T., Wagner, D., and Pfeiffer, E. M.: Methane emission from Siberian arctic polygonal tundra: Eddy covariance measurements and modeling, Glob. Change Biol., 14, 1395–1408, 2008.

Chapter 4. *The net exchange of carbon greenhouse gases with aquatic systems in a high Arctic watershed and its role in whole-ecosystem carbon transfer*

Introduction

Freshwater ecosystems cover less than 10% of global ice-free land area (Lehner and Doll, 2004) and have been typically overlooked as substantial contributors to, or sinks of, atmospheric carbon greenhouse gases (GHGs; Bastviken *et al.*, 2011). However, recent studies suggest that inland lakes receive and process carbon at magnitudes similar to oceanic uptake and sediment burial, making them important systems within the global carbon cycle (Cole *et al.*, 2007; Battin *et al.*, 2009; Tranvik *et al.*, 2009; Maberly *et al.*, 2013; Raymond *et al.*, 2013). Unimpacted lakes often are net emitters of the GHG carbon dioxide (CO_2) to the atmosphere (Rautio *et al.*, 2011) because they continuously respire allochthounous and autothounous organic carbon (OC) while uptake of CO_2 by autotrophs occurs typically over shorter seasonal periods (Cole *et al.*, 2000; Huttunen *et al.*, 2003; Breton *et al.*, 2009; Bastviken *et al.*, 2011; Callaghan *et al.*, 2012). Many lakes and wetlands are also strong net sources of the powerful GHG methane (CH_4; Breton *et al.*, 2009), perhaps contributing up to 12% of all CH_4 emissions to the atmosphere (Lai, 2009). Saturated soils, lake sediments and even oxic waters can be prime environments for bacterial methanogenesis (Bogard *et al.*, 2014). Further, because of its poor solubility, CH_4 can be efficiently vented to the atmospheric via turbulence and ebullition (Walter *et al.*, 2006).

Lakes, ponds and wetlands are globally most abundant in northern regions largely due to historical periods of glaciation and resulting land deformation. Lakes may cover greater than half of the terrain in portions of northern regions, and can account for more than three-quarters of a landscape's net CO_2 exchange with the atmosphere (Abnizova *et al.*, 2012), depending on in-lake productivity and OC loading from watersheds. Saturated northern landscapes can also be intense emitters of CH_4 because permafrost impedes drainage of soils, promoting anoxia (Tagesson *et al.*, 2012). However, at the highest latitudes of northern regions, landscapes have relatively well-drained soils (Campbell *et al.*, 1992) and experience little precipitation, resulting in often less than 5% of the ice-free landscape being covered by lakes, ponds and wetlands. Though the majority of high Arctic landscapes are comprised of desiccated polar semidesert soils, these

environments do support some plant growth and soil decomposition, however net near-zero exchanges of CO_2 with the atmosphere generally prevail (Soegaard *et al.*, 2000; Lloyd, 2001; Lund *et al.*, 2012; Lafleur *et al.*, 2012). In the rarer wet environments with greater plant growth but temperature-constrained decomposition, net uptake of CO_2 may be comparable to the southern Arctic (Emmerton *et al.*, 2014). Therefore, in this otherwise dry ecoregion, the potential exists for productive ecosystems where there is ample water supply.

However, a rapidly changing high-latitude climate is substantially altering polar watersheds at unprecedented rates (Climate Change, 2007; Emmerton *et al.*, 2014). Some climate models predict that in the Canadian Arctic, autumn and winter temperatures may rise 3-5°C by 2100, but up to 9°C in the high Arctic (~>70°N; ACIA, 2004; Climate Change 2007). Mean annual precipitation is projected to increase ~12% for the Arctic as a whole over the same period, but up to 35% in localized regions where the most warming will occur (Climate Change, 2007). Such warming and wetting is anticipated to greatly alter the energy balance of Arctic landscapes (ACIA, 2004) resulting in glacial melt (Pfeffer *et al.*, 2008), permafrost thaw (Froese *et al.*, 2008), altered hydrological regimes (i.e., drying or wetting; Peterson *et al.*, 2002) and extended growing seasons (Smith *et al.*, 2008). These changes are also expected to perturb watershed carbon cycling through the emergence of labile carbon from thawing or disturbed permafrost, and increases in biological productivity on landscapes and in lakes, ponds and wetlands (Mack *et al.*, 2004; Smol *et al.*, 2005; Walker *et al.*, 2006; Smol *et al.*, 2007). Considering the extensive cover of the polar semidesert (>10^6 km^2) in the high Arctic, these changes may have considerable effects on the future exchange of carbon between watersheds and the atmosphere, and on global carbon feedbacks (Anthony *et al.*, 2014). However, few studies exist that quantify high Arctic aquatic GHG exchange with the atmosphere, investigate possible drivers of this exchange, or compare the relative contributions of GHGs by high Arctic aquatic ecosystems with those of their terrestrial counterparts.

The first objective of our study was to measure the net exchange of CO_2 and CH_4 between common, but distinctly different types of high Arctic aquatic ecosystems and the atmosphere. Our second objective was to better understand the processes underlying the production of CO_2 and CH_4 by investigating how, for example, aqueous concentrations changed

with water chemistry and hydrology. Our final objective was to compare the relative strength of CO_2 and CH_4 exchange of aquatic systems with those from surrounding terrestrial landscapes, to calculate watershed-scale exchange of CO_2 and CH_4 for a typical high Arctic region.

Methods

Site description and sampling overview

We conducted our research at the Lake Hazen base camp in central Quttinirpaaq National Park, Ellesmere Island, Nunavut (81.8º N, 71.4º W), Canada's most northerly protected area. Lake Hazen (area: 545 km^2; max. depth: 267 m) is the world's largest lake by volume north of the Arctic Circle, and is surrounded by a substantial watershed (~8,400 km^2). About 40% of the Lake Hazen watershed is glaciated with the balance of area covered by polar semidesert soils (>90% of ice–free area; Edlund, 1994), meadow wetlands, ponds and small lakes. The lower Lake Hazen watershed is a high Arctic thermal oasis (France, 1993) as it experiences anomalously warm growing season (June–August) conditions because it is protected from cold coastal weather by the Grant Land Mountains and Hazen Plateau. For example, mean July air temperature is typically 8-9 ºC at the camp, compared to July 1981-2010 climate normals of 6.1 ºC and 3.4 ºC at the coastal Eureka and Alert weather stations on Ellesmere Island, respectively (Environment Canada, 2014). These warm conditions, coupled with continuous daylight during the growing season, have resulted in a greater diversity and abundance of vegetation and wildlife in the Lake Hazen watershed compared to surrounding areas, despite receiving only ~95 mm of precipitation annually (France, 1993).

The aquatic environment in the watershed is dominated by ultra-oligotrophic Lake Hazen (Keatley *et al.*, 2007), which receives most of its water annually from rivers discharging seasonal melt water from glaciers. Water exits Lake Hazen via the Ruggles River. Ice-cover can remain on Lake Hazen throughout the growing season, though in recent years the lake has gone ice-free more frequently, usually by late July. As glacial melt accelerates throughout the growing season, the water level of Lake Hazen rises, inundating its shoreline and wetlands and ponds that develop along its margin. Margin wetlands/ponds are often isolated by porous gravel berms when Lake Hazen water levels are low, but become directly connected to Lake Hazen when water levels are high and the berms are breached. Wetlands, ponds and lakes higher up in the watershed receive

their water primarily from snowmelt, permafrost thaw water and/or upstream lake drainage, and typically go ice-free mid-June to early July.

Between 2005 and 2012, we collected, or measured in-situ, surface waters for dissolved CO_2 and CH_4 concentrations and general water chemistry from Lake Hazen, as well as from Skeleton Lake and Pond 01 (Figure 4.1; Table A3.1). Skeleton Lake (area: 2 ha; max depth: 4.2 m) is a typical upland lake flushed in summer by permafrost thaw streams draining surrounding hill slopes before exiting to a meadow wetland valley. Pond 01 (area: 0.1-0.7 ha; max depth: 0.3-1.1 m) is a margin wetland/pond separated from Lake Hazen by a gravel berm. Just after ice-off each year, Pond 01 was in a drier, wetland-like state with extensive sedge growth surrounding two central ponds. By mid to late July, Lake Hazen typically rose sufficiently to seep through the berm causing flooding of the pond, before breaching the berm and extensively flushing the pond's entirety (Figure A3.1). In addition to intensively sampling these three aquatic systems, we periodically collected water from an additional margin wetland/pond (Pond 02) and four ponds further up on the landscape (Ponds 03, 07, 10-12, 16; Table A3.1).

Quantifying concentrations of dissolved CO_2 and CH_4 in surface waters

Two approaches were used to quantify concentrations of dissolved CO_2 and CH_4 in surface waters. The first approach (bottle samples; CO_{2-B}, CH_{4-B}; Hamilton *et al.*, 1994; Kelly *et al.*, 1997) was used at all sites and involved water collection directly into evacuated 160-mL Wheaton glass serum bottles capped with butyl rubber stoppers. Each bottle contained 8.9 g of potassium chloride (KCl) preservative and backfilled with 10 mL of ultra high purity dinitrogen (N_2) gas headspace. To collect a sample, bottles were submersed ~5 cm below the water surface and punctured with an 18-gauge needle. All samples were collected while standing on the shoreline of the aquatic system. In situ barometric pressure and water temperature were recorded. Dissolved gas samples were stored in the dark at ~5°C for up to 5 weeks until return to the University of Alberta, where they were analyzed in the accredited Biogeochemical Analytical Service Laboratory (BASL). At the BASL, samples were placed in a wrist-action shaker for 20 minutes to equilibrate dissolved CO_2 and CH_4 with the N_2 headspace. Headspace CO_2 and CH_4 concentrations were quantified on a Varian 3800 gas chromatograph (GC) using a flame ionization detector at 250°C with ultra high purity hydrogen (H_2) as a carrier gas passing through
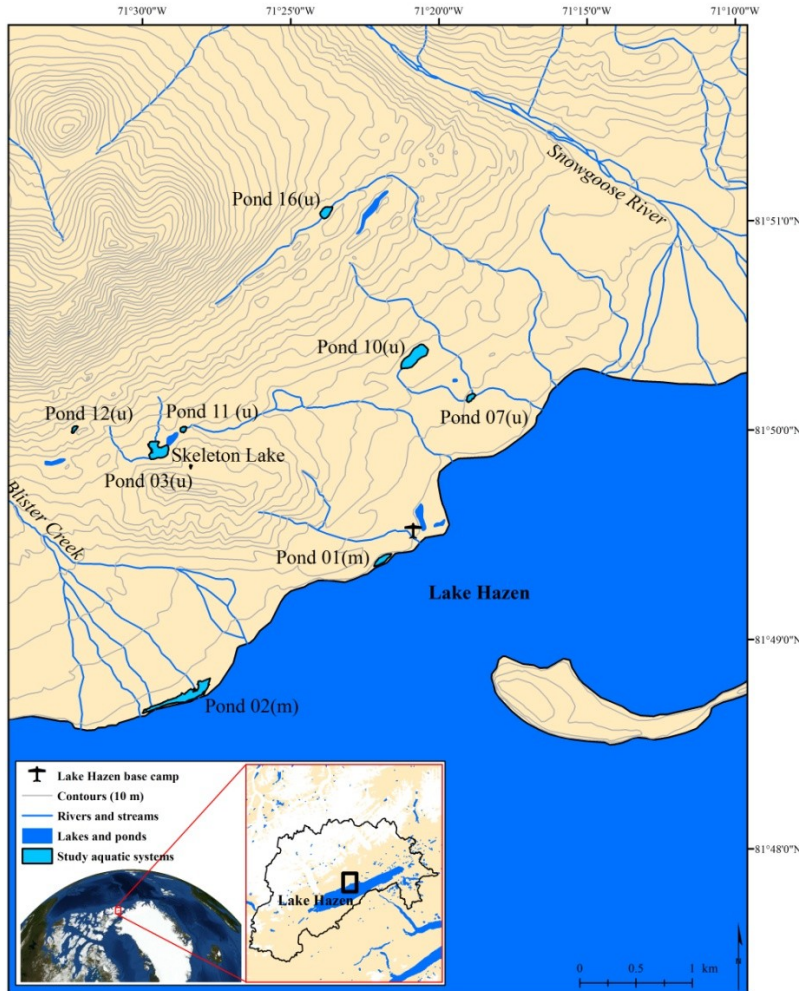
Figure 4.1 Lake Hazen camp in Quttinirpaaq National Park, Nunavut, Canada. Upland (u) and margin (m) study wetlands, ponds and lakes are indicated. Shown inset are the general locator and Lake Hazen watershed.

a hayesep D column at 80°C. A ruthenium methanizer converted CO_2 to CH_4. Four gas standards (Praxair, Linde-Union Carbide), ranging from 75 to 6000 ppm for both CO_2 and CH_4, were used to calibrate the GC. A Varian Star Workstation program integrated peak areas and standardcalibration curves with an $r^2 > 0.99$ were accepted for analyses. A standard was re-analyzed every 10 samples to reconfirm the GC calibration and duplicate injections were performed on all samples. Headspace CO_2 and CH_4 concentrations were converted to dissolved molar concentrations using Henry's Law, corrected for temperature and barometric pressure differences between sample collection and analyses. To quantify total dissolved inorganic carbon (DIC), samples were acidified with 0.5 mL H_3PO_4 to convert all DIC to CO_2, and then immediately reanalyzed on the GC. DIC concentrations were then calculated as above.

The second approach (automated system; $CO_{2\text{-AS}}$) was used to determine detailed diel

changes in dissolved surface water CO_2 concentrations at two of our sites (Skeleton Lake and Pond 01). We deployed automated systems that quantified in-situ dissolved CO_2 concentrations every three hours in conjunction with our bottle sampling at those sites (Table A3.1). These systems functioned by equilibrating, over a 20-minute period, dissolved CO_2 from pumped surface waters with a gas cell in a Celgard MiniModule Liqui-Cel. The equilibrated gas in the cell was then analysed for CO_2 concentration with a LI-COR 820 infrared gas analyzer. We also measured dissolved oxygen (O_2) concentrations with a Qubit flow-through sensor. Concentrations were then converted to aqueous molar concentrations using Henry's Law and water temperature quantified with a CS 107-L thermistor. The systems were in watertight cases, upon which was mounted a CS 014A anemometer (1 m height) and Kipp and Zonen photosynthetically-active radiation (PAR) LITE quantum sensor. All data were recorded on Campbell Scientific CR10X dataloggers.

Quantifying net diffusive CO_2 and CH_4 fluxes with the atmosphere

We used the stagnant film model described by Liss and Slater (1974) to quantify net CO_2 and CH_4 mass fluxes between surface waters and the atmosphere. The stagnant film model assumes gas concentrations in both surface waters and the atmosphere are well-mixed, and that gas transfer between the phases occurs via diffusion across a diminutive stagnant boundary layer. Diffusive gas transfer across the boundary layer is assumed to follow Fick's First Law:

$$\text{Gas flux } (\mu\text{mol m}^{-2}\text{ hr}^{-1}) = k\ (C_{SUR} - C_{EQL}) \tag{1}$$

where C_{SUR} (μmol L^{-1}) is the concentration of the gas in surface waters, C_{EQL} (μmol L^{-1}) is the atmospheric equilibrium concentration, and k is the gas exchange coefficient, or the depth of water per unit time in which the concentration of the gas equalizes with the atmosphere (i.e., piston velocity). We used measured dissolved CO_2 and CH_4 concentrations and Equation 1 to quantify gas exchange between surface waters and the atmosphere. Values of k (cm hr^{-1}) were calculated using wind speed and published empirical relationships (Hamilton *et al.*, 1994; Table A3.2). To determine the direction of the flux, atmospheric equilibrium CO_2 and CH_4 concentrations were quantified using Henry's law, in-situ barometric pressure and air temperature, and mean CO_2 and CH_4 mixing ratios in the atmosphere during the year of sampling. If dissolved CO_2 and CH_4 concentrations in surface waters were above or below their

corresponding calculated atmospheric equilibrium concentrations, the aquatic systems were considered a source or sink relative to the atmosphere, respectively.

Ebullition fluxes of CO_2 and CH_4 can also liberate from aquatic systems. We used floating inverted 30-cm plastic funnels with a bubble collection chamber to trap ebullition releases of CO_2 and CH_4 at the surface of Skeleton Lake and Pond 01. Traps were deployed continuously at both sites during the 2007 and 2008 summers and checked weekly for bubble volume accumulation. Ebullition volume was measured by drawing into a syringe, through a rubber septum in the collection chamber, the accumulated gas. However, we did not measure gas concentrations in this trapped gas because CO_2 and CH_4 can diffuse back into surface waters while sitting in the trap. Instead, fresh bubbles were collected for CO_2 and CH_4 analyses by probing the sediments and collecting them into a hand held bubble trap. Samples were then immediately transferred to evacuated, stoppered 30 ml Wheaton bottles and analyzed for CO_2 and CH_4 concentrations on the GC in a manner similar to that described above for water samples. Bubble CO_2 and CH_4 concentrations were multiplied by bubble volume collected over the weeklong period to determine ebullition fluxes.

Other physical and chemical measurements

At the same depth and location as GHG samples, we measured or collected water for general biogeochemical analyses at selected aquatic systems and frequencies (Table A3.1). At each site, temperature, pH, specific conductivity and dissolved O_2 were measured in-situ using a YSI 556 MPS multi-probe. Water samples were also collected for general chemical analyses (total dissolved nitrogen [N], particulate N, NO_3^-/NO_2^-, NH_4^+, total phosphorus [P], total dissolved P, alkalinity, dissolved organic carbon [DOC], total dissolved solids, major cations/anions, chlorophyll-*a*) into pre-cleaned HDPE bottles, immediately processed in the Lake Hazen/Quttinirpaaq Field Laboratory clean room after water collection, and stored in the dark at ~5ºC until analyzed at the BASL.

Results and Discussion

Concentrations and diffusive fluxes of dissolved CO_2 and CH_4 in surface waters

Lake Hazen - The near atmospheric equilibrium concentrations of dissolved CO_2 (daily mean of all CO_{2-B} samples: 20.1 ± 0.6 μmol L^{-1}) and CH_4 (daily mean CH_{4-B}: 0.059 ± 0.014 μmol L^{-1}) in Lake Hazen (Figure 4.2) were typical of deep lakes with extremely low nutrient, organic matter and chlorophyll-*a* (0.20 μg L^{-1}) concentrations (Keatley *et al.*, 2007; Babaluk *et al.*, 2009). CO_2 concentrations across all years were related strongly and positively with DIC, HCO_3^-, major ions and wind speed (Table A3.3, A3.4), suggesting supply and dissociation of carbonate material, as well as wind mixing, were important factors contributing to Lake Hazen surface water CO_2 concentrations, rather than primary productivity or heterotrophic decomposition. The former was supported by a positive and strong relationship between Lake Hazen water levels (Water Survey of Canada, 2015) and DIC and TDS concentrations (Figure A3.2), suggesting that inflowing glacial rivers were a source of carbonate to Lake Hazen, contributing to increasing CO_2 concentrations. After standardizing to a common time period across years when samples existed (July 6-20), there were only minor significant differences in CO_2 concentration between years which followed closely with the availability of dissolved ions (Table 4.1; Figure 4.3). Driven by near-equilibrium concentrations, only rare storm events and relatively consistent water temperatures, diffusive fluxes of CO_2 from Lake Hazen were also stable and near zero throughout the season (daily mean CO_{2-B}: -12.1 ± 4.1 mg C m^{-2} d^{-1}). An exception was during a storm event in mid-July 2010, which showed strong CO_2 uptake (Figure 4.3, A3.3), which was possibly from mixing of the water column and exposure of very low CO_2 concentration water at the surface (Figure 4.2). CH_4 concentrations in Lake Hazen within and between all years were very low (Table 4.1; Figure 4.2, 4.3) and changed closely with wind speed (Table A3.3, A3.4), highlighting the poor solubility of CH_4 in water and release to the atmosphere with turbulence. However, mostly because CH_4 concentrations were low along the sandy shoreline of the sampling site, Lake Hazen was a very weak source of CH_4 to the atmosphere (daily mean CH_{4-B}: 0.19 ± 0.05 mg C m^{-2} d^{-1}).
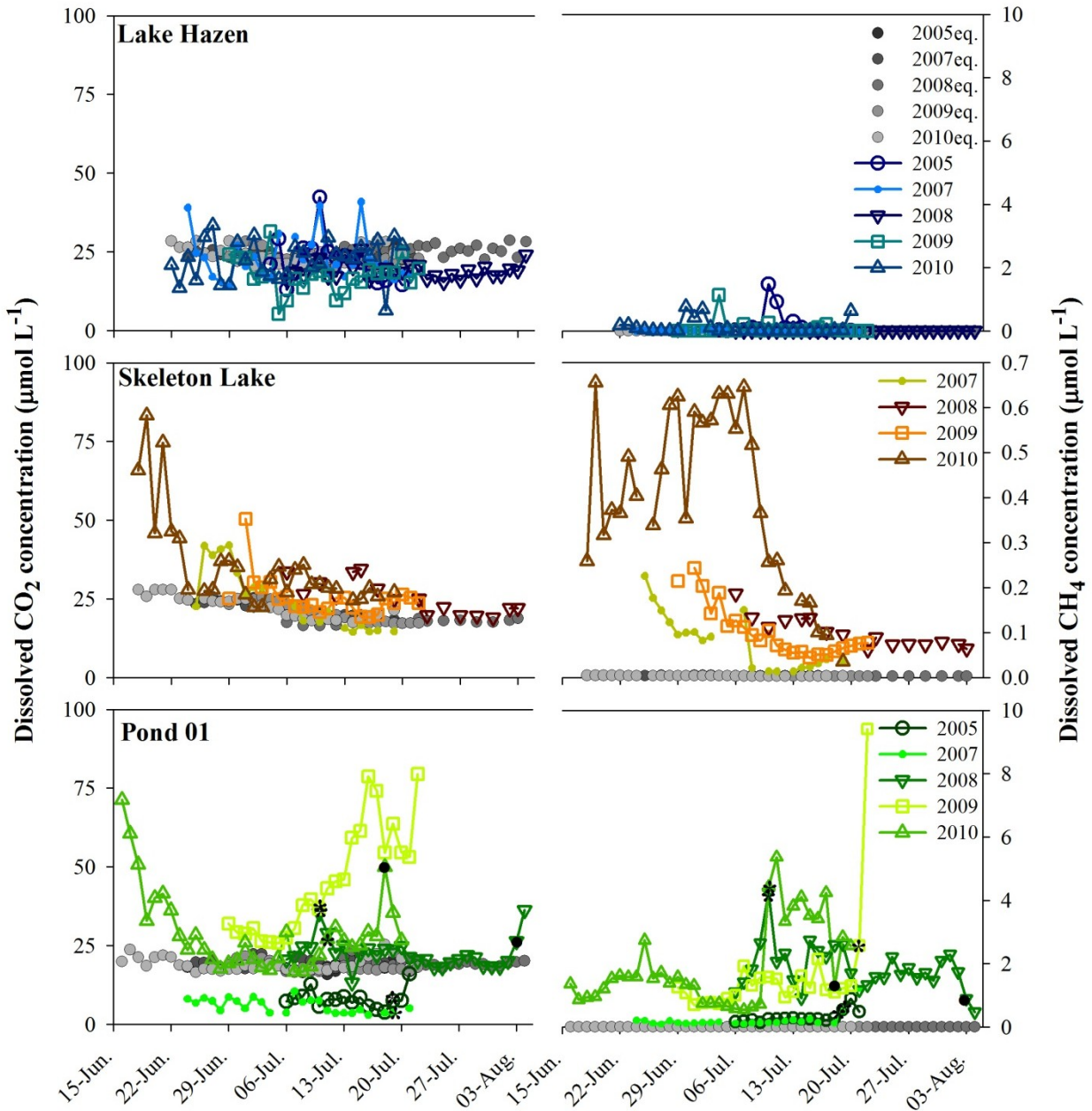
Figure 4.2 Dissolved carbon dioxide (CO_2) and methane (CH_4) concentrations during the 2005-10 growing seasons (June-August) at an upland lake (Skeleton Lake), margin wetland/pond (Pond 01) and large ultra-oligrotrophic great lake (Lake Hazen) in a high Arctic watershed. Asterisk (*) indicates general beginning of seepage to Pond 01 by Lake Hazen, and a dot (●) indicates full flushing of Pond 01 by Lake Hazen.

Table 4.1 Mean (±SE) carbon dioxide (CO_2) and methane (CH_4) concentrations and fluxes measured by bottle (B) and automated system (AS) methods from three lake types in the Lake Hazen watershed, standardized for the period July 6-20 in 2005 and 2007-10. For all the data, please see Figure 4.2.

	Lake Hazen		Skeleton Lake			Pond 01		
	CO_{2-B}	CH_{4-B}	CO_{2-B}	CO_{2-AS}	CH_{4-B}	CO_{2-B}	CO_{2-AS}	CH_{4-B}
µmol L^{-1}								
2005	21.5±1.9	0.21±0.11	-	-	-	7.5±0.5	-	0.30±0.05
2007	24.0±2.1	0.00±0.00	17.1±0.9	-	0.04±0.01	5.1±0.6	4.5±0.2	0.18±0.03
2008	19.6±0.8	0.00±0.00	29.7±1.4	32.7±0.7	0.13±0.01	23.8±1.2	23.0±0.7	2.15±0.21
2009	16.4±1.0	0.07±0.02	22.9±0.6	22.3±0.6	0.07±0.01	50.2±3.9	38.9±3.8	1.38±0.09
2010	23.5±1.5	0.05±0.04	28.7±1.0	30.4±1.0	0.28±0.06	27.1±2.1	27.8±0.9	2.75±0.42
Mean	21.0±0.7	0.07±0.03	24.3±0.8	28.2±0.4	0.13±0.02	23.2±2.1	21.3±1.4	1.38±0.15
mg C m^{-2} d^{-1}								
2005	4±8	0.6±0.3	-	-	-	-45±9	-	1.1±0.2
2007	24±20	0.0±0.0	-22±8	-	0.7±0.5	-155±48	-137±38	1.7±0.5
2008	-19±5	0.0±0.0	41±12	112±24	0.4±0.1	50±23	37±16	17.6±5.6
2009	-12±2	0.1±0.0	14±3	30±10	0.3±0.1	88±14	110±24	3.8±0.4
2010	-50±44	0.2±0.1	161±52	210±41	3.9±1.4	97±35	80±29	35.8±17.1
Mean	-11±10	0.2±0.1	50±17	113±15	1.4±0.5	11±16	-13±25	12.3±3.9

The lake's CO_2 concentrations (daily mean CO_{2-B}: 29.8±2.0 µmol L^{-1}; daily mean CO_{2-AS}: 26.3±0.8 µmol L^{-1}) were mostly above atmospheric equilibrium, with close agreement between bottle and automated system approaches (Table 4.1; Figure A3.4). This suggested that midday bottle sampling was suitable for quantifying integrated mean daily CO_2 concentrations in the lake. CH_4 concentrations in Skeleton Lake were relatively low, but higher, than in Lake Hazen (daily mean CH_{4-B}: 0.195±0.021 µmol L^{-1}). Both CO_2 and CH_4 concentrations correlated closely together during the earlier portion of summers (Table A3.3, A3.4), progressing from higher to lower concentrations as ice cover retreated (Figure 4.2). This trend was consistent with many ice-covered lakes where there is a build-up of heterotrophic metabolism by-products in the water over winter before venting to the atmosphere upon loss of ice cover (Kling *et al.,* 1992; Karlsson *et al.*, 2013). During mid-summer after accumulated gases vented, CO_2 and CH_4 concentrations were lower and showed some variability (Figure 4.2). Diurnal trends measured by the automated system (Figure 4.54) showed that CO_2 and O_2 concentrations associated positively together, rather than negatively, as would be expected if planktonic primary productivity was important. This suggested that CO_2 and O_2 concentrations were mostly affected by temperature-related solubility changes (Figure 4.4). Alternatively, the predominance of benthic vegetation growth
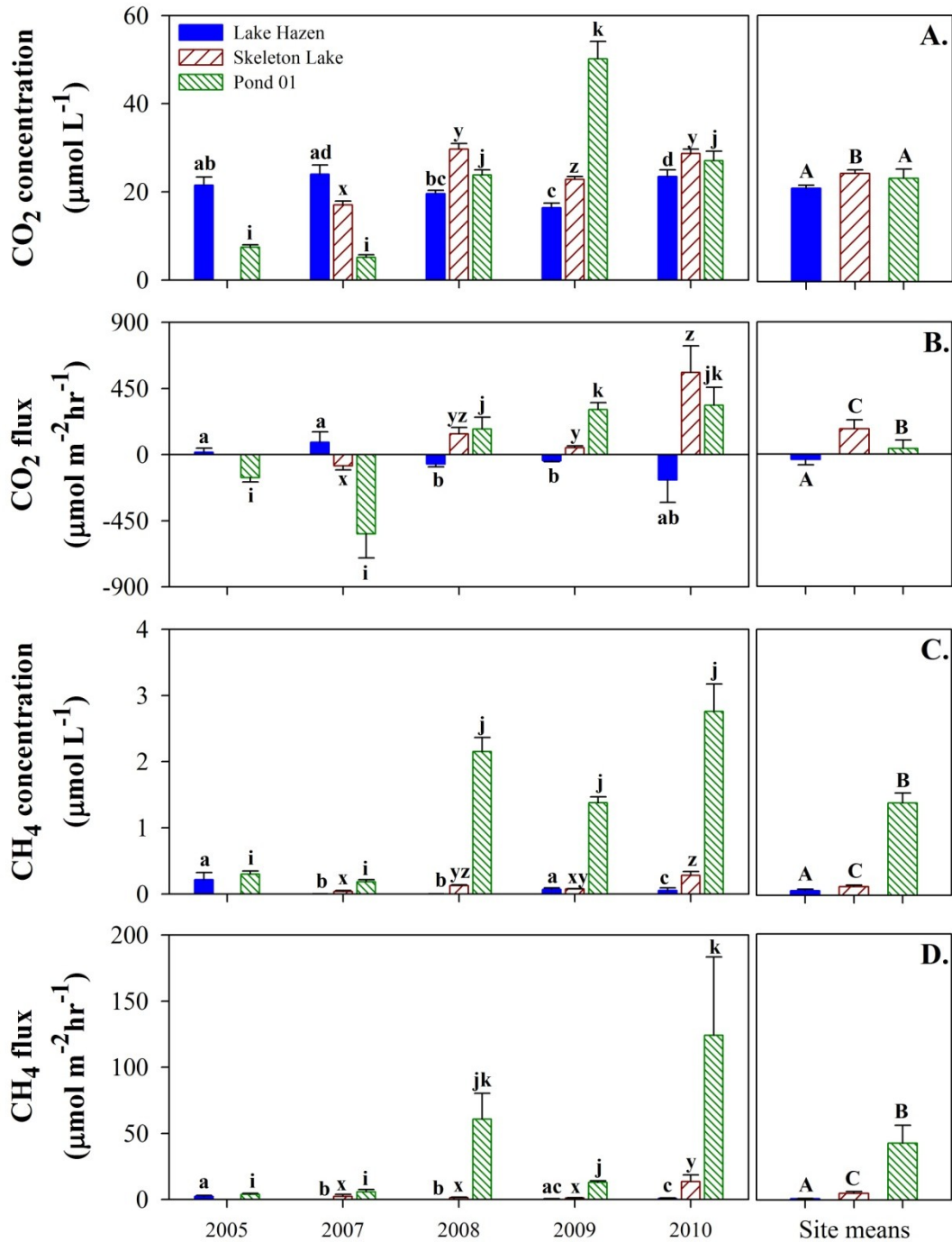
Figure 4.3 Mean (±SE) dissolved carbon dioxide (CO_2) and methane (CH_4) concentrations and fluxes during the 2005-10 growing seasons (July 6-20) at an upland lake (Skeleton Lake), margin wetland/pond (Pond 01) and large ultra-oligrotrophic lake (Lake Hazen) in a high Arctic watershed. Letters denote statistical differences between years at each site (one-way ANOVA).

and midday maximums of chlorophyll-*a* concentration may have meant that productivity did impact CO_2 and O_2 concentrations, but was affected by mixing and stratification in the lake. However, despite diurnal tendencies, seasonal changes in CO_2 associated strongest and positively with changes in CH_4 concentration. This suggested that heterotrophic activity, which may release both CO_2 and CH_4 (especially from sediments), was a strong influence on the net
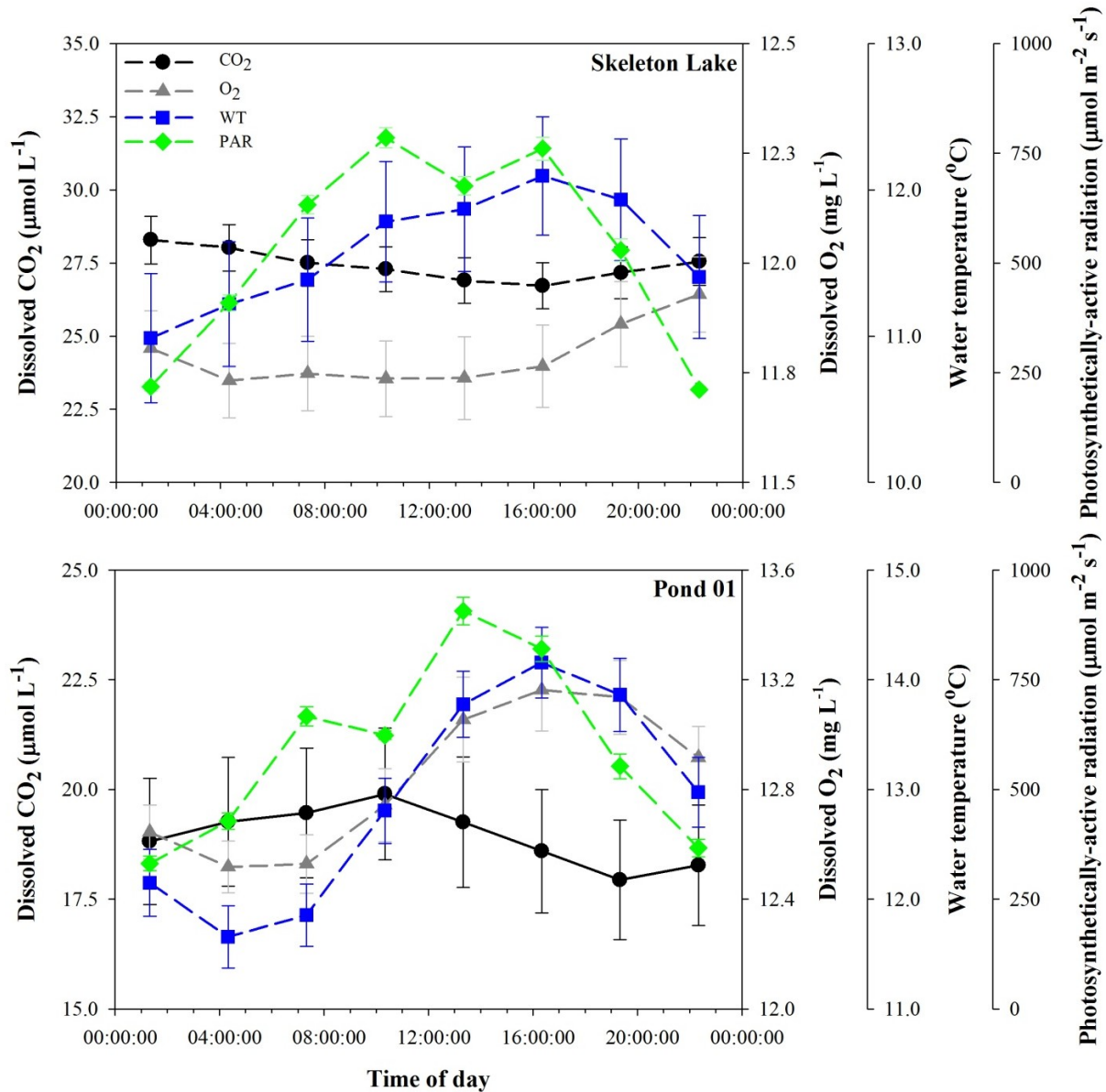
Figure 4.4 Three-hour diurnal dissolved CO_2, O_2, water temperature and PAR data measured by automated systems deployed at the shorelines of Skeleton Lake (2008-10) and Pond 01 (2007-10) during the growing season.

CO_2 exchange from the lake, compared to autotrophy (Table A3.4).This resulted in Skeleton Lake being a net emitter of CO_2 to the atmosphere during a typical summer (daily mean CO_{2-B}: 58.1±14.5 mg C m^{-2} d^{-1}; daily mean CO_{2-AS}: 70.5±11.7 mg C m^{-2} d^{-1}; Figure A3.4).

CH_4 concentrations in Skeleton Lake decreased to variable but low levels post ice-cover. When re-connected to the atmosphere in spring, accumulated CH_4 was emitted to the atmosphere, oxygen diffused into the water, and permafrost melt streams delivered waters high in concentrations of DIC, SO_4^{2-} and major ions to the lake (Table A3.3, A3.5). This indicated that CH_4 generation in sediments was possibly limited due oxygenation of the water column, or competition between SO_4^{2-}-reducing and methanogenic bacteria. This hypothesis was supported by the prevalence of H_2S gas in collected sediment cores (unpublished) and by trivial volumes and CH_4 concentrations of bubbles (0.000-0.013 mg m^{-2} d^{-1}) measured from sediments during the summer (Figure A3.5). Therefore, mean seasonal CH_4 emissions were low from the lake (1.31±0.23 mg C m^{-2} d^{-1}) and were generally stable between years (Figure 4.3).

Pond 01 - Periodic flooding of Pond 01 drastically altered its CO_2 and CH_4 concentrations. From 2005 to 2007 (Table 4.1; Figure 4.3), Pond 01 received little Lake Hazen water and mean July dissolved CO_2 concentrations (CO_{2-B}: 5.1-7.5 µmol L^{-1}; CO_{2-AS}: 4.5 µmol L^{-1}) were far below atmospheric equilibrium. CH_4 concentrations were also very low (0.18-0.30 µmol L^{-1}) and relatively stable over time (Figure 4.2). Low CO_2 concentrations in Pond 01 could be attributed to DIC use by autotrophic plankton (mean chlorophyll-*a* concentration: 0.94 µg L^{-1} pre-flood vs. 0.19 µg L^{-1} post-flood) and observed robust macrophyte productivity (Tank *et al.*, 2009). Consequently, CO_2 uptake (CO_{2-B}: -45--155 mg C m^{-2} d^{-1}; CO_{2-AS}: -137 mg C m^{-2} d^{-1}) was occurring in the pond during non-flooding years (Figure A3.4). CH_4 concentrations, and therefore CH_4 fluxes (CH_{4-B} 1.1-1.7 mg C m^{-2} d^{-1}), were also very low because most of the wetland's soils were dry, exposed to the atmosphere and not connected to the central pond where we sampled. Post 2007 sampling (Water Survey of Canada, 2015), substantial rises in Lake Hazen water levels resulted in Pond 01 receiving substantial seepage water from the lake each year (Figure 4.2, A3.6). Consequently, concentrations of CO_2 from 2008-10 (mean July CO_{2-B}: 23.8-50.2 µmol L^{-1}; CO_{2-AS}: 23.0-38.9 µmol L^{-1}) and CH_4 (CH_{4-B}: 1.38-2.76 µmol L^{-1}) increased considerably, as did emissions of each gas to the atmosphere (CO_{2-B}: 50-97 mg C m^{-2} d^{-1}; CO_2-

$_{AS}$: 37-110 mg C m^{-2} d^{-1}; CH$_{4-B}$: 3.8-35.8 mg C m^{-2} d^{-1}; Figure A3.4). This strong flooding of Pond 01, best delineated by bottle measurements, overall resulted in daily mean concentrations of CO$_2$ and CH$_4$ above equilibrium concentrations (mean daily CO$_{2-B}$: 23.5±1.2 µmol L^{-1}; CH$_{4-}$: 1.404±0.111 µmol L^{-1}; Figure 4.2). For CO$_2$, these drastic seasonal changes overwhelmed diurnal changes (measured by automated systems) which showed a classic CO$_2$ and O$_2$ relationship; a signature of in-lake primary productivity (Figure 4.4). Further, seasonal water chemistry indicated that increases in iron concentration and other reduced compounds (e.g., NH$_4^+$; Table A3.3, A3.4) coincided with the increases in CO$_2$ concentration, suggesting that widespread flooding led to a die-off of wetland plants, and heterotrophic CO$_2$ release to the water column, similar to results from other flooded wetland systems (Kelly *et al.*, 1997). CH$_4$ production was strongly coincident with increasing NO$_3^-$ concentration following flooding, which was likely a signature of intruding Lake Hazen water (Table A3.5) with some possible NO$_3^-$ release from remineralization of organic matter. CH$_4$ production was also aided by naturally low SO$_4^{2-}$ concentrations in Lake Hazen water, possibly limiting the influence of SO$_4^{2-}$-reducing bacteria in sediments and offering advantage to methanogenic bacteria. Considering all samples together and acknowledging substantial variability due to flooding, mean seasonal CO$_2$ fluxes showed that Pond 01 was a net emitter of CO$_2$ to the atmosphere (CO$_{2-B}$: 16.0±16.2 mg C m^{-2} d^{-1}) and a strong source, per unit area, of CH$_4$ to the atmosphere (CH$_{4-B}$: 8.0±1.5 mg C m^{-2} d^{-1}).

Factors affecting CO$_2$ and CH$_4$ concentrations in other aquatic systems on the landscape

We also sampled other aquatic systems in the northeastern portion of the Lake Hazen watershed to investigate broader trends of CO$_2$ and CH$_4$ concentrations and the influence of water quality on these concentrations. These systems varied from upland lakes/ponds flushed by permafrost seep streams, to margin wetlands/ponds seasonally inundated by Lake Hazen. Seepage water flushing upland lakes was sourced from surrounding hill slopes composed of evaporite, dolomite and carbonate rock (Trettin, 1994), leading to water rich in concentrations of SO$_4^{2-}$, HCO$_3^-$ and other major ions (Table A3.5). Margin wetlands/ponds were periodically flushed by cold, ultra-oligotrophic Lake Hazen water, dilute in major ions, nutrients and DOC, but higher in NO$_3$-NO$_2$. We found that lakes and ponds with greater concentrations of DIC, DOC, and carbonate-related ions (e.g., Ca^{2+}, SiO$_2$) generally had higher dissolved CO$_2$ concentrations than the more dilute systems (Table A3.5, A3.6, Figure A3.7). Chlorophyll-*a*

concentrations were low in all lakes (max. 2.4 μg L^{-1}) and showed only weak association with CO_2 concentration, likely reflecting challenging high Arctic growing conditions and the prevalence of these shallow systems to support benthic productivity not easily measureable in the water column. Therefore, these results suggested that watershed supply of carbon from the dissolution of carbonate rock (Marcé *et al.*, 2015), or from photodegradation (Bertilsson and Tranvik, 2000) or respiration of organic matter, rather than primary productivity, were the key processes controlling CO_2 exchange in the Lake Hazen watershed. Our results showed most lakes and ponds (78%) in the northeastern portion of the Lake Hazen watershed had either similar or higher concentrations of CO_2 relative to atmospheric equilibrium concentrations. This was further supported by CO_2 modelling of previously studied lakes throughout the watershed which suggested 79% of lakes had neutral or higher CO_2 concentrations relative to the atmosphere (see supplementary information; Table A3.7; Figure A3.8; Keatley *et al.*, 2007; Babaluk *et al.*, 2009). Despite the indications that Lake Hazen watershed lakes were typically sources of CO_2 to the atmosphere, CO_2 fluxes were generally higher in other lakes of the low and sub Arctic (as defined by AMAP, 1998; Table 4.2).

Table 4.2 Ranges or means of CO_2 and CH_4 fluxes from various studies investigating lake GHG exchange during the ice-free season from the high, low and sub arctic regions. Positive values represent emission to the atmosphere.

Biome*	General locator	CO2 flux mg C m^{-2} d^{-1}	CH4 flux mg C m^{-2} d^{-1}	Study
High arctic	Canadian arctic archipelago	-11-58	0.2-8.0	This study
High arctic	Canadian arctic archipelago	-246-1,374	0.4-67.5	Laurion *et al.*, 2010
Low arctic	northern Alaska	-78-718	1.0-12.3	Kling *et al.*, 1992
Low arctic	northern Alaska	300-1,100	-	Sturtevant *et al.*, 2007
Low arctic	north central Russia	381-1,095	-	Abnizova *et al.*, 2012
Low arctic	north central Russia	500-2,600	4.1-9.4	Repo *et al.*, 2007
Low arctic	western Alaska	-	2.0-14.7	Bartlett *et al.*, 1992
Low arctic	western Siberia	-	18.6	Zimov *et al.*, 1997
Sub arctic	western Siberia	-	68.2	Walter *et al.*, 2006
Sub arctic	northern Sweden	-29-126	1.0-21.3	Karlsson *et al.*, 2013
Sub arctic	east central Canada	107-747	0.4-5.4	Laurion *et al.*, 2010
Sub arctic	northwestern Canada	-650-1,550	-	Tank *et al.*, 2009

as delineated by AMAP[0].

Whereas CO_2 concentrations were higher in lakes and ponds supplied with dissolved rock and organic matter, high CH_4 concentrations generally coincided with waters poorer in dissolved rock signatures and organic matter. We observed a clear decline in lake CH_4 concentrations along with increasing Ca^{2+} and SO_4^{2-} concentrations (Figure A3.7, Table A3.5, A3.6). High concentrations of SO_4^{2-} in aquatic systems would generally support the metabolism of SO_4^{2-}-reducing bacteria, which typically out-compete methanogenic bacteria for required H^+ ions. Concentrations of CH_4 also increased with higher NO_3^- concentrations in the lakes (Table A3.6), highlighting the flooding influence of Lake Hazen (high in NO_3^-) on Pond 01 and 02 margin wetlands/ponds (Table A3.5). Because most of the lakes we sampled were relatively high in SO_4^{2-} concentrations, CH_4 concentrations (and likely emissions to the atmosphere) were low (Table A3.5). However, other lakes in the watershed (Keatley *et al.*, 2007; Babaluk *et al.*, 2009) were less influenced by evaporite rock formations and thus had lower aqueous concentrations of SO_4^{2-}, and potentially higher emissions of CH_4 to the atmosphere. Alternatively, all margin wetlands/ponds adjacent to Lake Hazen would be expected to be emitters of CH_4 because of ubiquitous flooding.

Exchange of CO_2 and CH_4 in a rapidly changing watershed

Landscapes rich with lakes and wetlands, such as those in the southern Arctic, may contribute to well over 50% of all landscape GHG exchange with the atmosphere (Abnizova *et al.,* 2012). However, little is known about the relative contributions of GHGs exchange from the different landscape types in the dry high Arctic ecoregion, despite its extensive area and rapidly changing climate. In the Lake Hazen watershed, polar semidesert and poorly vegetated landscapes cover the vast majority of glacier-free area (>80%), followed by Lake Hazen itself (12%) and more productive meadow wetlands (3%) and upland (3%) and margin (<<1%) lakes and ponds (Figure 4.5). Emmerton *et al.*(2014; unpublished) measured, using eddy covariance flux towers (CO_2, CH_4) and static chambers (CH_4), growing season GHG exchange with polar semidesert and meadow wetland landscapes from 2008-2012. They found that the polar semidesert was among the most unproductive terrestrial ecosystems on Earth (60.2 ± 36.2 mg C m^{-2} d^{-1}), similar to findings from other studies (Soegaard *et al.*, 2000; Lloyd, 2001; Lund *et al.*, 2012). However, they also found the polar semidesert was a considerable atmospheric sink of CH_4 (1.0 ± 0.1 mg C m^{-2} d^{-1}). The moist and vegetated meadow wetland, however, was a very
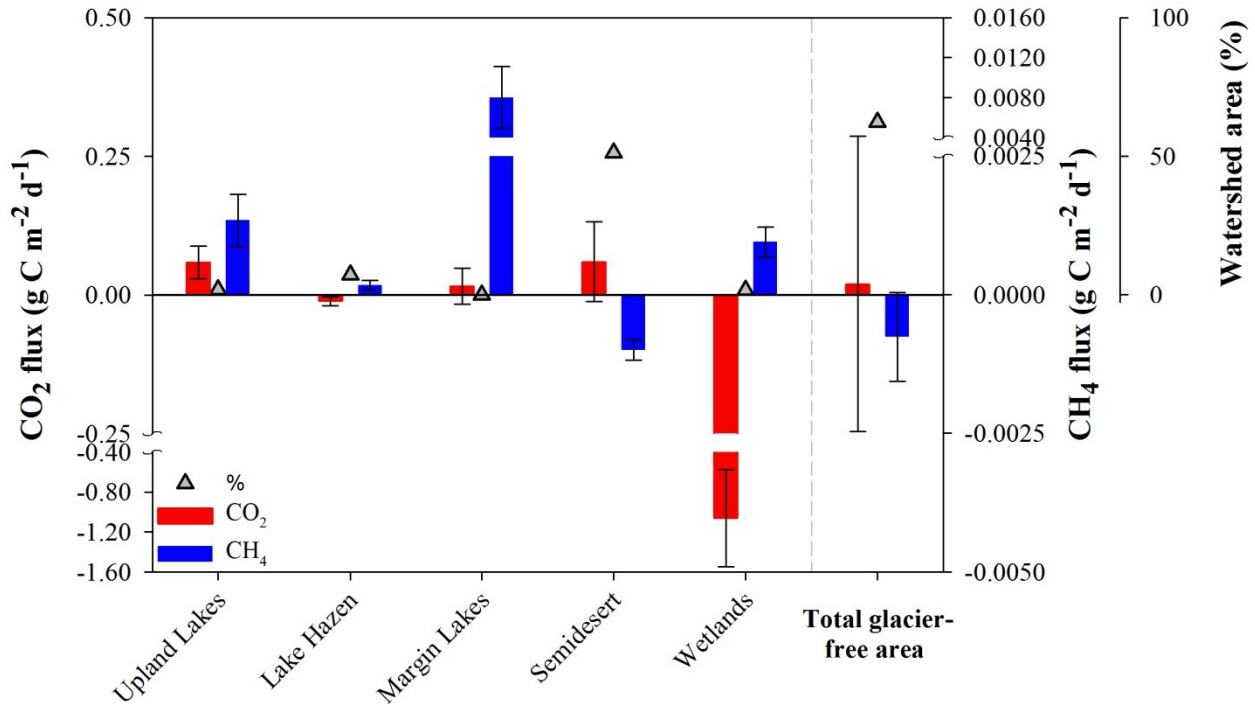
Figure 4.5 Mean growing season (47-64 d.) carbon dioxide (CO_2) and methane (CH_4) fluxes from several Lake Hazen waterhsed aquatic and terrestrial environments. Total fluxes and errors weighted by glacier-free watershed area shown in the right panel

productive ecosystem driven by ample water availability and 24-hour daylight (-1,063.1±243.6 mg C m^{-2} d^{-1}), but was a weaker emitter of CH_4 than expected (1.0±0.1 mg C m^{-2} d^{-1}), likely because of poor quantities of organic substrate in the active layer soils (Emmerton *et al.*, 2014).

There are over 3,500 upland ponds and lakes covering just over 140 km^2 of the Lake Hazen watershed, whereas ~50 margin wetlands/ponds covered only 0.5 km^2. Using mean growing season CO_2 and CH_4 fluxes from Lake Hazen (CO_2: -11.1±3.8 mg C m^{-2} d^{-1}; CH_4: 0.2±0.0 mg C m^{-2} d^{-1}), Pond 01 (CO_2: 16.0±16.2 mg C m^{-2} d^{-1}; CH_4: 8.0±1.5 mg C m^{-2} d^{-1}) and Skeleton Lake (CO_2: 58.1±14.5 mg C m^{-2} d^{-1}; CH_4: 1.3±0.2 mg C m^{-2} d^{-1}) and the assumption that Pond 01 and Skeleton were representative of other watershed lakes (Figure A3.8), we quantified mean growing season CO_2 and CH_4 exchange of the total of all aquatic systems with the atmosphere in the watershed. Integrating terrestrial results, we then weighted aquatic and terrestrial CO_2 and CH_4 exchange by land cover in the watershed (Edlund, 1994). We found that more productive environments (wetlands, margin wetlands/ponds), covering by far the least area

in the watershed (<4%), were inconsequential contributors to GHG exchange in the watershed. Most land area was covered by large, ultra-oligotrophic lakes (Lake Hazen) and nutrient-poor soils (polar semidesert), therefore reducing mean CO_2 exchange in the watershed to only a near-zero source to the atmosphere, and a near-zero sink of atmospheric CH_4. However, this may be poised to change substantially in the future.

The Lake Hazen watershed, similar to other high Arctic regions (Hill and Henry, 2011), is rapidly changing in many respects due to intense warming, including increasing glacial runoff to Lake Hazen (Water Survey of Canada, 2015). Changes in the heating and hydrology of lake systems and desiccated landscapes can have monumental effects on their productivity, nutrient cycling, and food web structures, all of which can influence the ultimate exchange of carbon between lakes and the atmosphere. Warming soils in permafrost regions have the potential to pulse-release water to the landscape that has been sequestered for many years. Because of the high relief surroundings on the northeast portion of the Hazen watershed, permafrost seeps, similar to those feeding Skeleton Lake, have the potential to flow more intensely, and for longer periods, thus flushing upland lakes with high SO_4^{2-}-waters. This may work to maintain the currently low CH_4 concentrations and fluxes, and keep in check emissions of this strong GHG. CO_2 concentrations, however, appeared slightly more affected by biological activity which may strengthen with decreasing ice-cover, longer growing seasons, and warmer water temperatures, potentially lowering CO_2 emission to the atmosphere.

Unlike upland lakes, glacial warming and increasing water levels in Lake Hazen should drive greater GHG emissions to the atmosphere from margin wetlands/ponds as flooding periods extend in time as growing seasons lengthen. With less connection to the landscape and earlier summer conditions excellent for plant growth, these lakes may have the potential to become sustained hot spots of decomposition and GHG emission upon flooding. However, the future exchange of GHG from the watershed will ultimately depend on how polar semideserts, and Lake Hazen, change within a warming climate. Loss of ice cover from Lake Hazen earlier in the season and greater river inflow could induce more intense mixing and nutrient availability in the water column and perhaps higher productivity and CO_2 sequestration. For example, there is evidence from recent Lake Hazen sediment core analyses (unpublished) suggesting an increase

in pelagic algae prevalence in the lake in concert with greater nutrient availability and increasingly ice-free conditions. Under warming and wetting climate conditions, polar semideserts are expected to become more productive (Climate Change, 2007) and strengthen as a sink of atmospheric CO_2, but not necessarily change its status as a strong CH_4 sink (Emmerton *et al.*, 2014). This then suggests that the semidesert may also become a stronger GHG sink in a warmer future. However, increasing productivity of each landscape in the watershed will be dependent on nutrient availability that may take several centuries to improve and support greater productivity (Wookey *et al.*, 1995). So the expected increase in sink strength of the Lake Hazen watershed will likely be a long-term progression.

Overall, we found that there were wide ranges of GHG exchange between different lake types in the high Arctic Lake Hazen watershed which were affected by hydrology and dissolved ions, and less-so by biological productivity. However, GHG exchange in the watershed was dominated in area by dry polar semidesert landscapes and a large ultra-oligotrophic great lake, resulting in a watershed exchanging near-neutral amounts of GHGs with the atmosphere. Future climate changes and strengthening GHG uptake in the watershed may occur very slowly until relatively barren landscapes become more hospitable to primary productivity.

References

Abnizova, A.; Siemens, J.; Langer, M.; Boike, J. Small ponds with major impact: The relevance of ponds and lakes in permafrost landscapes to carbon dioxide emissions. Global Biogeochemical Cycles 2012, 26,GB2040.

AMAP: AMAP Assessment Report: Arctic Pollution Issues, Arctic Monitoring and Assessment Programme (AMAP), Oslo, Norway, xii+859 pp., 1998.

Anthony, K. M. W.; Zimov, S. A.; Grosse, G.; Jones, M. C.; Anthony, P. M.; Chapin, F. S., III; Finlay, J. C.; Mack, M. C.; Davydov, S.; Frenzel, P.; Frolking, S. A shift of thermokarst lakes from carbon sources to sinks during the Holocene epoch. Nature 2014, 511(7510), 452-+.

ACIA, Arctic Climate Impact Assessment: Impacts of a Warming Arctic: Arctic Climate Impact Assessment. 2004. Cambridge University Press, Cambridge, UK.

Babaluk, J.A.; Gantner, N.; Michaud, W.; Muir, D.C.G.; Power, M.; Reist, J.D.; Sinnatamby, R.; Wang, X. Chemical Analyses of water from lakes and streams in Quttinirpaaq National park, Nunavut, 2001-2008. Canadian Data Report of Fisheries and Aquatic Sciences 1217. 2009. Government of Canada. Winnipeg.

Bartlett, K.B.; Crill, P.M.; Sass, R.L.; Harriss, R.C.; Dise, N.B. Methane emissions from tundra environments in the Yukon-Kuskokwim Delta, Alaska. J. of Geophysical Research 1992, 97(D15), 16,645-16,660.

Bastviken, D.; Tranvik, L. J.; Downing, J. A.; Crill, P. M.; Enrich-Prast, A. Freshwater methane emissions offset the continental carbon sink. Science 2011, 331(6013), 50-50.

Battin, T. J.; Luyssaert, S.; Kaplan, L. A.; Aufdenkampe, A. K.; Richter, A.; Tranvik, L. J. The boundless carbon cycle. Nature Geoscience 2009, 2(9), 598-600.

Bertilsson, S.; Tranvik, L.J. Photochemical transformation of dissolved organic matter in lakes. Limnology and Oceanography 2000, 45(4), 753-762.

Bogard, M. J.; del Giorgio, P. A.; Boutet, L.; Chaves, M. C. G.; Prairie, Y. T.; Merante, A.; Derry, A. M. Oxic water column methanogenesis as a major component of aquatic CH4 fluxes. Nature Communications 2014, 5, 5350.

Breton, J.; Vallieres, C.; Laurion, I. Limnological properties of permafrost thaw ponds in northeastern Canada. Canadian Journal of Fisheries and Aquatic Sciences 2009, 66(10), 1635-1648.

Callaghan, T. V.; Johansson, M.; Key, J.; Prowse, T.; Ananicheva, M.; Klepikov, A. Feedbacks and interactions: From the arctic cryosphere to the climate system. Ambio 2012, 40, 75-86.

Campbell, I.B.; Claridge, G.G.C. Chapter 8 Soils of cold climate regions. In: Weathering, Soils & Paleosols Martini IP and Chesworth W (eds.) Elsevier Amsterdam, The Netherlands 1992. Pages 183-224.

Climate Change 2007 - The Physical Science Basis. Contribution of Working Group I to the Fourth Assessment Report of the IPCC. 2007. Cambridge University Press, Cambridge, UK.

Cole, J. J.; Pace, M. L.; Carpenter, S. R.; Kitchell, J. F. Persistence of net heterotrophy in lakes during nutrient addition and food web manipulations. Limnology and Oceanography 2000, 45(8), 1718-1730.

Cole, J. J.; Prairie, Y. T.; Caraco, N. F.; McDowell, W. H.; Tranvik, L. J.; Striegl, R. G.; Duarte, C. M.; Kortelainen, P.; Downing, J. A.; Middelburg, J. J.; Melack, J. Plumbing the global carbon cycle: Integrating inland waters into the terrestrial carbon budget. Ecosystems 2007, 10(1), 171-184.

Edlund, S. A.: Vegetation, in: Resource Description and Analysis –Ellesmere Island National Park Reserve, Natural Resource Conservation Section, Prairie and Northern Region, Parks Canada, Department of Canadian Heritage, Winnipeg, Canada, 55 pp., 1994.

Emmerton, C.A.; St. Louis, V.L.; Lehnherr, I.; Humphreys, E.R.; Rydz, E.; Kosolofski, H.R. The net exchange of methane with high Arctic landscapes during the summer growing season. Biogeosciences 2014, 11, 3095-3106.

Environment Canada. Canadian climate normals 1981-2000. 2014. Available from: http://climate.weather.gc.ca/climate_normals/.

France, R. L. The Lake Hazen trough - a late winter oasis in a polar desert. Biological Conservation 1993, 63(2), 149-151.

Froese, D.G., Westgate, J.A.; Reyes, A.V.; Enkin, R.J.; Preece, S.J. Ancient permafrost and a future, warmer Arctic. Science 2008, 321, 1648.

Hamilton, J. D.; Kelly, C. A.; Rudd, J. W. M.; Hesslein, R. H.; Roulet, N. T. Flux to the atmosphere of CH4 and CO2 from wetland ponds on the Hudson-Bay lowlands (hbls). Journal of Geophysical Research-Atmospheres 1994, 99(D1), 1495-1510.

Hill, G. B.; Henry, G. H. R. Responses of high arctic wet sedge tundra to climate warming since 1980. Global Change Biology 2011, 17(1), 276-287.

Huttunen, J. T.; Nykanen, H.; Turunen, J.; Martikainen, P. J. Methane emissions from natural peatlands in the northern boreal zone in Finland, Fennoscandia. Atmospheric Environment

2003, 37(1), 147-151.

Karlsson, J.; Giesler, R.; Persson, J.; Lundin, E. High emission of carbon dioxide and methane during ice thaw in high latitude lakes. Geophysical Research Letters 2013, 40(6), 1123-1127.

Keatley, B. E.; Douglas, M. S. V.; Smol, J. P. Limnological characteristics of a high arctic oasis and comparisons across northern Ellesmere island. Arctic 2007, 60(3), 294-308.

Kelly, C. A.; Rudd, J. W. M.; Bodaly, R. A.; Roulet, N. P.; StLouis, V. L.; Heyes, A.; Moore, T. R.; Schiff, S.; Aravena, R.; Scott, K. J.; Dyck, B.; Harris, R.; Warner, B.; Edwards, G. Increases in fluxes of greenhouse gases and methyl mercury following flooding of an experimental reservoir. Environmental Science & Technology 1997, 31(5), 1334-1344.

Kling, G. W.; Kipphut, G. W.; Miller, M. C. The flux of CO2 and CH4 from lakes and rivers in arctic alaska. Hydrobiologia 1992, 240(1-3), 23-36.

Lafleur, P.M.; Humphreys, E.R.; St Louis, V.L.; Myklebust, M.C.; Papakyriakou, T.; Poissant, L.; Barker, J.D.; Pilote, M.; Swystun, K.A. Variation in peak growing season net ecosystem production across the Canadian Arctic. Environ. Sci. Technol. 2012, 46, 7971–7977.

Lai, D. Y. F. Methane dynamics in northern peatlands: A review. Pedosphere 2009, 19(4), 409-421.

Laurion, I.; Vincent, W. F.; MacIntyre, S.; Retamal, L.; Dupont, C.; Francus, P.; Pienitz, R. Variability in greenhouse gas emissions from permafrost thaw ponds. Limnology and Oceanography 2010, 55(1), 115-133.

Liss, P. S.; Slater, P. G. Flux of gases across air-sea interface. Nature 1974, 247(5438), 181-184.

Lloyd, C. R. The measurement and modelling of the carbon dioxide exchange at a high arctic site in Svalbard. Global Change Biology 2001, 7(4), 405-426.

Lund, M.; Falk, J. M.; Friborg, T.; Mbufong, H. N.; Sigsgaard, C.; Soegaard, H.; Tamstorf, M. P. Trends in CO2 exchange in a high arctic tundra heath, 2000-2010. Journal of Geophysical Research-Biogeosciences 2012, 117, G02001.

Maberly, S. C.; Barker, P. A.; Stott, A. W.; De Ville, M. M. Catchment productivity controls CO2 emissions from lakes. Nature Climate Change 2013, 3(4), 391-394.

Mack, M.C.; Schuur, E.A.G.; Bret-Harte, M.S.; Shaver, G.R.; Chapin III, F.S. Ecosystem carbon storage in arctic tundra reduced by long-term nutrient fertilization. Nature 2004, 431, 440-443.

Marcé R.; Obrador, B.; Morgui, J.-A.; Riera, J.L.; Lopez, P.; Armengol, J. Carbonate weathering as a driver of CO_2 supersaturation in lakes. Nature Geoscience 2015, 8, 107-111.

Peterson, B. J.; Holmes, R. M.; McClelland, J. W.; Vorosmarty, C.J.; Lammers, R. B.; Shiklomanov, A. I.; Shiklomanov, I. A.; Rahmstorf, S. Increasing river discharge to the Arctic Ocean. Science 2002, 298, 2171-2173.

Pfeffer, W.T.; Harper, J.T.; O'Neel, S. Kinematic constraints on glacier contributions to 21st-century sea-level rise. Science 2008, 321, 1340-1343.

Raymond, P. A.; Hartmann, J.; Lauerwald, R.; Sobek, S.; McDonald, C.; Hoover, M.; Butman, D.; Striegl, R.; Mayorga, E.; Humborg, C.; Kortelainen, P.; Duerr, H.; Meybeck, M.; Ciais, P.; Guth, P. Global carbon dioxide emissions from inland waters. Nature 503(7476), 355-359.

Rautio, M.; Dufresne, F.; Laurion, I.; Bonilla, S.; Vincent, W. F.; Christoffersen, K. S. Shallow freshwater ecosystems of the circumpolar arctic. Ecoscience 2011, 18(3), 204-222.

Repo, M.E.; Huttunen, J.T.; Naumov, A.V.; Chichulin, A.V.; Lapshina, E.D.; Bleuten, W.; Martikainen, P.J. Release of CO2 and CH4 from small wetland lakes in western Siberia.

Tellus 2007, 59B, 788-796.

Smith, L.C.; Sheng, Y.; MacDonald, G.M.; Hinzman, L.D. Disappearing Arctic lakes. Science 2008, 308, 1429.

Smol, J. P.; Wolfe, A. P.; Birks, H. J. B.; Douglas, M. S. V.; Jones, V. J.; Korhola, A.; Pienitz, R.; Ruhland, K.; Sorvari, S.; Antoniades, D.; Brooks, S. J.; Fallu, M. A.; Hughes, M.; Keatley, B. E.; Laing, T. E.; Michelutti, N.; Nazarova, L.; Nyman, M.; Paterson, A. M.; Perren, B.; Quinlan, R.; Rautio, M.; Saulnier-Talbot, E.; Siitonen, S.; Solovieva, N.; Weckstrom, J. Climate-driven regime shifts in the biological communities of arctic lakes. Proceedings of the National Academy of Sciences of the United States of America 2005, 102(12), 4397-4402.

Smol, J.P.; Douglas, M.S.V. Crossing the final ecological threshold in high Arctic ponds. PNAS 2007, 104, 12395-1239.

Soegaard, H.; Nordstroem, C.; Friborg, T.; Hansen, B. U.; Christensen, T. R.; Bay, C. Trace gas exchange in a high-arctic valley 3. Integrating and scaling CO2 fluxes from canopy to landscape using flux data, footprint modeling, and remote sensing. Global Biogeochemical Cycles 2000, 14(3), 725-744.

Sturtevant, C.S.; Oechel, W.C. Spatial variation in landscape-level CO2 and CH4 fluxes from arctic coastal tundra: influence from vegetation, wetness, and the thaw lake cycle. Global Change Biology 2013, 19, 2853-2866.

Tagesson, T.; Molder, M.; Mastepanov, M.; Sigsgaard, C.; Tamstorf, M. P.; Lund, M.; Falk, J. M.; Lindroth, A.; Christensen, T. R.; Strom, L. Land-atmosphere exchange of methane from soil thawing to soil freezing in a high-arctic wet tundra ecosystem. Global Change Biology 2012, 18(6), 1928-1940.

Tank, S. E.; Lesack, L. F. W.; Hesslein, R. H. Northern delta lakes as summertime CO2 absorbers within the arctic landscape. Ecosystems 2009, 12(1), 144-157.

Tranvik, L. J.; Downing, J. A.; Cotner, J. B.; Loiselle, S. A.; Striegl, R. G.; Ballatore, T. J.; Dillon, P.; Finlay, K.; Fortino, K.; Knoll, L. B.; Kortelainen, P. L.; Kutser, T.; Larsen, S.; Laurion, I.; Leech, D. M.; McCallister, S. L.; McKnight, D. M.; Melack, J. M.; Overholt, E.; Porter, J. A.; Prairie, Y.; Renwick, W. H.; Roland, F.; Sherman, B. S.; Schindler, D. W.; Sobek, S.; Tremblay, A.; Vanni, M. J.; Verschoor, A. M.; von Wachenfeldt, E.; Weyhenmeyer, G. A. Lakes and reservoirs as regulators of carbon cycling and climate. Limnology and Oceanography 2009, 54(6), 2298-2314.

Trettin, H.P. Geology. In: Resource description and analysis - Ellesmere Island National Park Reserve, 1994, pp.1-78, Department of Canadian Heritage, Winnipeg, Canada

Walker, M. D.; Wahren, C. H.; Hollister, R. D.; Henry, G. H. R.; Ahlquist, L. E.; Alatalo, J. M.; Bret-Harte, M. S.; Calef, M. P.; Callaghan, T. V.; Carroll, A. B.; Epstein, H. E.; Jonsdottir, I. S.; Klein, J. A.; Magnusson, B.; Molau, U.; Oberbauer, S. F.; Rewa, S. P.; Robinson, C. H.; Shaver, G. R.; Suding, K. N.; Thompson, C. C.; Tolvanen, A.; Totland, O.; Turner, P. L.; Tweedie, C. E.; Webber, P. J.; Wookey, P. A. Plant community responses to experimental warming across the tundra biome. PNAS 2006, 103(5), 1342-1346.

Walter, K. M.; Zimov, S. A.; Chanton, J. P.; Verbyla, D.; Chapin, F. S., III Methane bubbling from Siberian thaw lakes as a positive feedback to climate warming. Nature 2006, 443(7107), 71-75.

Water Survey of Canada. Real time hydrometric data, 2015. Available from: http://www.wateroffice.ec.gc.ca/index_e.html.

Wookey, P.A.; Robinson, C.H.; Parsons, A.N.; Welker, J.M.; Press, M.C.; Callaghan, T.V.; Lee, J.A. Environmental constraints on the growth, photosynthesis and reproductive development of Dryas octopetala at a high Arctic polar semi-desert, Svalbard. Oecologia 1995, 102, 478-489.

Zimov, S.A.; Voropaev, Y.V.; Semiletov, I.P.; Davidov, S.P.; Prosiannikov, S.F.; Chapin III, F.S.; Chapin, M.C.; Trumbore, S.; Tyler, S. North Siberian lakes: a methane source fueled by Pleistocene carbon. Science 1997, 277(5327), 800-802.

Chapter 5. General Conclusion

Together, the data and findings presented in these research chapters represents one of the few comprehensive studies of greenhouse gases exchange from a high Arctic, polar semidesert watershed. Of the published literature, only work ongoing at the high Arctic research station at Zackenberg Valley in northeast Greenland (78ºN) have multiple year static chamber or eddy covariance measurements of CO_2 and CH_4 exchange from different types of high Arctic vegetation cover. Collection of GHG exchange data from high Arctic regions has historically been very difficult to perform not only because of remote locations and challenging weather, but also because the use of eddy covariance, the standard in hectare-scale measurement of GHG exchange, has been very reliant on consistent sources of electricity to power gas analyzers, sonic anemometers and other supplementary equipment. Only recently have CO_2 and CH_4 gas analyzers been available on the market which can be powered solely from practical solar power systems. This important breakthrough has allowed for full growing-season evaluation of GHG exchange at remote high Arctic landscapes with suitable optical conditions for solar power. This has also allowed for easier collection of multiple year GHG measurements as only the availability of functioning batteries and daylight limits the operation of the eddy covariance system. These technical advances allowed us to collected up to five years worth of growing season eddy covariance data at two contrasting landscape types for up to almost the entire period of daylight at our site (May to October).

The measurement and quantification of CO_2 exchange between contrasting high Arctic landscapes and the atmosphere is presented in Chapter 2. We showed slight seasonal emission of CO_2 and relatively flat seasonal trends of CO_2 at a semidesert site during the growing season. At the more productive meadow wetland, we observed a "classic" net growing season uptake of CO_2 and a well-resolved seasonal trend of CO_2 exchange, illustrating the impact of water availability on carbon uptake at a high Arctic location. We integrated concurrent measurements of weather and other environmental conditions to better understand factors influencing CO_2 exchange during the growing season at each landscape. We found that CO_2 emission at the semidesert landscape was most influenced by surface soil moisture and respiration rates (biotic and abiotic) while CO_2 exchange at the meadow wetland landscape was influenced mostly by the

timing and intensity of heating. Our upscaling assessment found that semidesert ground NDVI was low and similar to satellite measurements, however, faint seasonal changes and poor NEP-NDVI relationships created challenges for detecting changing productivity with satellite measurements alone. The wetland appeared more suitable to remotely-sense productivity, however high Arctic wetland extent is limited by topography and may be difficult to resolve with larger satellite pixels. Our findings suggested that future landscape change in the high Arctic may be restricted by poor soil moisture retention and topography, and therefore may have considerable inertia against substantial short-term changes in CO_2 exchange. As a result, under climate change scenarios, we predicted that future landscape change in the high Arctic may be restricted first by its ability to retain water, and secondly by the intensity of heating.

The exchange of CH_4 between contrasting high Arctic landscapes and the atmosphere is presented in Chapter 3, and coincides with the approach and findings from the previous chapter on CO_2 exchange. We made static chamber measurements over five and three growing seasons at a polar desert and wetland, respectively, and eddy covariance measurements at the wetland in 2012. We also presented a whole-ecosystem mass budget of CH_4 from a high Arctic wetland to investigate the sources and net aquatic and terrestrial exchange of CH_4 from the ecosystem. During the growing season, chamber measurements showed that desert soils consumed CH_4 whereas the wetland emitted CH_4, as measured by both static chambers and eddy covariance. Desert CH_4 consumption rates were positively associated with soil temperature among years, and were similar to temperate locations, whereas wetland CH_4 varied closely with stream discharge, soil temperature and carbon dioxide flux. Using the mass budgeting approach, we determined that methanogenesis within wetland soils was the dominant source of the measured flux of CH_4 by the eddy covariance tower. Overall low CH_4 emission at the wetland was likely due to a shallow organic soil layer, and thus limited carbon resources for methanogens. Considering the prevalence of dry soils in the high Arctic, our results suggested that these landscapes cannot be overlooked as important consumers of atmospheric CH_4.

The exchange of GHGs between high Arctic lakes and the atmosphere during a five year period is presented in Chapter 4. Both collection of water in bottles and subsequent laboratory analysis, and in-situ measurements by automated systems were used to quantify concentrations

of dissolved CO_2 and CH_4 in different types of high Arctic lakes. Mass fluxes between the lakes and the atmosphere were also quantified at three intensively studied lakes. Concurrent measurements of general chemistry in all sampled lakes were taken to evaluate the influential compounds and conditions which affected GHG exchange in lakes. We found that hydrology and the geochemistry of rock formations affected GHG exchange more so than biological activity in the water column. When integrating GHG exchange results from both terrestrial and aquatic ecosystems in the Lake Hazen watershed, we found that relatively productive aquatic systems and wetlands exchanged substantially more GHGs with the atmosphere than unproductive environments. However, the areal dominance of both the ultra-oligotrophic Lake Hazen and polar semidesert soils meant that the watershed as a whole exchanged near zero amounts of GHGs with the atmosphere. Future climate warming and changes in the GHG regime in the watershed will likely proceed very slowly until relatively unproductive lakes and landscapes become more hospitable to autotrophic activity.

Overall, our findings suggested that a high Arctic watershed was most likely a net-zero contributor of GHGs to the atmosphere, and was mostly defined by exchanges by nearly unproductive large lakes and polar semidesert cover. Hot-spots of GHG emission or uptake within the watershed were therefore less important when weighted by areal cover. An important data gap we recognized from this work was the near lack of eddy covariance measurements of GHG exchange from ice-covered regions in the high Arctic. Though GHG exchange from these environments may be extremely low, the direction of even very faint GHG exchange may be very important on a regional scale considering areal coverage of glacial ice can be over 50% in some regions. Similar approaches of integrating aquatic and terrestrial GHG exchange measurements in the future would benefit from not only extensive temporal sampling of GHG exchange using eddy covariance towers, but more extensive spatial surveying using other approaches (e.g., static chambers, water sampling, remote sensing etc.), so as to have more representation of each landscape type within the watershed. More investigation into the lateral transport of carbon in major rivers and runoff streams would also be important to quantify watershed-scale carbon cycling. Our scaling exercise to relate measurements of net vegetation productivity using optical and eddy covariance measurements on the ground, to similar measurements using orbiting sensors on satellites may have the broadest impact of all our work.

The Arctic has typically been a difficult part of Earth to measure using remote sensing because of extensive cloud cover, low sun angles and resulting shadow interference, lack of daylight for much of the annual period, and sparse plant cover to quantify vegetation growth indices. The Lake Hazen watershed is among the clearest locations in the high Arctic for satellites to view. We found that vegetation growth was, on average, too low to correctly assess vegetation growth, and thus broader GHG exchange across the high Arctic at this time. This finding perhaps has implications for recent studies that infer widespread "greening" of the high Arctic in a warming climate, and highlights the importance of hydrological effects (e.g., water-related greening rather than heating) on GHG exchange across the high Arctic.

Appendix 1. Supporting information for Chapter 2: Net ecosystem production of polar semidesert and wetland landscapes in the rapidly changing Canadian high Arctic

EddyPro flux calculation procedures and corrections

Half-hour fluxes were calculated using a block averaging approach. To correct for anemometer tilt, a double rotation was performed to force mean vertical and lateral wind components to zero. Fluxes were de-spiked and corrected for time lag between the anemometer and gas analyzer measurements using a covariance maximization approach. Fluxes measured by LI-7500s were corrected for density fluctuations using the Webb *et al.* (1980) approach while LI-7200s provided gas mixing ratios. We used spectral corrections to adjust for flux loss at low (after Moncrieff *et al.*, 2004) and high (after Ibrom *et al.*, 2007) frequencies for both sensors. Half-hour fluxes were rejected when EC sensors malfunctioned or returned poor diagnostic values (e.g., during rare rain events for the LI-7500s), when gas analyzer signals exceeded a 0.4 second lag with the CSAT3 measurement, when wind did not pass over the wetland or passed through the tower structures, and when the friction velocity fell below 0.1 m s^{-1}, as done in similar studies (Wille *et al.*, 2008). We also applied turbulence tests after Mauder and Foken (2006) to remove the poorest-quality fluxes (level 2) when they did occur. Half-hour fluxes that were beyond ±3 standard deviations of the growing season mean were also removed.

Tables

Table A1.1 Growing season measurement duration and frequency of eddy covariance and dark soil respiration measurements at the polar semidesert and wetland sites near Lake Hazen. LI–7500 and LI–7200 denotes open–path and enclosed–path infrared gas analyzer measurements, respectively.

	Eddy covariance			Dark soil respiration (LI–6400)		
	# Dailies	Start Date	End Date	# Measures	Start Date	End Date
Polar semidesert						
LI–7500						
2008	28	08–July	04–August	3	25–July	31–July
2009	90	19–May	16–August	9	02–July	20–July
2010	59	18–June	15–August	8	25–June	19–July
2011	75	20–May	02–August	13	29–June	03–August
2012	125	01–June	03–October	10	03–July	04–August
LI–7200						
2011	75	20–May	02–August	–	–	–
2012	65	01–June	04–August	–	–	–
Meadow wetland						
LI–7500						
2010	30	22–June	21–July	8	26–June	19–July
2011	76	19–May	02–August	13	29–June	03–August
2012	125	02–June	03–October	9	03–July	04–August
LI–7200						
2011	77	19–May	03–August	–	–	–
2012	67	31–May	05–August	–	–	–

Table A1.2 Eddy covariance, meteorological and soil measurements collected by sensors mounted on the eddy covariance towers at the polar semidesert and wetland sites.

Eddy covariance measurements	
CO_2 / H_2O gas density	Licor LI–7500 CO_2/H_2O open–path infrared gas analyzers
CO_2 / H_2O mixing ratio	Licor LI–7200 CO_2/H_2O enclosed–path infrared gas analyzers
All–direction wind speed	Campbell Scientific CSAT3 sonic anemometers

Meteorological measurements	
Air temperature	HMP45C212 temp./humidity probes inside radiation shields
Air pressure	Licor LI–7500 CO_2/H_2O gas analyzer
Wind speed and direction	Campbell Scientific CSAT3 sonic anemometers
Net, photosynthetically active radiation	Kipp & Zonen Net and PAR radiometers
Precipitation	TE525 Tipping Bucket rain gauge

Soil measurements	
Soil temperature	CS107B soil temperature probes
Soil moisture	CS616–L soil water content reflectometers
Soil heat flux	CSHFT3 soil heat flux plates

Notes:1. All soil sensors were buried at 5cm depth within 1m of each tower; 2. Precipitation was only periodically monitored during the study period because of high spatial variability and rare measureable events.

Table A1.3 Light response-respiration model parameters and correlation coefficients of models used to gap–fill missing half–hour data from eddy covariance measurements (*LI-7200 measurements, otherwise LI-7500) at the polar semidesert and meadow wetland sites.

	α	β	a	b	c	R_{10}	Q_{10}
Polar semidesert							
2008F	-3.59E+07	-0.02	0.02	-0.01	0.01	-0.01	0.01
2008UF	-5.88E+07	0.25	0.02	-0.03	-4.04E-05	-12.95	0.27
2009F	3.49E+08	0.18	-1,110.66	1.61E+004	0.32	-6.41E-05	0.55
2009UF	1.03E+10	1.78	-0.52	-0.16	-3.97E-05	-2.57	0.79
2010F	4.86E+08	0.21	-6,933.95	-1.52E+07	-56.82	-5.48E+07	2.13E+13
2010UF	1.02E+08	0.79	-0.47	0.12	-5.85E-04	-0.48	0.46
2011F*	1.67E+07	-0.04	-324.91	1.33E+04	0.02	2.09E-05	0.22
2011UF*	-1.04E+08	0.61	0.02	-0.15	8.37E-08	26.59	0.72
2012F*	1.68E+09	-0.12	-2.8E+05	-1.10E+08	5,248.58	4.12E+07	6.10E+14
2012UF*	1.03E+10	0.77	7.98	72.73	2.48E-03	0.05	0.50
2012F	-1.66E+09	0.80	0.84	-4.00	1.43E-04	0.35	0.38
Meadow wetland							
2010F	1.81E+08	0.73	-0.21	-1.34	1.91E-05	-5.01	0.86
2010UF	1.02E+10	1.92	4.79	100.12	-0.16	-0.15	0.30
2011F*	1.68E+09	-4.18	-1.52E+05	-1.00E+05	1.22	2.79E-05	1.01
2011UF*	1.00E+08	-0.20	-5,130.75	-4,048.77	-1.77	1.16-04	7.96
2012F*	-4.69E+09	-0.75	-2.45E+04	1.98E+06	86.97	3.76E+11	2.41E+15
2012UF*	5.32E+10	201.94	456.54	-10.75	-5.44E-04	0.44	0.98
2012F	6.27E+07	9.96E-04	101.97	-438.76	92.10	1.21E-03	106.84

Notes: F indicates the frozen period; UF indicates the unfrozen period; α (initial slope of the light–response curve), β (maximum GEP), R_{10} (base ecosystem respiration at 10ºC) and Q_{10} (temperature sensitivity parameter); a-c are parameters.

Table A1.4 Parameters from heating correction (T_s^{bot}) used at the polar semidesert and meadow wetland sites.

Site	Correction equation
Polar semidesert	$T_s^{bot} = 0.9583*T + 0.0055*\max(\text{solar}-500,0) + 0.3936*U$
Meadow wetland	$T_s^{bot} = 1.169*T + 0.0059*\max(\text{solar}-500,0) + 0.44*U$

Notes: T = air temperature (ºC); U = wind speed (m s^{-1})

Table A1.5 Fitted parameters for the hybrid Q_{10}–hyperbolic soil moisture model (μmol m^{-2} s^{-1}) used to gap fill R_{ECO} at the polar semidesert and meadow wetland landscapes.

	a	b	c	Q_{10}	R_{10}
Polar semidesert	14.843	97.896	-0.070	0.038	1.057
Meadow wetland	398.813	682.819	-5.617	0.009	1.264

Figures
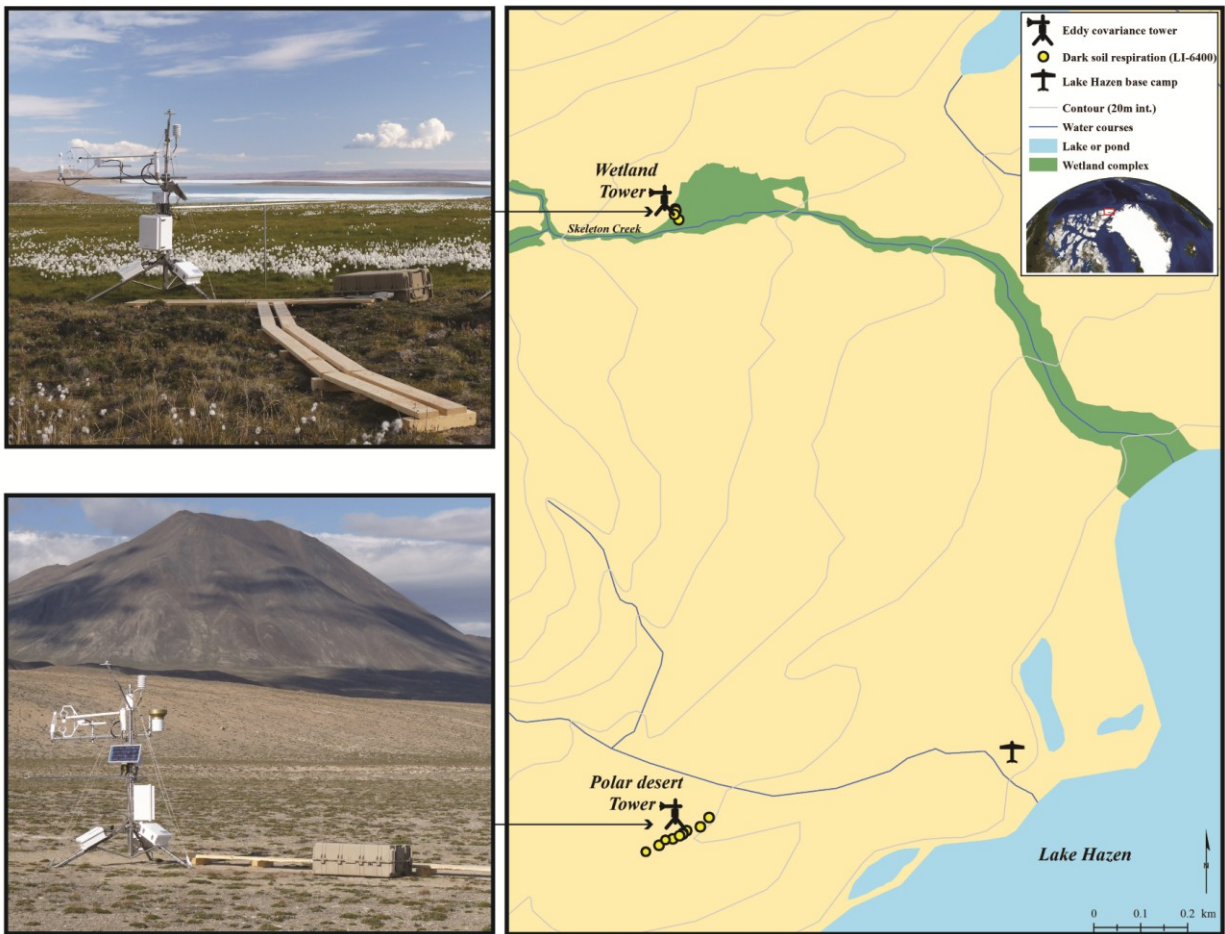
Figure A1.1 Lake Hazen camp in Quttinirpaaq National Park, Nunavut, Canada (81.8°N, 71.4°W). Photographs of eddy covariance towers deployed at the polar semidesert site (lower left panel) and the meadow wetland site (upper left panel) are shown. Polar semidesert and meadow wetland study sites are shown with eddy covariance towers and dark soil respiration collars (right panel).
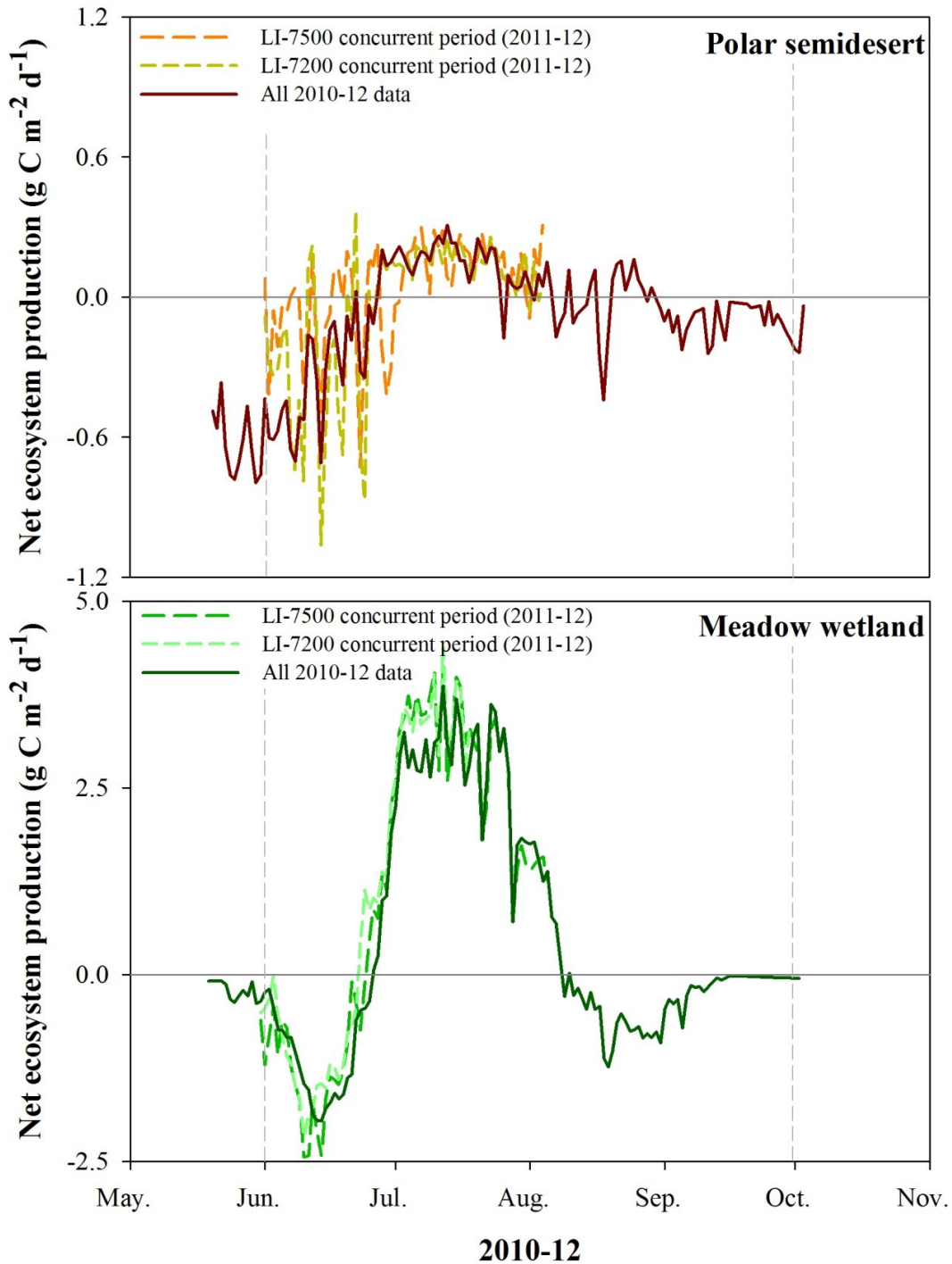
Figure A1.2 Comparison of LI-7500 and LI-7200 NEP fluxes running concurrently at each EC tower during portions of the growing season. These data are overlain with all 2010-12 data, which includes LI-7500 (2010; autumn 2012) and LI-7200 (2011, summer 2012) data together.

Desert Dark Soil Respiration Collars - Vegetated

Desert Dark Soil Respiration Collars - Unvegetated

Wetland Dark Soil Respiration Collars

Figure A1.3 Photos of collars used to measure dark soil respiration using the LI–6400. Vegetated and unvegetated soils at the polar semidesert and soils at the wetland are shown. Collars used from 2010–12 at both sites are shown only.
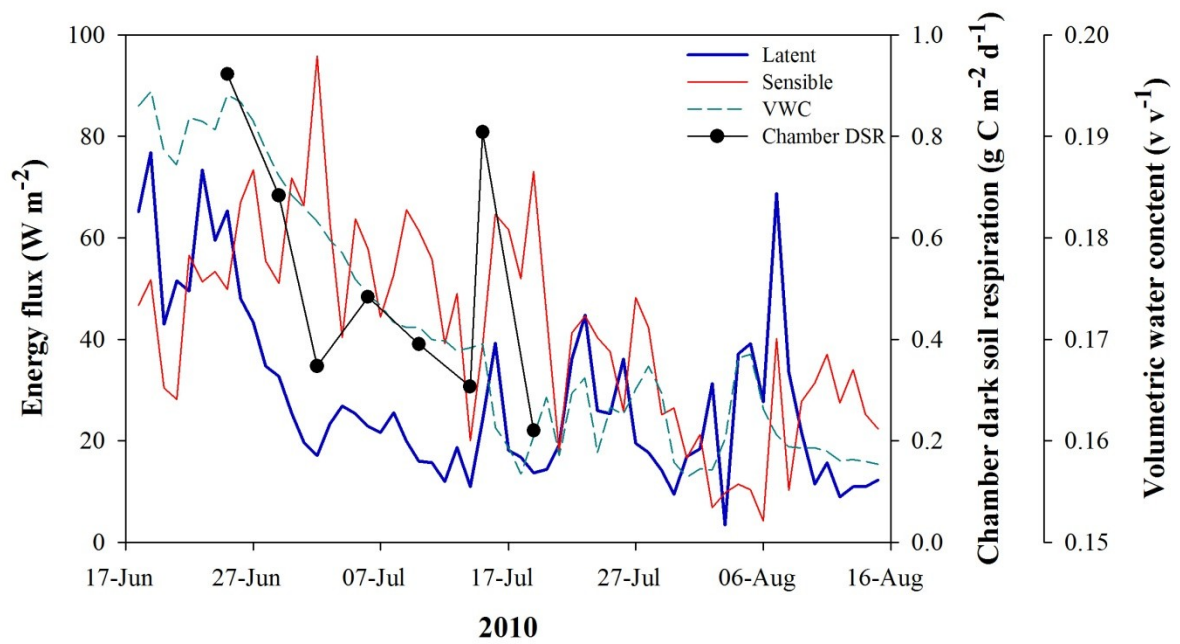
Figure A1.4 Time-series plots of latent and sensible energy fluxes, soil volumetric water content (at 5 cm depth) and chamber dark soil respiration fluxes from the polar semidesert in 2010. Note that mid-June is just after snowmelt while 15-Jul. a rainfall occurred.
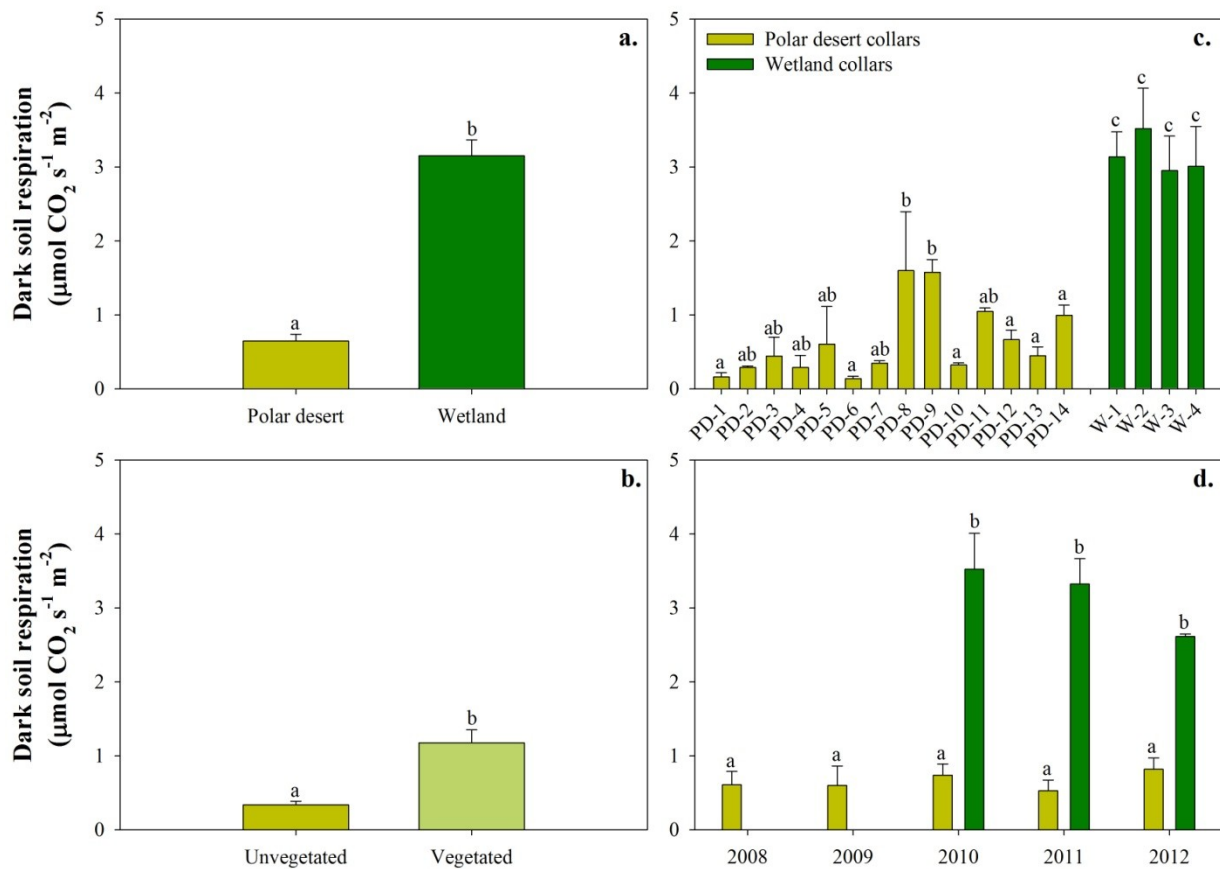
Figure A1.5 Multiple comparisons of replicates of dark soil respiration measured at the polar semidesert and wetland sites using the LI–6400: a. mean polar semidesert versus wetland measurements; b. mean unvegetated versus vegetated measurements at the polar semidesert; c. mean individual collar measurements at the polar semidesert and wetland; d. mean polar semidesert and wetland measurements between years. Letter differences indicate statistically significant differences between means using two–sample t–tests (a., b.) and one–way ANOVA (c., d.). PD–1 to PD–9 used during 2008 and 2009 growing seasons; PD–10 to PD–14 used during 2010 to 2012 growing seasons.
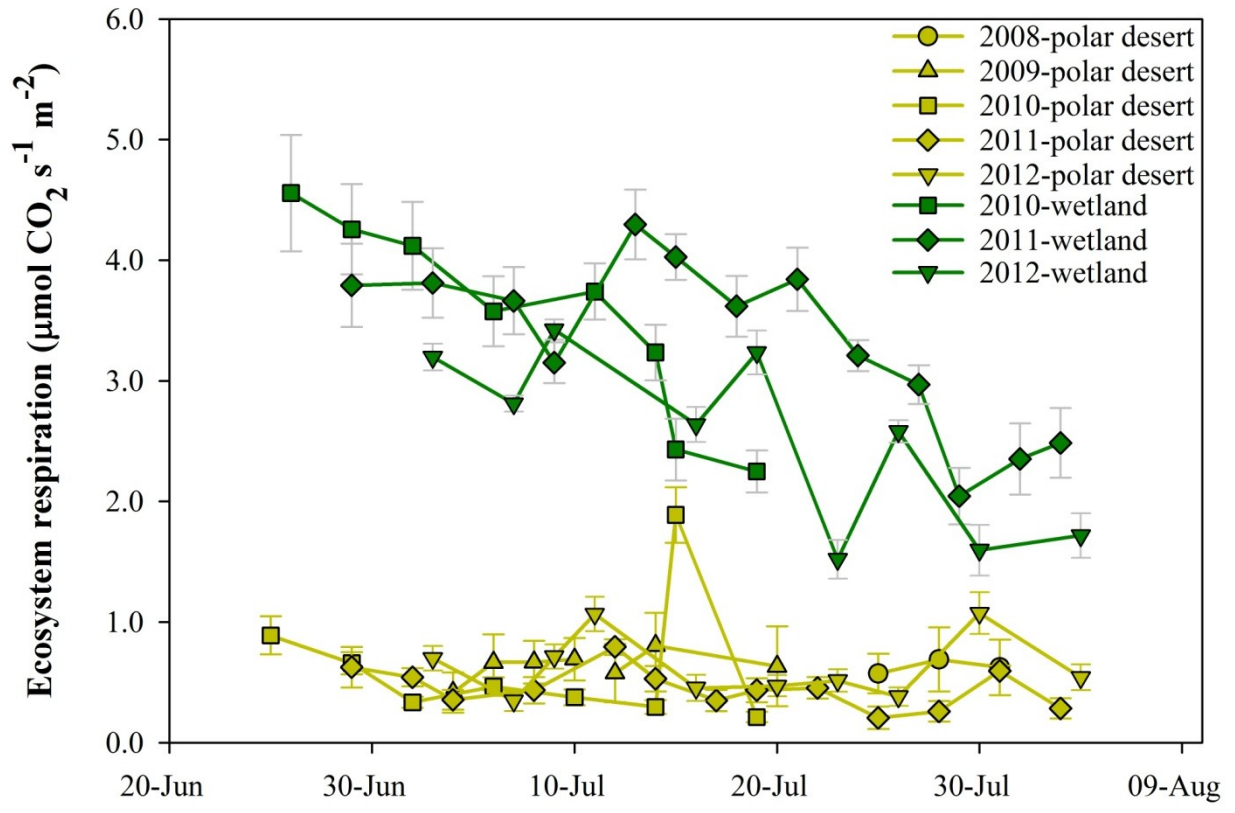
Figure A1.6 Mean dark soil respiration fluxes (±SE) measured by the LI–6400 on polar semidesert and wetland landscapes during portions of the 2008 to 2012 growing seasons. The 15-July-2010 semidesert measurements included those taken following a rainfall event, while the first 2010 measurements at the same site were taken while the landscape was still wet following snowmelt.
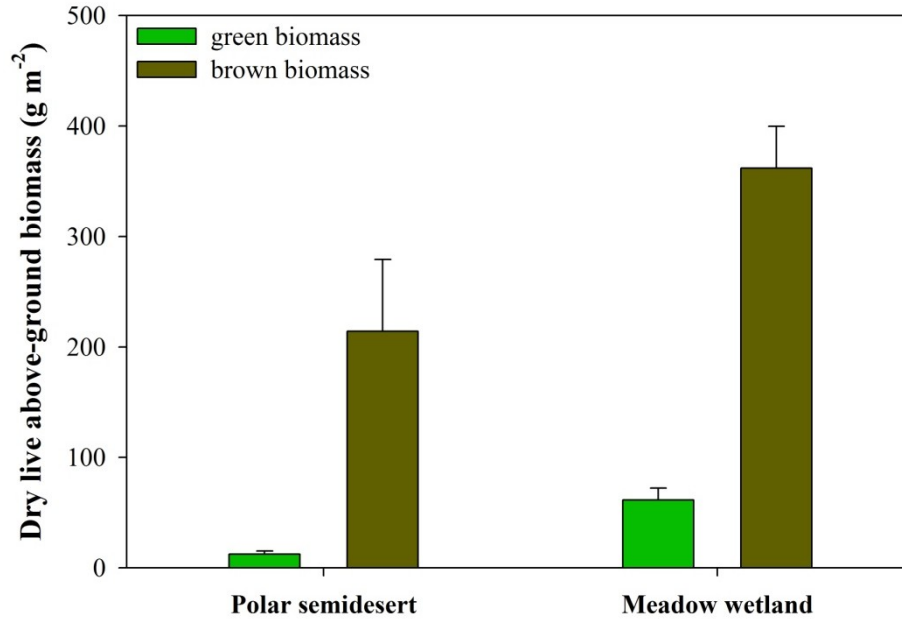
Figure A1.7 Mean (±1SE) green and brown leaf biomass from plot harvests across transects at both the polar semidesert and meadow wetland eddy covariance tower flux footprints.

References

Ibrom A, Dellwik E, Flyvbjerg H, Jensen NO, Pilegaard K (2007) Strong low-pass filtering effects on water vapour flux measurements with closed-path eddy correlation systems. Agricultural and Forest Meteorology, 147, 140-156.

Mauder M, Foken T (2006) Impact of post-field data processing on eddy covariance flux estimates and energy balance closure. Meteorologische Zeitschrift, 15, 597-609.

Moncrieff J, Clement R, Finnigan J, Meyers T (2004) Averaging, detrending, and filtering of eddy covariance time series. Handbook of Micrometeorology: A Guide for Surface Flux Measurement and Analysis, 29, 7-31.

Webb EK, Pearman GI, Leuning R (1980) Correction of flux measurements for density effects due to heat and water-vapor transfer. Quarterly Journal of the Royal Meteorological Society, 106, 85-100.

Wille C, Kutzbach L, Sachs T, Wagner D, Pfeiffer EM (2008) Methane emission from Siberian Arctic polygonal tundra: eddy covariance measurements and modeling. Global Change Biology, 14, 1395-1408.

Appendix 2. *Supporting information for Chapter 3: The net exchange of methane with high Arctic landscapes during the summer growing season*

Tables

Table A2.1 Meteorological and soil measurements collected by sensors mounted on the eddy covariance towers at the polar semidesert and wetland sites.

Meteorological measurements	
air temperature	HMP45C212 temp./humidity probes inside radiation shields
air pressure	Licor LI-7500 CO_2/H_2O gas analyzer
wind speed and direction	Campbell Scientific CSAT3 sonic anemometers
Net, photosynthetically active radiation	Kipp & Zonen net and PAR radiometers
Precipitation	TE525 Tipping Bucket rain gauge

Soil measurements	
soil temperature	CS107B soil temperature probes
soil moisture	CS616-L soil water content reflectometers
soil heat flux at 5 cm depth	CSHFT3 soil heat flux plates

Notes:1. All soil sensors were buried at 5cm depth within 1m of each tower; 2. Precipitation was only periodically monitored during the study period because of high spatial variability and rare measureable events.

Table A2.2 Spearman rank correlation matrix of daily mean environmental parameters and mean CH_4 fluxes from desert chambers (A.) and wetland chambers (B.) during the 2008-12 growing seasons. Bold indicates statistical significance at α=0.05.

A. Desert chambers

	1	2	3	4	5	6	7	8	9	10	11
1.CH_4 NEE	1										
2.Air pressure	-0.16	1									
3.Air temperature	-0.02	0.02	1								
4.Water vapor flux	0.07	-0.02	-0.20	1							
5.Air density	-0.03	**0.48**	**-0.78**	0.02	1						
6. Soil thaw depth	-0.01	-0.32	0.00	**0.46**	-0.29	1					
7.Net radiation	-0.13	-0.04	0.06	-0.16	0.02	**-0.43**	1				
8.PAR	-0.28	-0.07	0.20	-0.27	-0.08	**-0.46**	**0.93**	1			
9.Soil heat flux (5 cm)	-0.14	-0.24	**0.37**	-0.20	**-0.34**	-0.09	**0.65**	**0.71**	1		
10.Soil moisture	-0.20	0.06	-0.02	-0.27	0.07	**-0.43**	**0.40**	**0.39**	**0.35**	1	
11.Soil temperature	0.01	0.13	**0.84**	-0.26	**-0.50**	**-0.36**	0.21	**0.38**	**0.41**	0.16	1

B. Wetland chambers

	1	2	3	4	5	6	7	8	9	10	11	12
1.CH_4 NEE	1											
2.Air pressure	-0.26	1										
3.Air temperature	0.08	-0.33	1									
4.Water vapor flux	0.36	-0.01	0.13	1								
5.Air density	-0.12	**0.69**	**-0.88**	0.01	1							
6. Soil thaw depth	**0.51**	**-0.48**	-0.04	**0.53**	-0.11	1						
7.Net radiation	**-0.53**	0.27	**0.54**	**-0.38**	-0.37	**-0.61**	1					
8.PAR	**-0.52**	0.29	**0.53**	-0.41	-0.35	**-0.66**	**0.99**	1				
9.Soil heat flux (5 cm)	**-0.52**	0.32	0.38	**-0.52**	-0.16	**-0.58**	**0.80**	**0.81**	1			
10.Soil moisture	0.34	0.25	0.06	-0.04	0.05	0.21	0.17	0.14	-0.03	1		
11.Soil temperature	0.22	0.06	**0.47**	-0.20	-0.35	-0.23	**0.51**	**0.49**	0.31	**0.66**	1	
12. Stream discharge	**0.72**	-0.20	0.05	**0.53**	-0.04	**0.77**	**-0.43**	**-0.47**	**-0.51**	**0.50**	0.23	1

Table A2.3 Spearman rank correlation matrix of environmental factors and mean EC CH_4 fluxes from wetland LI-7700 measurements during the 2012 growing season. Bold indicates statistical significance at α=0.05.

	1.	2.	3.	4.	5.	6.	7.	8.	9.	10.	11.	12.	13.	14.
1. CH$_4$ NEE	1													
2. Momentum flux	**0.35**	1												
3. Sensible heat flux	0.09	**0.32**	1											
4. Latent energy flux	0.22	**0.40**	**0.59**	1										
5. CO$_2$ flux	**-0.71**	-0.01	0.19	0.03	1									
6. Water vapor flux	0.21	**0.39**	**0.59**	**1.00**	0.03	1								
7. Friction velocity	**0.36**	**0.99**	**0.30**	**0.39**	0.00	**0.39**	1							
8. Net radiation	**-0.38**	0.20	**0.73**	**0.49**	**0.60**	**0.49**	0.18	1						
9. PAR	0.00	0.26	**0.79**	**0.74**	0.14	**0.74**	0.24	**0.80**	1					
10. Soil heat flux (5cm)	0.03	-0.11	0.11	0.25	-0.04	0.25	-0.15	**0.29**	**0.33**	1				
11. Soil moisture	0.09	**0.46**	**0.37**	**0.38**	**0.31**	**0.37**	**0.52**	0.26	0.21	**-0.48**	1			
12. Soil temperature	**0.65**	0.18	0.15	**0.53**	**-0.58**	**0.53**	0.17	-0.22	**0.28**	0.09	0.12	1		
13. Air pressure	**-0.36**	-0.19	**0.35**	0.05	**0.39**	0.06	-0.22	**0.54**	**0.44**	**0.47**	-0.26	-0.21	1	
14. Air temperature	**0.49**	0.25	0.18	**0.70**	**-0.43**	**0.70**	0.27	-0.03	**0.45**	0.17	**0.29**	**0.82**	-0.27	1

EC measurements: rows 1–7. Other measurements: rows 8–14.

Table A2.4 Summary table of site mean CH_4 fluxes (F_{CH4}) measured in high-, low- and subarctic tundra (as defined by *AMAP*, 1998) for some portion of the northern growing season (May-October). Fluxes organized by chamber and eddy covariance measurements and by terrestrial sites predominantly emitting or consuming CH_4. All fluxes in mg CH_4 m^{-2} d^{-1}.

Location	Lat Lon	LANDSCAPE / METHOD				Reference
		Emission Sites		Consumption Sites		
		Chambers	Eddy Cov.	Chambers	Eddy Cov.	
High Arctic						
Ellesmere I., CA	81°49' -71° 20'	0.2	1.3	-1.4		*This study*
Ellesmere I., CA	77-82° -63-75			-0.9 – -0.3		*1-2*
Zackenberg, GL	74°28' -20° 34'	71 – 202	40 – 90	-0.3		*3-8*
Northern RU	72-73° 140-143°	0.1 – 78				*9*
Low Arctic						
Lena Delta, RU	72°22' 126° 30'	16 – 55	19 – 30			*10-13*
Tiski, RU	71°30' 130° 00'	23				*14*
Barrow, US	71°17' -156° 41'	23 – 52	32			*15-18*
Alaska, US	68-71° -148-158°	49 – 5				*19,20*
Toolik, US	68°38' -149° 38'	5 – 78				*21-26*
Yamal, RU	68°08' 71° 42'	58				*27*
Northern RU	67-77° 40-179°	27		-0.5		*11*
Vorkuta, RU	67°20' 63° 44'	5-83				*28,29*
Daring Lake, CA	64°52' -111° 35'	62				*30*
Bethel, US	60°45' -161° 45'	96	20			*31,32*
Churchill, CA	58°45' -94° 09'	54				*33*
Skan Bay, US	53° 39' -167° 04'			-3		*34*
Sub Arctic						
Indigirka, RU	70°49' 147° 29'	103	63			*35,36*
Cherskii, RU	69°36' 161° 20'	165-281		-1		*14,37,38*
Kaamanen, FI	69°08' 27° 16'	68	29			*39,40*
Stordalen, SE	68°21' 19° 02'	10-203	28-38	-1		*41-47*
Schefferville, CA	54°47' -66° 49'	30		-3		*48,49*
James Bay, CA	51°31' -80° 27'	16-52				*33,50*

1-Lamb et al., 2011
2-Stewart et al., 2012
3-Christensen et al., 2000
4-Mastepanov et al., 2008
5-Ström et al., 2012
6-Joabsson and Christensen, 2001
7-Tagesson et al., 2012
8-Friborg et al., 2000
9-Christensen et al., 1995
10-Kutzbach et al., 2004
11-Sachs et al., 2008
12-Sachs et al., 2010
13-Wille et all, 2008
14-Nakano et al., 2000
15-Lara et al., 2012
16-Rhew et al., 2007
17-Sturtevant et al., 2012

18-von Fischer et al., 2010
19-Morrissey and Livingston, 1992
20-Sebacher et al., 1986
21-King et al., 1998
22-Moosavi and Crill, 1998
23-Schimel, 1995
24-Torn and Chapin, 1993
25-Verville et al, 1998
26-Oberbauer et al., 1998
27-Heyer et al., 2002
28-Berestovakaya et al., 2005
29-Heikkinen et al., 2002a
30-Wilson and Humphreys, 2012
31-Bartlett et al., 1992
32-Fan et al., 1992
33-Roulet et al., 1994
34-Whalen and Reeburgh, 1990

35-Parmentier et al., 2011
36-van Huissteden et al., 2005
37-Merbold et al., 2009
38-Corradi et al., 2005
39-Hargreaves et al., 2001
40-Heikkinen et al., 2002b
41-Friborg et al., 1997
42-Jackowicz-Korczynski et al., 2010
43-Oquist and Svensson, 2002
44-Ström et al., 2007
45-Svensson and Rosswell, 1984
46-Svensson et al., 1999
47-Christensen et al., 1997
48-Bubier, 1995
49-Adamsen and King, 1993
50-Moore et al., 1994

Table A2.5 Concentrations ($\pm$1SD) of several chemicals downstream through the Skeleton Creek wetland complex. All chemicals are reported in μmol L^{-1}.

Location	Dissolved CH$_4$	Dissolved CO$_2$	Water$_T$	NO$_3^-$:NH$_4^+$	DIN:TDN	DOC	PN	Ca^{2+}
PF-1	0.00±0.00	40±1	4±1	205	1.0	67	0.08	3.1
PF-2	0.00±0.01	45±9	11±2	-	-	-	-	-
Skeleton	0.18±0.22	23±9	12±3	0.14±0.20	0.03±0.02	425±100	0.05±0.02	1.4±0.5
Pond 11	0.04±0.02	25±8	14±2	0.20±0.66	0.03±0.02	389±13	0.04±0.02	2.2±0.6
Stream-1	0.03±0.02	106±35	12±2	-	-	-	-	-
Stream-2	0.00±0.00	69±21	12±2	-	-	-	-	-
Wet-In	0.01±0.01	80±41	9±2	0.11±0.14	0.04±0.03	471±48	0.03±0.04	3.0±0.5
Wet-Out	0.00±0.01	77±24	9±2	0.07±0.13	0.04±0.02	524±47	0.05±0.05	3.0±0.5

← Downstream

Water$_T$: water temperature; NH$_4$: dissolved ammonium; NO$_3$: dissolved nitrate; DIN: dissolved inorganic nitrogen; TDN: total dissolved nitrogen; DOC: dissolved organic carbon; PN: particle-bound nitrogen; Ca^{2+}: dissolved calcium

Figures
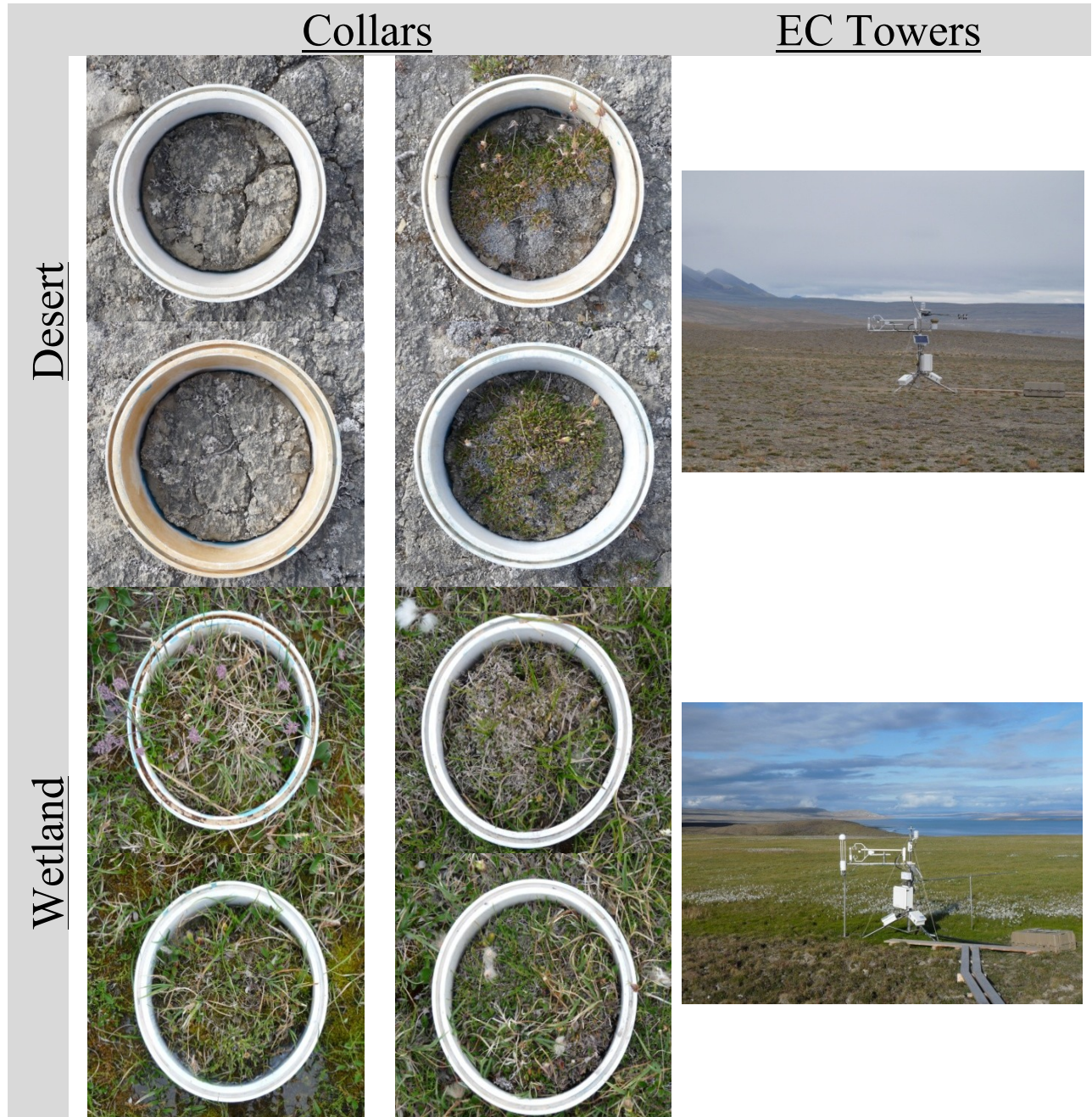
Figure A2.1 Photos of all chambers and enclosed vegetation, and EC towers and footprints at the desert and wetland sites. Photos taken during the growing season.
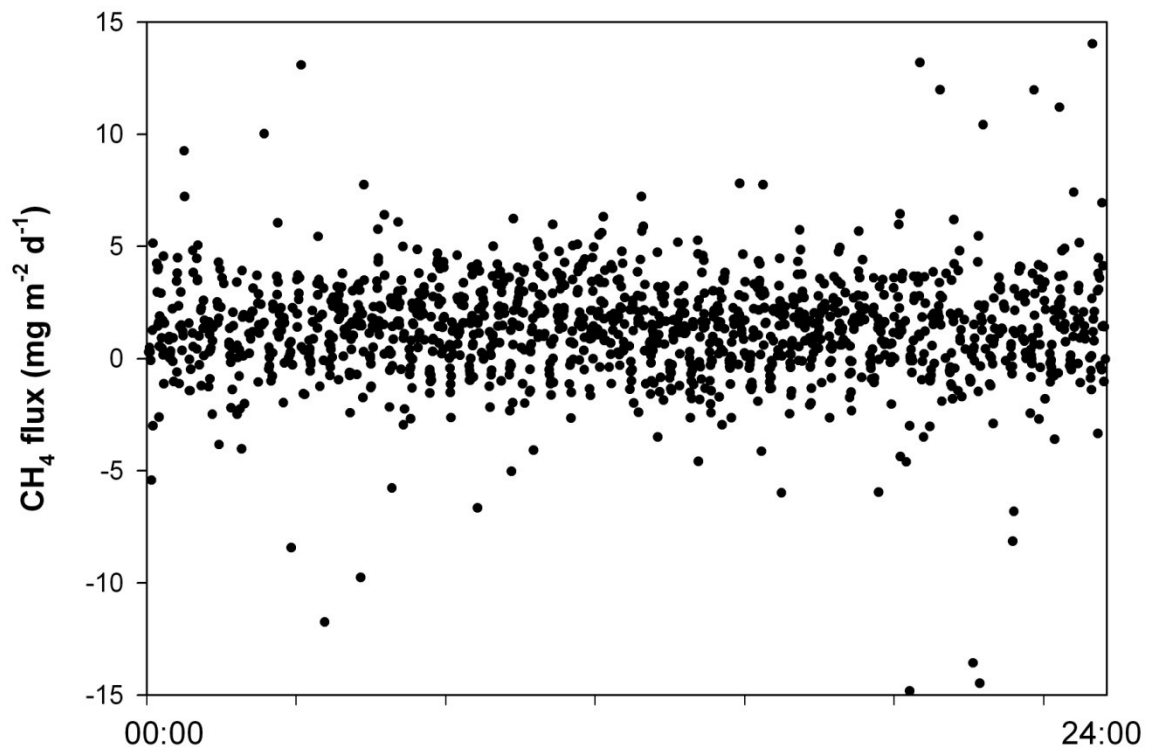
Figure A2.2 Diurnal organization of all half-hourly CH$_4$ NEE fluxes for the 2012 growing season at the wetland as measured by the EC tower.
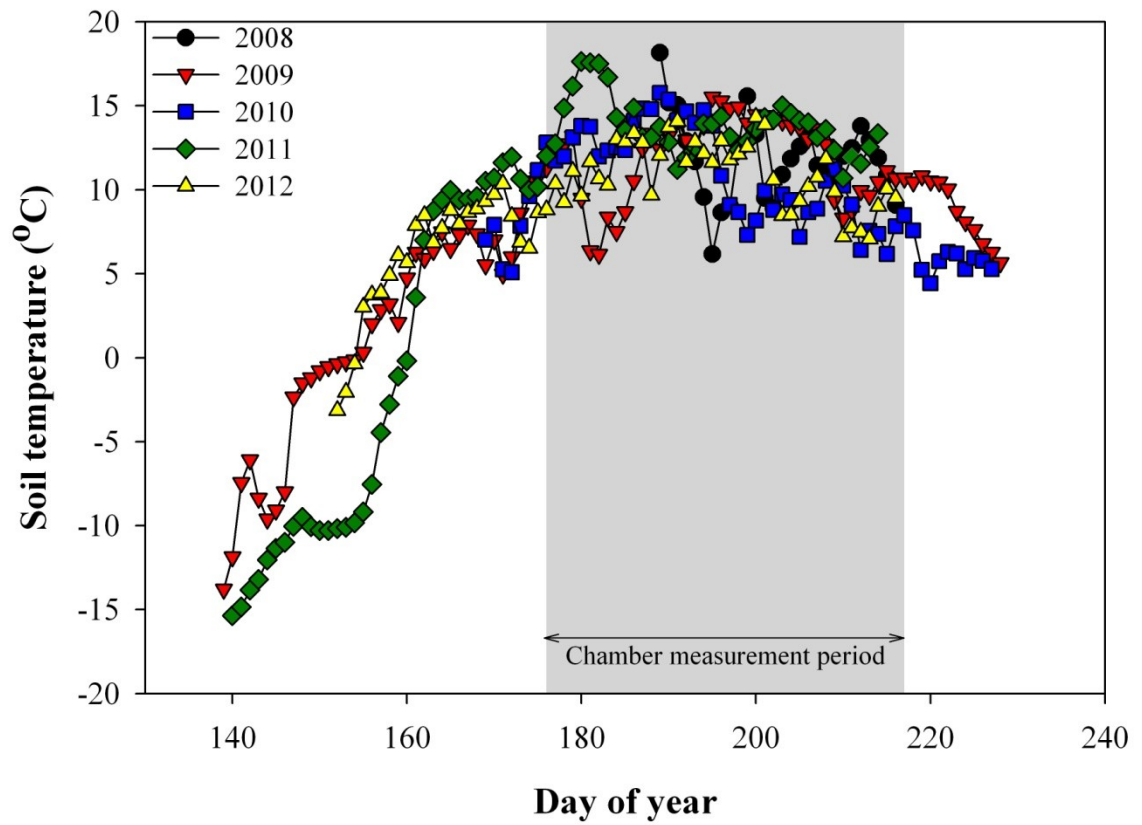
Figure A2.3 Soil temperatures at 5 cm depth during the growing seasons of 2008 to 2012 at the desert eddy covariance flux tower.
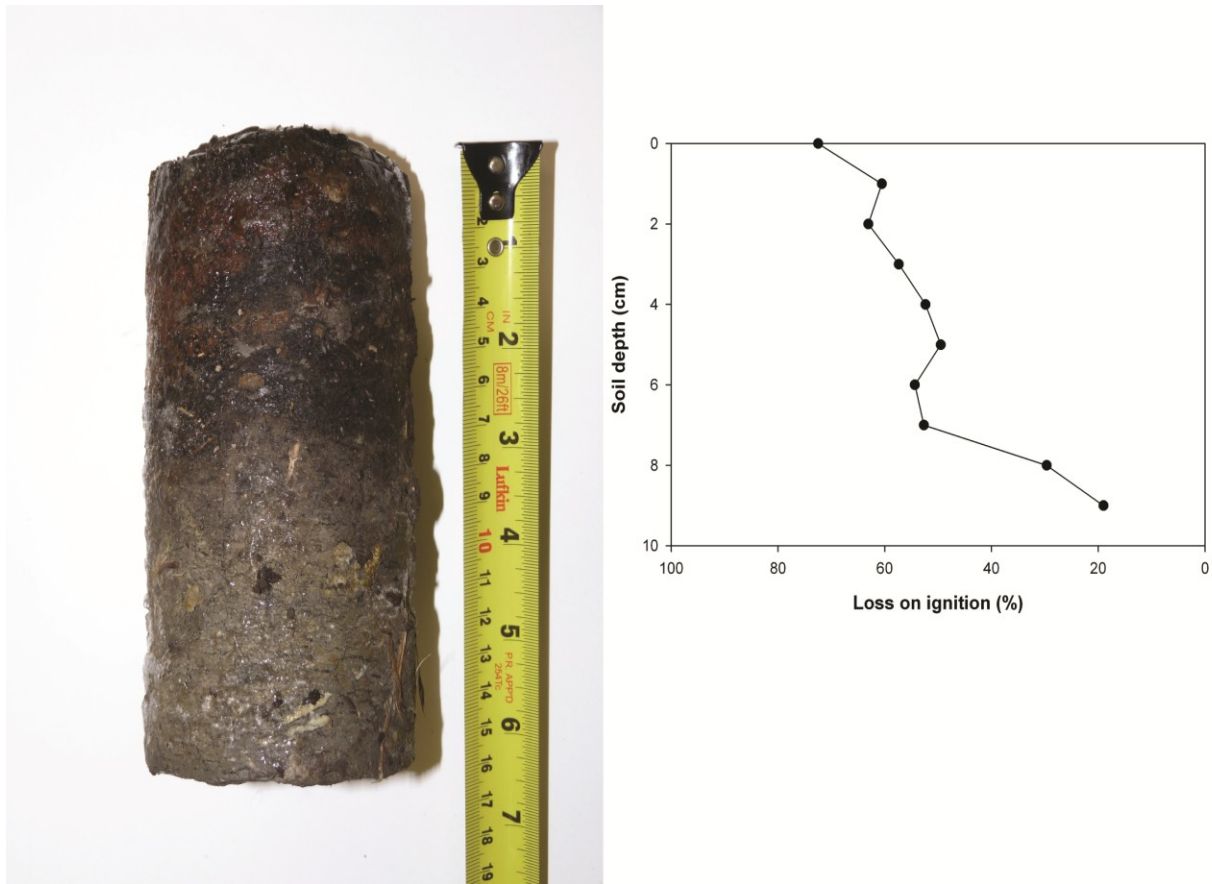
Figure A2.4 Photograph of a soil core extracted from the approximate middle of the wetland in May 2011 during frozen conditions (left). Graph of loss of ignition values (550°C) by depth for 0.5 cm portions of the wetland core (right).

References

Adamsen, A.P.S., and G.M. King (1993), Methane Consumption in Temperate and Sub-Arctic Forest Soils - Rates, Vertical Zonation, and Responses to Water and Nitrogen, *Applied and Environmental Microbiology, 59*, 485-490.

Bartlett, K.B., P.M. Crill, R.L. Sass, R.C. Harriss, and N.B. Dise (1992), Methane Emissions from Tundra Environments in the Yukon-Kuskokwim Delta, Alaska, *Journal of Geophysical Research-Atmospheres, 97*, 16645-16660.

Berestovskaya, Y.Y., I.I. Rusanov, L.V. Vasil'eva, and N.V. Pimenov (2005), The processes of methane production and oxidation in the soils of the Russian Arctic tundra. *Microbiology, 74*, 221-229.

Bubier, J.L. (1995), The Relationship of Vegetation to Methane Emission and Hydrochemical Gradients in Northern Peatlands, *Journal of Ecology, 83*, 403-420.

Christensen, T.R., S. Jonasson, T.V. Callaghan, and M. Havstrom (1995), Spatial Variation in High-Latitude Methane Flux Along a Transect across Siberian and European Tundra Environments, *Journal of Geophysical Research-Atmospheres, 100*, 21035-21045.

Christensen, T.R., A. Michelsen, S. Jonasson, and I.K. Schmidt (1997), Carbon dioxide and methane exchange of a subarctic heath in response to climate change related environmental manipulations, *Oikos, 79*, 34-44.

Christensen, T.R., T. Friborg, M. Sommerkorn, J. Kaplan, L. Illeris, H. Soegaard, C. Nordstroem, and S. Jonasson (2000), Trace gas exchange in a high-arctic valley 1. Variations in CO2 and CH4 flux between tundra vegetation types, *Global Biogeochemical Cycles, 14*, 701-713.

Corradi, C., O. Kolle, K. Walter, S.A. Zimov, and E.D. Schulze (2005), Carbon dioxide and methane exchange of a north-east Siberian tussock tundra, *Global Change Biology, 11*, 1910-1925.

Fan, S.M., S.C. Wofsy, P.S. Bakwin, D.J. Jacob, S.M. Anderson, P.L. Kebabian, J.B. McManus, C.E. Kolb, and D.R. Fitzjarrald (1992), Micrometeorological Measurements of Ch4 and Co2 Exchange between the Atmosphere and Sub-Arctic Tundra, *Journal of Geophysical Research-Atmospheres, 97*, 16627-16643.

Friborg, T., T.R. Christensen, and H. Sogaard (1997), Rapid response of greenhouse gas emission to early spring thaw in a subarctic mire as shown by micrometeorological techniques, *Geophysical Research Letters, 24*, 3061-3064.

Friborg, T., T.R. Christensen, B.U. Hansen, C. Nordstroem, and H. Soegaard (2000), Trace gas exchange in a high-arctic valley 2. Landscape CH4 fluxes measured and modeled using eddy correlation data, *Global Biogeochemical Cycles, 14*, 715-723.

Hargreaves, K.J., D. Fowler, C.E.R. Pitcairn, and M. Aurela (2001), Annual methane emission from Finnish mires estimated from eddy covariance campaign measurements, *Theoretical and Applied Climatology, 70*, 203-213.

Heikkinen, J.E.P., V. Elsakov, and P.J. Martikainen (2002a), Carbon dioxide and methane dynamics and annual carbon balance in tundra wetland in NE Europe, Russia, *Global Biogeochemical Cycles, 16*.

Heikkinen, J.E.P., M. Maljanen, M. Aurela, K.J. Hargreaves, and P.J. Martikainen (2002b), Carbon dioxide and methane dynamics in a sub-Arctic peatland in northern Finland, *Polar Research, 21*, 49-62.

Heyer, J., U. Berger, I.L. Kuzin, and O.N. Yakovlev (2002), Methane emissions from different ecosystem structures of the subarctic tundra in Western Siberia during midsummer and during the thawing period, *Tellus Series B-Chemical and Physical Meteorology, 54*, 231-249.

Jackowicz-Korczynski, M., T.R. Christensen, K. Backstrand, P. Crill, T. Friborg, M. Mastepanov, and L. Strom (2010), Annual cycle of methane emission from a subarctic peatland, *Journal of Geophysical Research-Biogeosciences, 115*.

Joabsson, A., and T.R. Christensen (2001), Methane emissions from wetlands and their relationship with vascular plants: an Arctic example, *Global Change Biology, 7*, 919-932.

King, J.Y., W.S. Reeburgh, and S.K. Regli (1998), Methane emission and transport by arctic sedges in Alaska: Results of a vegetation removal experiment, *Journal of Geophysical Research-Atmospheres, 103*, 29083-29092.

Kutzbach, L., D. Wagner, and E.M. Pfeiffer (2004), Effect of microrelief and vegetation on methane emission from wet polygonal tundra, Lena Delta, Northern Siberia, *Biogeochemistry, 69*, 341-362.

Lamb, E.G., S. Han, B.D. Lanoil, G.H.R. Henry, M.E. Brummell, S. Banerjee, and S.D. Siciliano (2011), A High Arctic soil ecosystem resists long-term environmental manipulations, *Global*

Change Biology, 17, 3187-3194.

Lara, M.J., S. Villarreal, D.R. Johnson, R.D. Hollister, P.J. Webber, and C.E. Tweedie (2012), Estimated change in tundra ecosystem function near Barrow, Alaska between 1972 and 2010, *Environmental Research Letters, 7*.

Mastepanov, M., C. Sigsgaard, E.J. Dlugokencky, S. Houweling, L. Strom, M.P. Tamstorf, and T.R. Christensen (2008), Large tundra methane burst during onset of freezing, *Nature, 456*, 628-U58.

Merbold, L., W.L. Kutsch, C. Corradi, O. Kolle, C. Rebmann, P.C. Stoy, S.A. Zimov, and E.D. Schulze (2009), Artificial drainage and associated carbon fluxes (CO2/CH4) in a tundra ecosystem, *Global Change Biology, 15*, 2599-2614.

Moore, T.R., A. Heyes, and N.T. Roulet (1994), Methane emissions from wetlands, southern Hudson Bay lowland, *Journal of Geophysical Research, 99*, 1455-1467.

Moosavi, S.C., and P.M. Crill (1998), CH4 oxidation by tundra wetlands as measured by a selective inhibitor technique, *Journal of Geophysical Research-Atmospheres, 103*, 29093-29106.

Morrissey, L.A., and G.P. Livingston (1992), Methane Emissions from Alaska Arctic Tundra - an Assessment of Local Spatial Variability, *Journal of Geophysical Research-Atmospheres, 97*, 16661-16670.

Nakano, T., S. Kuniyoshi, and M. Fukuda (2000), Temporal variation in methane emission from tundra wetlands in a permafrost area, northeastern Siberia, *Atmospheric Environment, 34*, 1205-1213.

Oberbauer, S.F., G. Starr, and E.W. Pop (1998), Effects of extended growing season and soil warming on carbon dioxide and methane exchange of tussock tundra in Alaska, *Journal of Geophysical Research-Atmospheres, 103*, 29075-29082.

Oquist, M.G., and B.H. Svensson (2002), Vascular plants as regulators of methane emissions from a subarctic mire ecosystem, *Journal of Geophysical Research-Atmospheres, 107*.

Parmentier, F.J.W., J. van Huissteden, M.K. van der Molen, G. Schaepman-Strub, S.A. Karsanaev, T.C. Maximov, and A.J. Dolman (2011), Spatial and temporal dynamics in eddy covariance observations of methane fluxes at a tundra site in northeastern Siberia, *Journal of Geophysical Research-Biogeosciences, 116*.

Rhew, R.C., Y.A. Teh, and T. Abel (2007), Methyl halide and methane fluxes in the northern Alaskan coastal tundra, *Journal of Geophysical Research-Biogeosciences, 112*.

Roulet, N.T., A. Jano, C.A. Kelly, L.F. Klinger, T.R. Moore, R. Protz, J.A. Ritter, and W.R. Rouse (1994), Role of the Hudson-Bay Lowland as a Source of Atmospheric Methane, *Journal of Geophysical Research-Atmospheres, 99*, 1439-1454.

Sachs, T., C. Wille, J. Boike, and L. Kutzbach (2008), Environmental controls on ecosystem-scale CH4 emission from polygonal tundra in the Lena River Delta, Siberia, *J. Geophys. Res., 113*, G00A03.

Sachs, T., M. Giebels, J. Boike, and L. Kutzbach (2010), Environmental controls on CH4 emission from polygonal tundra on the microsite scale in the Lena river delta, Siberia,. *Global Change Biology, 16*, 3096-3110.

Schimel, J.P. (1995), Plant-Transport and Methane Production as Controls on Methane Flux from Arctic Wet Meadow Tundra, *Biogeochemistry, 28*, 183-200.

Sebacher, D.I., R.C. Harriss, K.B. Bartlett, S.M. Sebacher, and S.S. Grice (1986), Atmospheric methane sources: Alaskan tundra bogs, an alpine fen, and a subarctic boreal marsh. *Tellus*

38B, 1-10.

Stewart, K.J., M.E. Brummell, R.E. Farrell, and S.D. Siciliano (2012), N2O flux from plant-soil systems in polar deserts switch between sources and sinks under different light conditions, *Soil Biology & Biochemistry, 48*, 69-77.

Strom, L., and T.R. Christensen (2007), Below ground carbon turnover and greenhouse gas exchanges in a sub-arctic wetland, *Soil Biology & Biochemistry, 39*, 1689-1698.

Strom, L., T. Tagesson, M. Mastepanov, and T.R. Christensen (2012), Presence of Eriophorum scheuchzeri enhances substrate availability and methane emission in an Arctic wetland, *Soil Biology & Biochemistry, 45*, 61-70.

Sturtevant, C.S., W.C. Oechel, D. Zona, Y. Kim, and C.E. Emerson (2012), Soil moisture control over autumn season methane flux, Arctic Coastal Plain of Alaska, *Biogeosciences, 9*, 1423-1440.

Svensson, B.H., and T. Rosswall (1984), Insitu Methane Production from Acid Peat in Plant-Communities with Different Moisture Regimes in a Subarctic Mire, *Oikos, 43*, 341-350.

Svensson, B.H., T.R. Christensen, E. Johansson, and M. Oquist (1999), Interdecadal changes in CO(2) and CH(4) fluxes of a subarctic mire: Stordalen revisited after 20 years, *Oikos, 85*, 22-30.

Tagesson, T., M. Molder, M. Mastepanov, C. Sigsgaard, M.P. Tamstorf, M. Lund, J.M. Falk, A. Lindroth, T.R. Christensen, and L. Strom (2012), Land-atmosphere exchange of methane from soil thawing to soil freezing in a high-Arctic wet tundra ecosystem, *Global Change Biology, 18*, 1928-1940.

Torn, M.S., and F.S. Chapin (1993), Environmental and Biotic Controls over Methane Flux from Arctic Tundra, *Chemosphere, 26*, 357-368.

van Huissteden, J., T.C. Maximov, and A.J. Dolman (2005), High methane flux from an arctic floodplain (Indigirka lowlands, eastern Siberia), *Journal of Geophysical Research-Biogeosciences, 110*.

Verville, J.H., S.E. Hobbie, F.S. Chapin, and D.U. Hooper (1998), Response of tundra CH4 and CO2 flux to manipulation of temperature and vegetation, *Biogeochemistry, 41*, 215-235.

von Fischer, J.C., R.C. Rhew, G.M. Ames, B.K. Fosdick, and P.E. von Fischer (2010), Vegetation height and other controls of spatial variability in methane emissions from the Arctic coastal tundra at Barrow, Alaska, *Journal of Geophysical Research-Biogeosciences, 115*.

Whalen, S.C., and W.S. Reeburgh (1990), Consumption of Atmospheric Methane by Tundra Soils, *Nature, 346*, 160-162.

Wille, C., L. Kutzbach, T. Sachs, D. Wagner, and E.M. Pfeiffer (2008), Methane emission from Siberian arctic polygonal tundra: eddy covariance measurements and modeling, *Global Change Biology, 14*, 1395-1408.

Wilson, K.S., and E.R. Humphreys (2010), Carbon dioxide and methane fluxes from Arctic mudboils, *Canadian Journal of Soil Science, 90*, 441-449.

Appendix 3. Supporting information for Chapter 4: The net exchange of carbon greenhouse gases with aquatic systems in a high Arctic watershed and its role in whole-ecosystem carbon transfer

Dissolved CO_2 model

The water quality of the aquatic environment in the Lake Hazen watershed has been investigated previously, though sporadically. In conjunction with our multiple growing season data set, papers by Keatley *et al.* (2007) and Babaluk *et al.* (2009) complete the most comprehensive survey of water quality in the watershed. We used published water quality data from both studies to construct a more complete picture of CO_2 concentrations in the Hazen watershed to determine if aquatic environments were typically sinks or sources of CO_2 relative to the atmosphere. Though Keatley *et al.* and Babaluk *et al.* do not report dissolved CO_2 concentrations in waters of sampled streams, lakes and ponds, we modeled dissolved CO_2 concentrations using DIC concentrations and pH from both studies. We used an empirical linear model:

$$\text{Dissolved } CO_2 \text{ (µmol L}^{-1}) = a + b*DIC + c*10^{pH} \qquad (A3.1)$$

where a, b and c are coefficients (Table A3.7), DIC is the concentration (µmol L^{-1}) of total DIC in a sample and pH is measured in-situ the time of sampling. We then compared dissolved CO_2 concentrations of all lakes against mean equilibrium CO_2 concentration measured closely at our 3-lake set between 2005 and 2012.

Tables

Table A3.1 Sampling dates for GHG concentrations, collected using bottles (B) or automated systems (AS), and general chemical analyses (C) of several aquatic sites throughout the Lake Hazen watershed.

Water body		2005	2007	2008	2009	2010	2011	2012
L. Hazen	B	4-20/7	24/6-21/7	6/7-4/8	29/6-22/7	22/6-20/7	6-30/7	-
	C	6-13/7	-	10/7-3/8	2-22/7	28/6-20/7	-	-
Upland ponds								
Skeleton L.	B	-	25/6-19/7	6/7-3/8	29/6-22/7	18/6-19/7	4-30/7	4-31/7
	AS	-	-	8/7-3/8	1-21/7	25/6-20/7	-	-
	C	-	14/7	10/7-2/8	2-22/7	28/6-17/7	-	-
Pond 03	B	10/7	13-14/7	29/7	-	12-17/7	6-30/7	-
	C	-	14/7	-	-	12-17/7	-	-
Pond 07	B	15/7	9/7	29/7	-	13-18/7	6-30/7	-
	C	-	10/7	-	-	13-18/7	-	-
Pond 10	B	15/7	-	-	-	13-18/7	6-30/7	-
	C	-	-	-	-	13-18/7	-	-
Pond 11	B	15/7	-	-	-	12-17/7	4-30/7	4-31/7
	C	-	-	-	-	12-17/7	-	-
Pond 12	B	15/7	14-16/7	29/7	-	12-17/7	-	31/7
	C	-	14/7	-	-	12-17/7	-	-
Pond 16	B	-	-	-	-	13-18/7	6-30/7	-
	C	-	-	-	-	13-18/7	-	-
Margin ponds								
Pond 01	B	6-21/7	24/6-21/7	6/7-4/8	29/6-22/7	16/6-20/7	6-30/7	-
	AS	-	24/6-21/7	10/7-2/8	29/6-21/7	19/6-5/7	-	-
	C	6-23/7	28/6-18/7	9/7-2/8	2-22/7	28/6-20/7	-	-
Pond 02	B	6-21/7	8/7	9/7-2/8	-	10-20/7	6-30/7	-
	C	6-22/7	6/7	9/7-2/8	-	10-20/7	-	-

Table A3.2 Empirical relationships for k (cm hr^{-1}; Hamilton *et al.*, 1994) used in the mass flux equation for greenhouse gases samples (Equation 2).

if U<3 m s^{-1}:

$$k_{600} = 0.76U$$
$$k_{CO2} = k_{600} * (600^{0.67}/SC_{CO2}^{0.67})$$
$$k_{CH4} = k_{600} * (600^{0.67}/SC_{CO2}^{0.67})$$

if U≥3 m s^{-1}:

$$k_{600} = 5.6U - 14.14$$
$$k_{CO2} = k_{600} * (600^{0.50}/SC_{CO2}^{0.50})$$
$$k_{CH4} = k_{600} * (600^{0.50}/SC_{CO2}^{0.50})$$

Notes: U was the in situ wind speed (m s^{-1}) measured on automated systems or a nearby meteorological tower; k_{600} (cm hr^{-1}) was the exchange coefficient normalized to a Schmidt number (SC) of 600.

Table A3.3 Correlation coefficients of samples for greenhouse gas and general chemical concentrations from Skeleton Lake (df=12), Lake Hazen (df=12) and Pond 01 (df=13). Statistical significance at α=0.05 indicated in **bold**. Correlation performed using Systat v13; Systat Software.

	Lake Hazen		Skeleton Lake		Pond 01	
	CO_2	CH_4	CO_2	CH_4	CO_2	CH_4
CH_4	0.42	-	**0.78**	-	0.48	-
Air_P	**-0.56**	-0.43	-0.38	-0.09	0.50	0.06
$Water_T$	-0.31	0.19	-0.46	**-0.58**	0.31	0.10
W_S	**0.62**	-0.28	-0.22	-0.22	-0.17	0.37
CO_2 flux	0.46	0.43	0.04	-0.11	**0.83**	**0.72**
CH_4 flux	0.43	**1.00**	0.17	0.24	0.03	**0.62**
DIC	**0.69**	0.29	**-0.71**	**-0.95**	**0.86**	0.25
NH_4^+	-0.25	-0.14	-0.07	-0.33	**0.80**	0.30
$NO_2^--NO_3^-$	**0.69**	0.16	-0.30	-0.19	0.43	**0.84**
TDN	0.35	0.33	-0.48	**-0.67**	**0.70**	0.48
PN	0.47	0.40	-0.41	-0.38	0.29	-0.31
TN	0.39	0.36	-0.51	**-0.66**	**0.72**	0.41
TP	0.35	-0.12	0.43	**-0.56**	0.47	0.06
TDP	**0.62**	-0.02	0.01	0.29	0.51	0.28
PC	**0.53**	**0.61**	-0.42	-0.43	0.25	-0.26
DOC	-0.51	-0.03	0.03	-0.06	0.35	0.17
Cl^-	**0.64**	0.15	-0.45	-0.52	0.37	0.14
SO_4^{2-}	**0.67**	0.28	**-0.72**	**-0.69**	**-0.54**	-0.17
Na^+	**0.71**	0.33	-0.47	-0.52	**0.59**	0.45
K^+	**0.71**	0.42	**-0.63**	**-0.91**	**0.86**	0.30
Ca^{2+}	**0.70**	0.20	**-0.75**	**-0.95**	**0.60**	0.19
Mg^{2+}	**0.72**	0.38	**-0.64**	**-0.79**	0.09	0.27
Fe^{2+}	-	-	-	-	**0.76**	0.08
Alkalinity	**0.70**	0.27	**-0.61**	**-0.86**	**0.87**	0.39
HCO_3^-	**0.70**	0.27	**-0.61**	**-0.86**	**0.87**	0.39
TDS	**0.80**	0.01	-0.17	-0.33	0.33	0.22
Chl-*a*	-0.07	-0.04	**-0.59**	-0.29	0.23	-0.16
pH	-0.26	-0.17	**-0.69**	**-0.62**	**-0.84**	**-0.61**

Table A3.4 Regression tree analysis of dissolved CO_2 and CH_4 with general chemical elements for Skeleton Lake, Lake Hazen and Pond 01. Positive ($\uparrow$) or negative ($\downarrow$) relationships between CO_2 and CH_4 and general chemical elements are also indicated.

Lake	CO₂			CH₄		
	Split Variable	Model Improvement	Relate w/CO₂	Split Variable	Model Improvement	Relate w/CH₄
Lake Hazen	DIC	0.545	$\uparrow$	DOC	0.209	$\uparrow$
	TDS	0.222	$\uparrow$	W_S	0.076	$\downarrow$
Skeleton Lake	CH_4^+	0.763	$\uparrow$	DIC	0.727	$\downarrow$
	Chl-*a*	0.075	$\downarrow$			
Pond 01	Fe^{2+}	0.803	$\uparrow$	$NO_2^--NO_3^-$	0.611	$\uparrow$
				Chl-*a*	0.052	$\downarrow$

Note: Regression tree analysis performed using Systat v13; Systat Software. For a partition of the data to occur, a minimum of five daily values was required with a minimum model improvement of 0.05.

Table A3.5 Water chemistry summary of three high Arctic lakes/ponds between 2005 and 2010.

Site	md	CO_2	CH_4	DIC	NO_3^-	NH_4^+	DOC	SO_4^{2-}	Fe	TDS	pH	Cond	Chl-a_F
	m					μmol L^{-1}				mg L^{-1}		μS cm^{-1}	μg L^{-1}
Lake Hazen													
LH	95	21±1	0.07±0.02	503±26	0.23±0.04	1.5±0.5	51±32	69±11	0.0±0.0	68±20	7.9±0.1	124±29	0.2±0.
Upland ponds													
SL	1.9	28±1	0.19±0.02	1491±33	0.02±0.00	2.2±0.6	390±42	1583±129	0.0±0.0	312±29	8.2±0.0	476±13	0.5±0.1
P03	0.3	43±10	0.19±0.07	2782±103	0.02±0.01	0.8±0.7	1707±103	1279±393	1.2±0.3	414±69	8.1±0.1	613±35	0.9±0.0
P12	0.8	11±1	0.04±0.01	1585±64	0.04±0.02	2.1±2.0	1407±138	4387±2068	0.2±0.1	891±168	8.4±0.1	957±18	0.8±0.3
P11	1.1	28±2	0.04±0.01	1400±70	0.02±0.01	0.4±0.2	389±7	2437±205	0.2±0.2	508±58	8.0±0.0	500±10	0.6±0.1
P16	1.1	18±4	0.20±0.05	934±38	0.01±0.00	0.3±0.2	554±12	1885±35	0.1±0.1	328±9	8.1±0.1	352±17	0.3±0.1
P10	1.1	17±4	0.33±0.29	2510±53	0.01±0.00	0.5±0.4	1982±75	4676±80	0.0±0.0	934±23	8.6±0.0	1028±40	2.4±0.6
P07	0.1	68±17	0.01±0.00	3051±129	0.02±0.01	1.7±0.7	3699±164	6603±80	3.2±0.7	1316±23	7.7±0.1	1087±127	0.9±0.4
Margin ponds													
P01	0.4	24±1	1.34±0.11	1604±40	0.09±0.03	2.5±0.5	536±75	524±75	2.1±0.4	231±16	8.3±0.1	351±28	0.7±0.2
P02	0.2	12±2	0.49±0.07	938±70	0.08±0.04	1.5±0.5	173±70	260±37	0.3±0.1	107±10	8.1±0.1	143±26	0.7±0.2
Streams, rivers													
PF1	-	**40±1**	**0.0±0.0**	812±36	7.7	0.1	67	3318	0.6	731	7.6±0.0	376±54	2.1
PF2	-	**45±4**	**0.00±0.00**	1526±112	-	-	-	-	-	-	7.8±0.1	453±32	-

Notes: NH_4^+: dissolved ammonium; NO_3^-: dissolved nitrite + nitrate; tdn:tdp: total dissolved nitrogen to phosphorus ratio; DOC: dissolved organic carbon;; Chl-a_F: cholorophyll-a by fluorescence; PF sites are drainage streams from hills surrounding Skeleton Lake, sampled five times during the summers of 2011 and 2012.

Table A3.6 Correlation coefficients of samples for greenhouse gas and general chemical concentrations from all sampled upland and margin ponds and lakes. Statistical significance at α=0.05 (df=8) indicated in **bold**. Correlation performed using Systat v13; Systat Software.

	CO_2	CH_4
CH_4	-0.26	-
Air_P	0.20	-0.32
$Water_T$	0.11	-0.09
DIC	**0.75**	-0.21
NH_4^+	0.07	0.44
$NO_2^--NO_3^-$	-0.31	**0.78**
TDN	0.52	-0.23
PN	0.38	0.33
TN	0.53	-0.23
TP	0.36	-0.17
TDP	0.59	-0.07
PP	0.30	-0.18
PC	**0.72**	-0.07
DOC	**0.74**	-0.35
TC	**0.78**	-0.31
Cl^-	0.38	-0.21
SO_4^{2-}	0.46	-0.53
Na^+	0.00	-0.12
K^+	0.37	-0.04
Ca^{2+}	0.54	-0.56
Mg^{2+}	0.43	-0.43
Fe^{2+}	**0.79**	0.26
Al	-0.43	0.20
SiO_2	**0.75**	-0.50
Alkalinity	**0.73**	-0.15
HCO_3^-	**0.75**	-0.16
CO_3^{2-}	-0.19	0.03
TDS	0.51	-0.48
Chl-*a*	-0.07	0.01
pH	**-0.75**	0.28
Cond.	0.48	-0.45
DO	0.44	0.16

Table A3.7 Regression coefficients for Equation S1 (Dissolved $CO_2 = a + b*DIC + c*10^{pH}$) for several aquatic ecosystem types in the Lake Hazen watershed.

	a	b	c
Lake Hazen	12.0	0.011	62809649
Upland lakes	-9.6	0.010	2301083060
Skeleton Lake	13.0	-0.001	1712116124
Margin Lakes	2.9	0.018	-171617867
Pond 01	-48.3	0.042	348348675

Figures
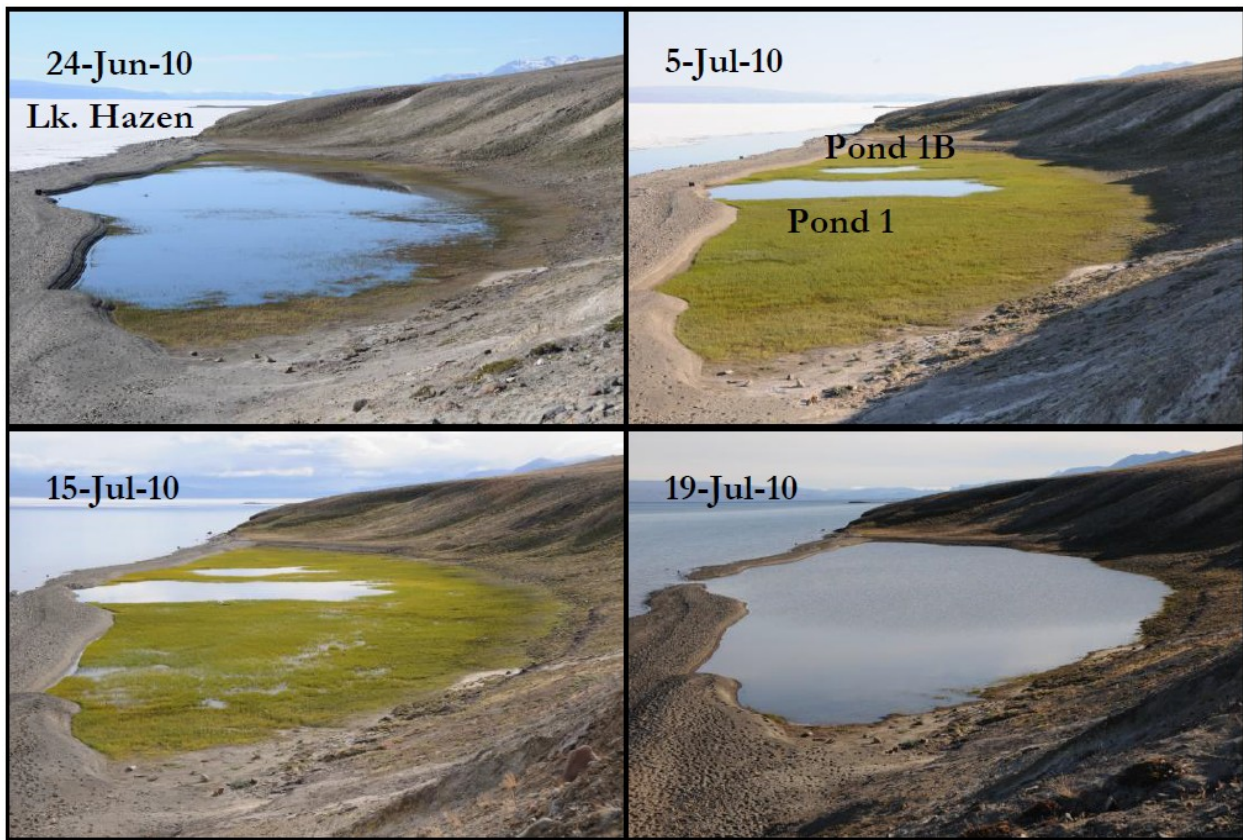
Figure A3.1 Photos of the increasing water levels in Pond 01 during the 2010 summer growing season.

Figure A3.2 Scatterplot of Lake Hazen water level measured at Ruggles River (Water Survey of Canada, 2015) against dissolved inorganic carbon and total dissolved solids concentration on the northeastern shore of Lake Hazen.
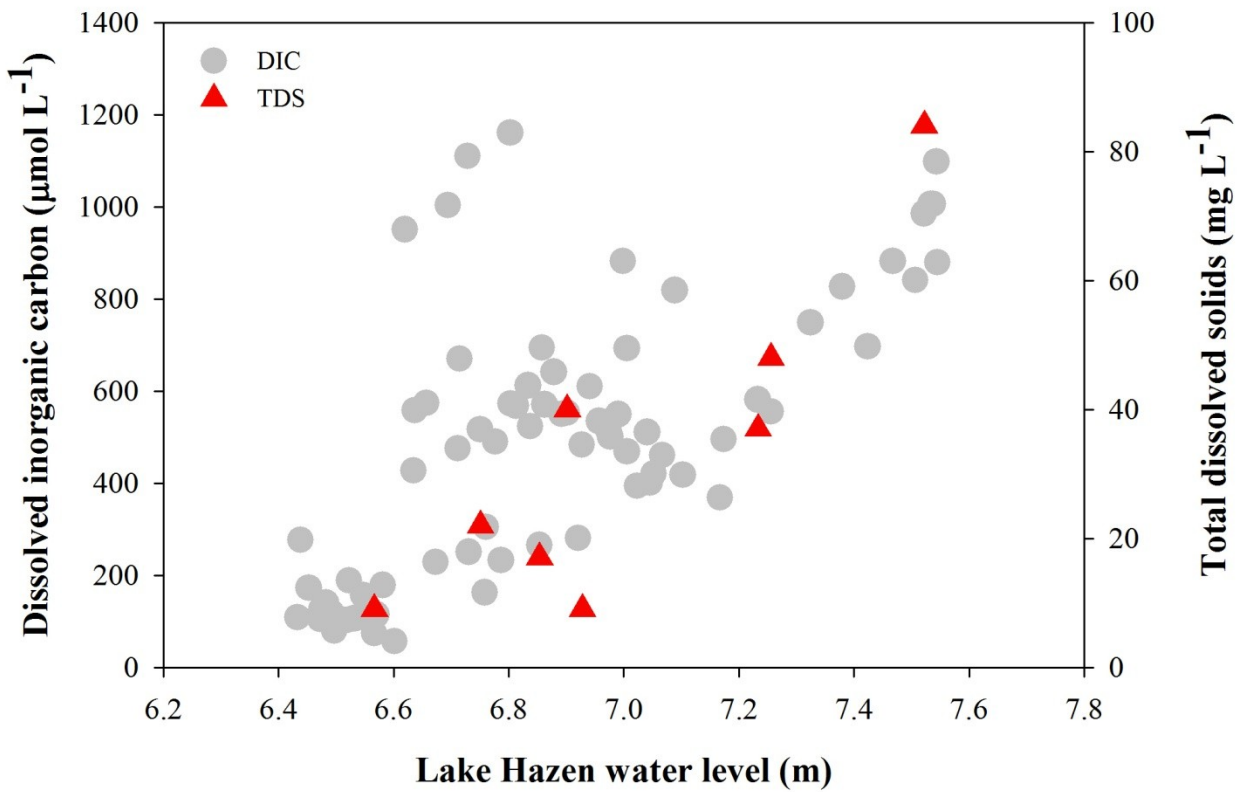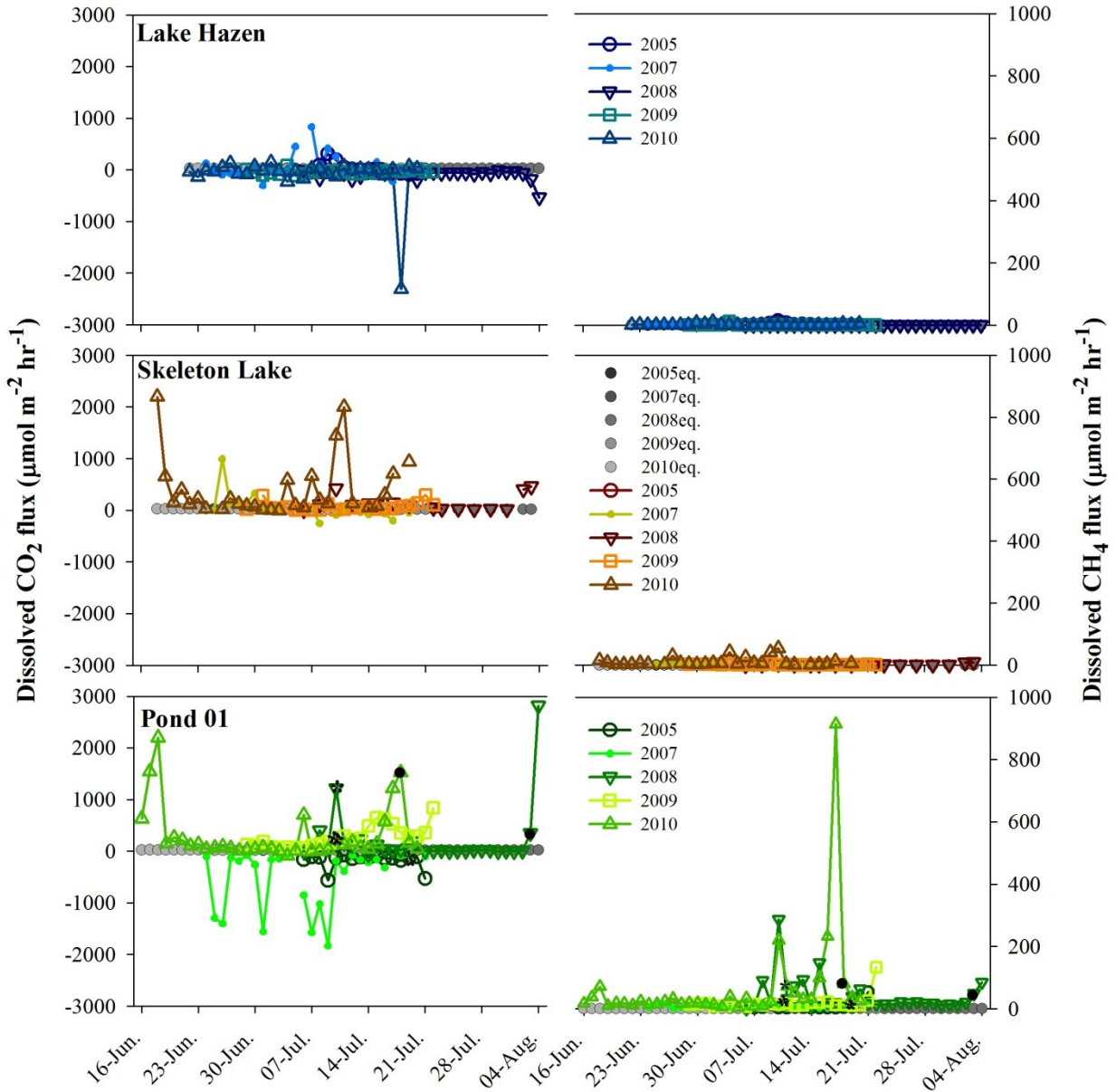
Figure A3.3 Carbon dioxide (CO$_2$) and methane (CH$_4$) fluxes during the 2005-10 growing seasons (June-August) at an upland (Skeleton Lake), margin lake (Pond 01) and large ultra-oligrotrophic lake (Lake Hazen) in a high Arctic watershed.
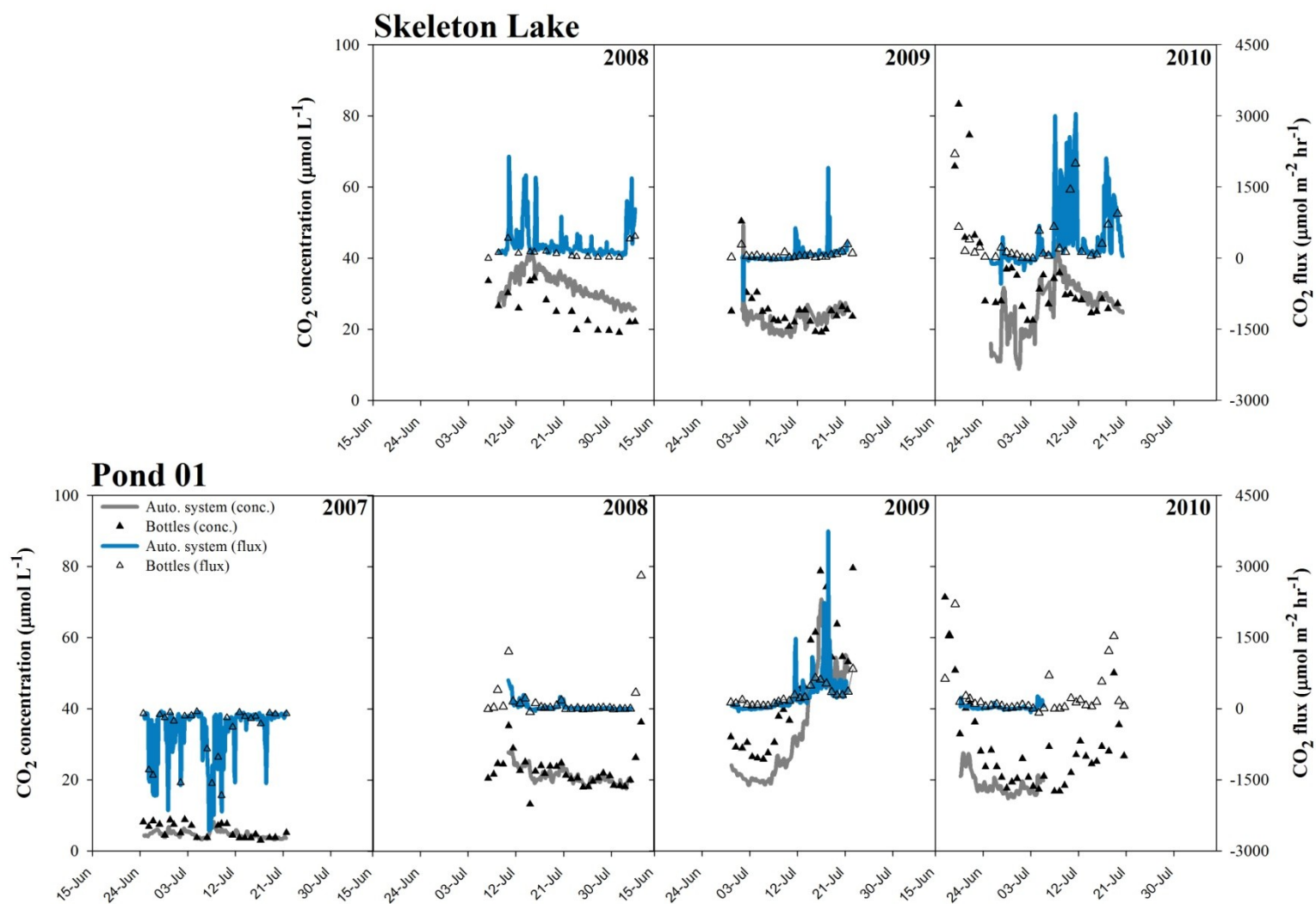
Figure A3.4 Seasonal comparison of bottle and automated system measurements of CO_2 and CH_4 concentrations and fluxes at Pond 01 and Skeleton Lake from 2007 to 2010.
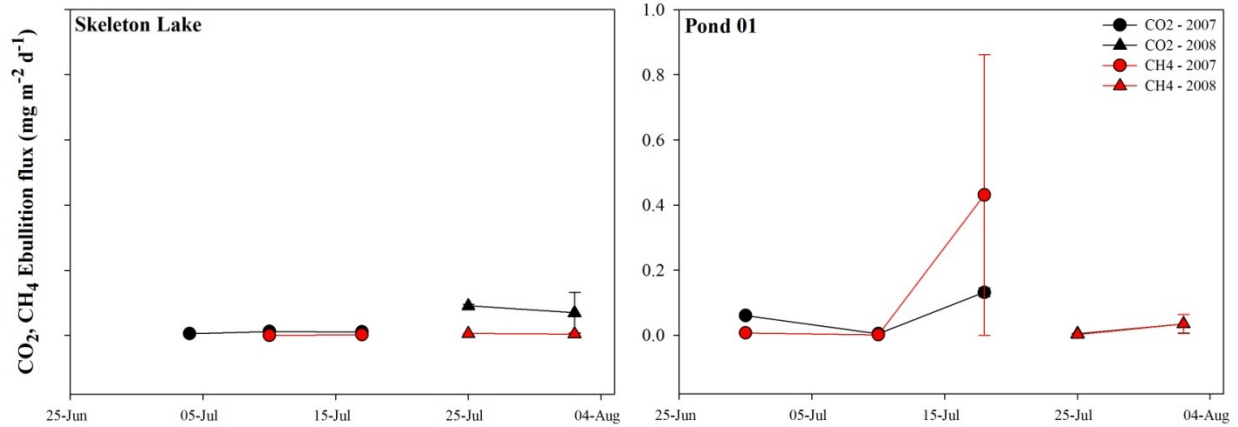
Figure A3.5 Ebullition fluxes during the growing seasons of 2007 and 2008 as measured by week-long deployments of floating traps and greenhouse gases analysis of manually captured bubbles in Pond 01 and Skeleton Lake in the Lake Hazen watershed.
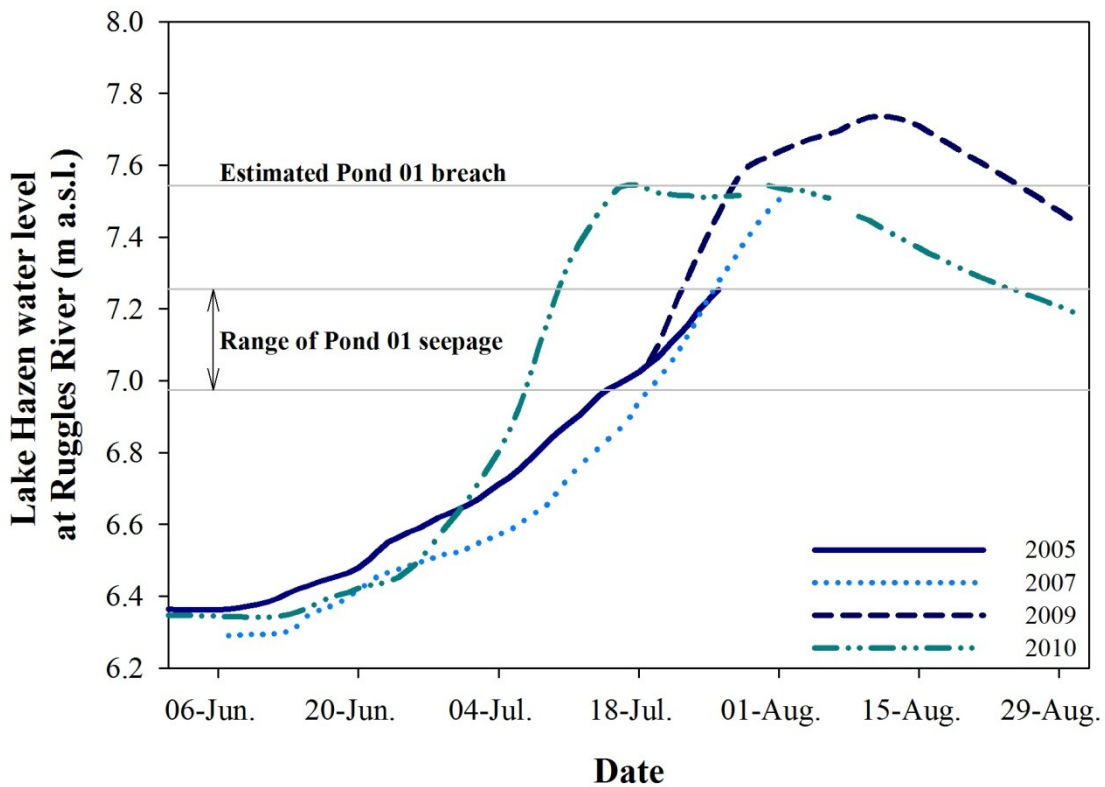
Figure A3.6 Available Lake Hazen water levels during the summer seasons of 2005, 2007, and 2009-10 at Ruggles River. The range of water levels when Pond 01 received Lake Hazen seepage water through its gravel berm are indicated and based on rapid changes in GHG concentrations. Rapid dilution of CH_4 concentrations and field observations were used to determine the water level of pond breach and flushing.

122
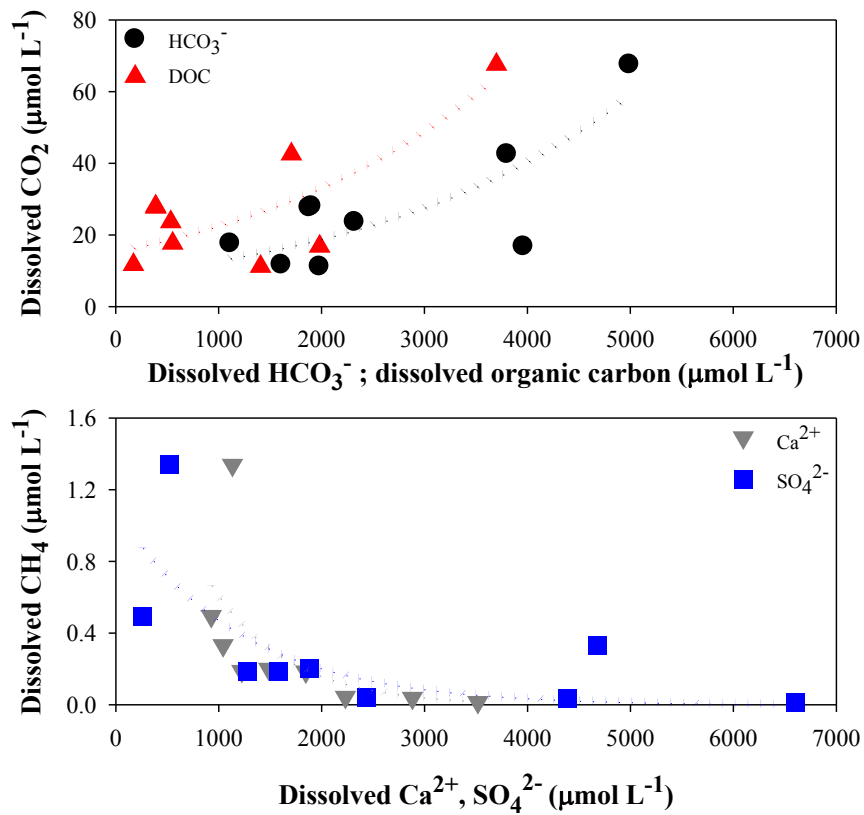
Figure A3.7 Dissolved CO_2 (upper panel) and CH_4 (lower panel) concentrations against key ions and organic matter measurements from nine sampled lakes in the Lake Hazen watershed between the summers of 2005 and 2010.
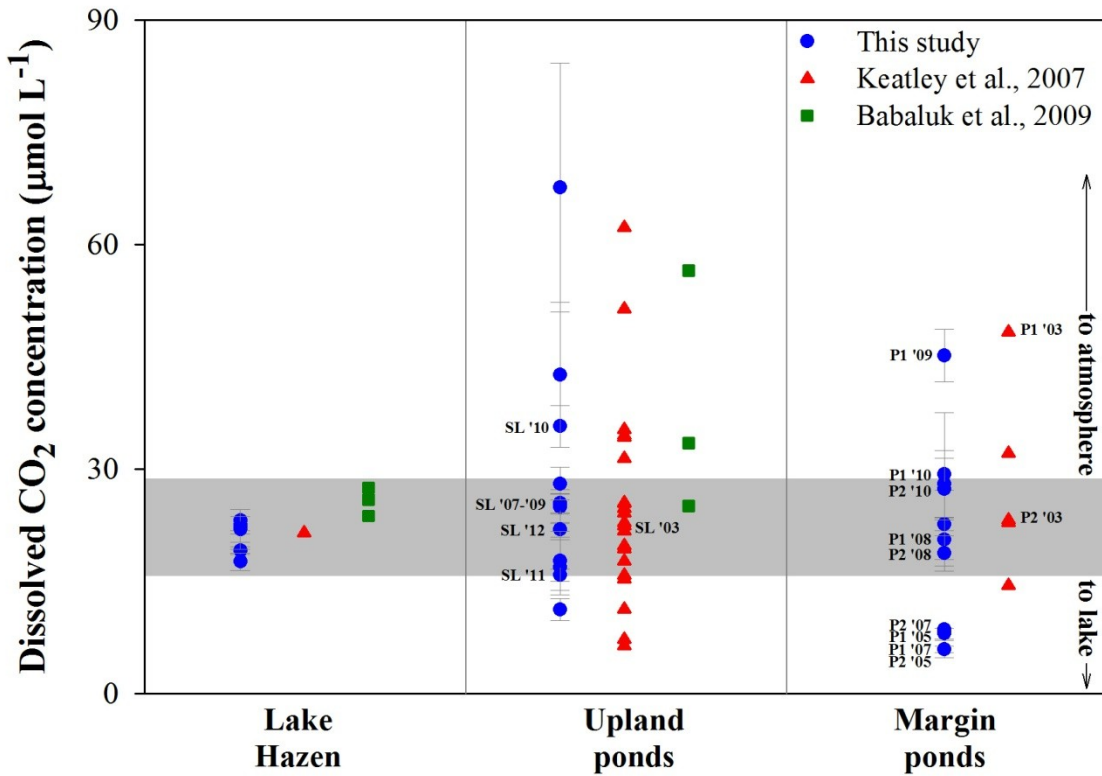
Figure A3.8 Mean measured (this study) and modelled (Keatley *et al.*, 2007; Babaluk *et al.*, 2009) dissolved carbon dioxide (CO_2) and methane (CH_4) concentrations in several streams, upland and margin ponds, and Lake Hazen between 2001 and 2010 in a high Arctic watershed. Grey bars indicate mean atmospheric equilibrium concentration range from measurements between 2005 and 2010 from this study.

References

Babaluk, J.A.; Gantner, N.; Michaud, W.; Muir, D.C.G.; Power, M.; Reist, J.D.; Sinnatamby, R.; Wang, X. Chemical Analyses of water from lakes and streams in Quttinirpaaq National park, Nunavut, 2001-2008. Canadian Data Report of Fisheries and Aquatic Sciences 1217. 2009. Government of Canada. Winnipeg.

Hamilton, J. D.; Kelly, C. A.; Rudd, J. W. M.; Hesslein, R. H.; Roulet, N. T. Flux to the atmosphere of ch4 and co2 from wetland ponds on the Hudson-Bay lowlands (hbls). *Journal of Geophysical Research-Atmospheres* **1994**, *99(D1)*, 1495-1510.

Keatley, B. E.; Douglas, M. S. V.; Smol, J. P. Limnological characteristics of a high arctic oasis and comparisons across northern Ellesmere island. *Arctic* **2007**, *60(3)*, 294-308.

Water Survey of Canada. Real time hydrometric data, **2015**. Available from: http://www.wateroffice.ec.gc.ca/index_e.html.

Craig A. Emmerton

2-258 CCIS, University of Alberta, Edmonton, AB   T6G 2E9   *emmerton@ualberta.ca*
work phone:780-492-0900   *www.ualberta.ca/~emmerton*

Academic background

Doctor of Philosophy – Ecology (in progress)
University of Alberta, Edmonton, AB   *05/10–defense Mar. 2015*

Master of Science – Physical Geography
Simon Fraser University, Burnaby, BC   *09/03–04/06*

Bachelor of Science (Honours) – Environmental Science (Co-op)
McMaster University, Hamilton, ON   *09/97–04/02*

Research experience

The net exchange of carbon greenhouse gases with remote polar semidesert and wetland landscapes on northern Ellesmere Island, Nunavut, Canada
University of Alberta, Edmonton, AB   *05–08/06; 05/10–present*
Ph.D. Candidate, Supervisor: Dr. Vincent St. Louis

A rapidly warming and wetting Arctic climate is changing the net ecosystem exchange (NEE) of carbon dioxide (CO_2) and methane (CH_4) with polar landscapes. Assessments of northern terrestrial NEE have focused mostly on the rich peatland landscapes of the low Arctic, with far fewer studies from expansive, but sparse, high Arctic polar landscapes. Consequently, how these ecosystems may respond to a warming and wetting climate is still a key gap in our understanding of global carbon feedbacks. We used multi−season eddy covariance and static chamber measurements to quantify summer growing season NEE of CO_2 and CH_4 on contrasting polar semidesert and meadow wetland landscapes on northern Ellesmere Island (81ºN), in Canada's high Arctic. During a typical growing season, we found that a dry polar semidesert landscape weakly consumed CO_2 but strongly consumed CH_4. Because dry soils comprise the majority of land area in the high Arctic, we suspect that these landscapes are currently a net sink of carbon GHGs during the summer growing season, and that a warming and wetting climate should reinforce the sink strength of CO_2 and CH_4 on these landscapes.

Mercury dynamics in the Mackenzie River, delta and estuary
Simon Fraser University, Burnaby, BC; University of Alberta, Edmonton, AB   *05/04–06/13*
Supervisor:Dr. Vincent St. Louis

Circumpolar rivers, including the Mackenzie River in Canada, are sources of the contaminant mercury (Hg) to the Arctic Ocean, but few Hg export studies exist for these rivers. During the 2007−2010 freshet and open water seasons, we collected river water upstream and downstream of the Mackenzie River delta to quantify total mercury (THg) and methylmercury (MeHg) concentrations and export. Using concentration−discharge relationships, we calculated bulk THg and MeHg export into the delta of 2300−4200 kg yr−1 and 15−23 kg yr−1 over the course of the study. Bulk THg and MeHg concentrations decreased 19% and 11% through the delta, likely

125

because of particle settling and other floodplain processes. These results suggest that northern deltas may be important accumulators of river Hg in their floodplains before oceanic export.

Downstream nutrient changes through the Mackenzie River delta and estuary
Simon Fraser University, Burnaby, BC   *06/03–04/06*
M.Sc. Student; Supervisor: Dr. Lance Lesack

The role of large, north-flowing rivers on the productivity of the coastal Arctic Ocean is not well characterized in terms of total nutrient delivery or estuarine influence. This is crucial information in the context of climate change as shrinking ice cover and larger river flows may drive biogeochemical changes in the region. This research program quantified open water nutrient fluxes and the role of the lake-rich Mackenzie River delta in storing and biogeochemically altering river water before discharge to the ocean. Nutrient changes across the full salinity transition of the Mackenzie River estuary were also investigated and evaluated with respect to the unique coastal conditions of the Mackenzie Shelf region (Arctic-River Delta Experiment).

FLUDEX and METAALICUS projects
Experimental Lakes Area, Fisheries & Oceans Canada, Winnipeg, MB   *05–08/01; 05–10/02*
Research Assistant; Supervisors: Mr. Ken Beaty, Dr. Drew Bodaly

The FLooded Uplands Dynamics EXperiment assessed the effects of hydro reservoir impoundment on the biogeochemistry of greenhouse gases (CO_2, CH_4) and trace level mercury. Three artificial impoundments were constructed across a gradient of upland forest types to simulate the early conditions of hydro reservoir creation. The Mercury Experiment To Assess Atmospheric Loading In Canada and the United States research program assessed the role of increasing mercury deposition on methylmercury concentrations in fish through a novel stable isotope loading approach at the whole-ecosystem level.

Relevant work experience

Mitacs-Accelerate Intern (Contract)
Campbell Scientific [Canada] Corp., Edmonton, AB   *11/11-03/12*
Supervisor: Mr. Claude Labine
-Developed protocols and client instruction manuals for processing eddy covariance data
-Finalized eddy covariance data from an eddy covariance tower in operation in central Alberta

Water and Sediment Quality Scientist (Contract)
University of Alberta, Edmonton, AB   *10/10–05/11*
Supervisor: Dr. Mingsheng Ma
-Designed water and sediment quality sampling program at stormwater ponds in Central Alberta
-Performed water and sediment quality sampling of stormwater ponds
-Parameters collected: nutrients, basic chemistry, trace metals, organic contaminants, pesticides

Limnologist (Project)
Alberta Environment, Government of Alberta, Spruce Grove, AB   *01/07–04/10*
Supervisor: Dr. Chiadih Chang
-Developed and managed research priorities and water quality monitoring programs in Alberta
-Analyzed data and composed scientific reports from water quality monitoring programs

-Provided guidance and analysis for policy development and decisions
-Provided science support for community groups, the public and regulatory agencies
-Performed shoreline assessments of oiling in response to a spill in a large freshwater lake

Hydrometric Technician (Term)-*Environment Canada, AB*   *08–12/06*
Environmental Scientist (Contract)-*Rescan™ Environmental Services Ltd., BC*   *11–12/05*
Environmental Systems Coordinator (Co-op)-*Diagnostic Chemicals Ltd., PEI*   *09–12/01*
Field Hydrology Assistant (Co-op)-*Experimental Lakes Area, ON*   *05–08/01*
Sustainable Development Policy Analyst (Co-op)-*Natural Resources Canada, ON*   *01–08/00*

Teaching experience

Guest lecturer
University of Alberta, Edmonton, AB   *10/14*
-Class lecture for Dr. John A. Gamon's graduate-level Ecosystem Physiology (Biology 495/595) course. Lecture topic: Process and application of the eddy covariance method.

Teaching Assistant
University of Alberta, Edmonton, AB   *09/13–04/14*
-Department of Biological Sciences courses; responsibilities included: teaching seminars and laboratory sessions, marking lab reports and exams and counselling students.
Courses taught → Biology 208: Ecology; Biology 430: Biostatistics.

Graduate Teaching Program
University of Alberta, Edmonton, AB   *09/10–present*
-Level 1 completion of Faculty of Graduate Studies and Research Graduate Teaching Program consisting of 15 hours of teaching training; Level 2 training to be completed end 2014.

Teaching Assistant
Simon Fraser University, Burnaby, BC   *09/03–12/05*
-Departments of Geography and Biological Sciences courses; responsibilities included: teaching seminars and laboratory sessions, marking lab reports and exams, and counselling students.
Courses taught → Limnology, Biogeochemistry, Physical Geography, River geomorphology

Publications

a. Refereed publications

1.   Chételat, J., Amyot, M., Arp, P., Blais, J.M., Depew, D., Emmerton, C.A., Evans, M., Gamberg, M., Gantner, N., Girard, C., Graydon, J., Kirk, J., Lean, D., Lehnherr, I., Muir, D., Nasr, M., Poulain, A.J., Power, M., Roach, P., Stern, G., Swanson, H., van der Velden, S. (2014) Mercury in freshwater ecosystems of the Canadian Arctic: recent advances on its cycling and fate. Science of the Total Environment, in press. (IF: 3.163)

2. Emmerton, C.A., St. Louis, V.L., Lehnherr, I., Humphreys, E.R., Rydz, E., Kosolofski, H. (2014) The net exchange of methane with high Arctic landscapes during the summer growing season. Biogeosciences, 11, 3095-3106. (IF: 3.753)

3. Emmerton, C.A., Graydon, J.A., Gareis, J.A.L., St. Louis, V.L., Lesack, L.F.W., Banack, J.K.A., Hicks, F., Nafziger, J. (2013) Mercury export to the Arctic Ocean from the Mackenzie River, Canada. Environmental Science & Technology, 47,7644-7654. (IF:5.481)

4. Lehnherr, I., St. Louis, V.L., Emmerton, C.A., Barker, J.D., Kirk, J.L. (2012) Methylmercury Cycling in High Arctic Wetland Ponds: Sources and Sinks. Environmental Science & Technology, 46(19): 10514-10522. (IF: 5.481)

5. Graydon, J.G., St. Louis, V.L., Lindberg, S.E., Sandilands, K.A., Rudd, J.W.M., Kelly, C.A., Harris, R., Tate, M.T., Krabbenhoft, D.P., Emmerton, C.A., Asmath, H., Richardson, M. (2012) The role of terrestrial vegetation in atmospheric Hg deposition: pools and fluxes of spike and ambient Hg from the METAALICUS experiment. Global Biogeochemical Cycles, 26, GB1022. (IF: 4.528)

6. Graydon, J.A., Emmerton, C.A., Lesack, L.F.W., and Kelly, E. (2009) Mercury in the Mackenzie River delta and estuary: concentrations and fluxes during open-water conditions. Sci. Total Environ. 407: 2980-2988. (IF: 3.163)

7. Emmerton, C.A., Lesack, L.F.W., and Vincent, W.F. (2008b) Nutrient and organic matter patterns across the Mackenzie River, estuary and shelf during the seasonal recession of sea-ice. Journal of Marine Systems. 74: 741-755. (IF: 2.476)

8. Emmerton, C.A., Lesack, L.F.W., and Vincent, W.F. (2008a) Mackenzie River nutrient delivery to the Arctic Ocean and effects of the Mackenzie Delta during open-water conditions. Global Biogeochemical Cycles. 22: GB1024. (IF: 4.528)

9. Emmerton, C.A., Lesack, L.F.W., and Marsh, P. (2007) Lake abundance, potential water storage, and habitat distribution in the Mackenzie River Delta, western Canadian Arctic. Water Resour. Res. 43: W05419. (IF: 3.709)

b. Submitted refereed publications

c. Government reports, theses

1. Canadian Mercury Science Assessment. Chapter 5: Watershed and Aquatic Processes. Clean Air Regulatory Agenda (CARA) Hg Science Program (2014). Environment Canada, Ottawa, Canada (Contributing Author, in press).

2. Northern Contaminants Program—Canadian Arctic contaminants assessment report III (2013). Ottawa, Canada. Aboriginal Affairs and Northern Development Canada (Contributing author).

3.   Emmerton, C.A. (2011) Wabamun Lake phosphorus budget 2008: data report and review of lake phosphorus budgets in Alberta. Alberta Environment. ISBN ISSN: 978-0-7785-9977-7. 34 pp.

4.   Emmerton, C.A. (2006) Downstream nutrient changes through the Mackenzie River Delta and Estuary, western Canadian Arctic. M.Sc. Thesis, Simon Fraser University: 181pp.

5.   Emmerton, C.A. (2001) The effect of entrapped air on hydraulic conductivity. B.Sc. Hons. Thesis, McMaster University: 34pp.

Presentations

1.   Emmerton, C.A., St. Louis, V.L., Humphreys, E.R., Barker, J.D., Gamon, J.A., Pastorello, G.Z. Net ecosystem production of semidesert and meadow wetland landscapes in the rapidly changing Canadian high Arctic. American Geophysical Union Fall Meeting, December 15-19, 2014, San Francisco, U.S.A.

2.   St. Louis, V.L., Emmerton, C.A., Lehnherr, I., Humphreys E.R., Rydz, E.R., Kosolofski, H. The net exchange of methane with high Arctic landscapes during the summer growing season. American Geophysical Union Fall Meeting, December 15-19, 2014, San Francisco, U.S.A.

3.   Lehnherr, I., St. Louis, V.L., Muir, D., Emmerton, C.A., Gardner, A., Lamoureux, S., Michelutti, N., Schiff, S., Sharp, M., Smol, J., St-Pierre, K., Tarnocai, C. Coupled terrestrial-aquatic climate impacts on the watershed of the high Arctic's great lake (Lake Hazen, Nunavut). Arctic Change 2014, December 8-12, 2014, Ottawa, Canada.
4.   St. Louis, V.L., Emmerton, C.A., Humphreys, E.R., Lehnherr, I., Barker, J. The net exchange of carbon greenhouse gases with Canadian high Arctic landscapes during the summer growing season. Arctic Change 2014, December 8-12, 2014, Ottawa, Canada.

5.   St. Louis, V.L., St-Pierre, K., Lehnherr, I., Emmerton, C.A., Szostek, L., Muir, D.C.G., Talbot, C. Rapidly changing summer ice conditions on the world's largest high Arctic lake (Lake Hazen, Nunavut, Canada). Arctic Change 2014, December 8-12, 2014, Ottawa, Canada.

6.   Gamon, J.A., Huemmrich, K.F., Emmerton, C.A., Humphreys, E., Lafleur, P., Pastorello, G.Z., Rocha, A.V., Shaver, G.R., St. Louis, V.L., Tenuta, M., Thayer, D., Williamson, S. Observing dynamic Arctic surface optical properties with an optical sensor network. American Geophysical Union Fall Meeting, December 9-13, 2013, San Francisco, U.S.A.

7.   Graydon, J.A ., Emmerton, C.A., Gareis, J.A.L., St. Louis, V.L., Lesack, L.F.W., Banack, J.K.A., Hicks, F., Nafziger, J. Mercury export to the Arctic Ocean from the Mackenzie River. T3-0915. The 11th International Conference on Mercury as a Global Pollutant, July 28-August 02, 2013, Edinburgh, UK.

8.   Emmerton, C.A., St. Louis, V.L. Net ecosystem production on High Arctic semi-desert and wetland landscapes, northern Ellesmere Island, Nunavut, Canada. IPY 2012 Conference, April 22-27, 2012, Montreal, Quebec, Canada.

9.   Lehnherr, I., St. Louis, V.L., Kirk, J.L., Emmerton, C.A., Barker, J.D. Methylmercury cycling in High Arctic wetlands: What are the controls on methylmercury production? IPY 2012 Conference, April 22-27, Montreal, Quebec, Canada.

10.   St. Louis, V.L., Lehnherr, I., Lamoureux, S.F., Graydon, J.A., Barker, J.D., Emmerton, C.A., Kirk, J.L. Net ecosystem exchange of carbon dioxide and methane from lakes and wetlands in the Canadian High Arctic. IPY 2012 Conference, April 22-27, 2012, Montreal, Quebec, Canada.

11.   Emmerton, C.A., St. Louis, V.L. Methane exchange on remote semi-desert soils and wetlands on northern Ellesmere Island, Nunavut, Canada. IPY 2012 Conference, April 22-27, 2012, Montreal, Quebec, Canada.

12.   Graydon, J.A., Emmerton, C.A., Gareis, J.L., Nafziger, J., Lesack, L.F.W., St. Louis, V.L., Hicks, F. Mercury input to the Beaufort Sea from the Mackenzie River. IPY 2012 Conference, April 22-27, Montreal, Quebec, Canada.

13.   Graydon, J.A., Emmerton, C.A., Gareis, J.L., Nafziger, J., Lesack, L.F.W., St.Louis, V.L., Hicks, F. Mercury input to the Beaufort Sea from the Mackenzie River. The 10th International Conference on Mercury as a Global Pollutant, July 24-29, 2011, Halifax, Canada.

14.   St. Louis, V.L, Emmerton, C.A., Barker, J., Humphreys, E., Lafleur, P., Tarnocai, C. Primary productivity in the High Arctic: measurements and predictions for climate change. American Geophysical Union Fall Meeting, December 13-17, 2010, San Francisco, U.S.A.

15.   Emmerton, C.A., St. Louis, V.L, Barker, J., Humphreys, E., Lafleur, P., Tarnocai, C. Primary productivity in the high Arctic: Measurements and predictions for climate change. Understanding circumpolar ecosystems in a changing world: outcomes of the International Polar Year, November 3-6, 2010, Edmonton, Canada.

16.   Graydon, J.A., Emmerton, C.A., Gareis, J.L., Nafziger, J., Lesack, L.F.W., St.Louis, V.L., Hicks, F. Mercury input to the Beaufort Sea from the Mackenzie River. Understanding circumpolar ecosystems in a changing world: outcomes of the International Polar Year, November 3-6, 2010, Edmonton, Canada.

17.   Graydon, J.A., Emmerton, C.A., Gareis, J.L., Nafziger, J., Lesack, L.F.W., St.Louis, V.L., Hicks, F. Mercury input to the Beaufort Sea from the Mackenzie River. 18th Annual Results Workshop of the Northern Contaminants Program (INAC). September 28-30, 2010, Whitehorse, Canada.

18.   Graydon, J.A., St. Louis, V.L., Lindberg, S.E., Sandilands, K., Krabbenhoft, D.P., Tate, M.T., Harris, R., Emmerton, C.A., Richardson, and M., Asmath, H. The role of terrestrial vegetation in mercury deposition: fate of stable mercury isotopes applied to upland and wetland forest canopies during the METAALICUS experiment. American Geophysical Union Fall Meeting, December 14-18, 2009, San Francisco, U.S.A.

19.   Emmerton, C.A. Focused watershed monitoring and community stewardship at a large Alberta lake. North American Lake Management Society 28th International Symposium, November 11-14, 2008, Lake Louise, Canada.

20.   Graydon, J.A. and Emmerton, C.A. Mercury in the Mackenzie River delta: concentrations and fluxes during open-water conditions. North American Lake Management Society 28th International Symposium, November 11-14, 2008, Lake Louise, Canada.

21.   Emmerton, C.A., L.F.W. Lesack and W.F. Vincent. Changes in river-borne nutrients downstream through the Mackenzie River Delta during open-water 2004. American Society of Limnology and Oceanography Summer Meeting, June 4-9, 2006, Victoria, Canada.

22.   Emmerton, C.A. Downstream nutrient changes through the Mackenzie River Delta and Estuary, western Canadian Arctic. M.Sc. Thesis Seminar. Simon Fraser University, Department of Geography. April 6, 2006.

23.   Emmerton, C.A., Lesack, L.F.W., and Vincent, W.F. Nutrient changes through the channels of the Mackenzie Delta and Estuary. ArcticNet Annual Meeting, December 13-16, 2005, Banff, Canada.

24.   Graydon, J.A., Emmerton, C.A., Lesack, L.F.W., and Vincent, W.F. Temporal mercury and nutrient contents in floodplain lakes and channels, Mackenzie Delta, N.W.T. ArcticNet Annual Meeting, December 13-16, 2005, Banff, Canada. (Conference poster).

Awards

-University of Alberta Dissertation Fellowship, 2014 $22,000

-Queen Elizabeth II Graduate Scholarship. University of Alberta, 2013 $15,000

-Steve and Elaine Antoniuk Graduate Scholarship, University of Alberta, 2013 $6,000

-AAAS/Science Program for Excellence in Science, Membership award, 2012 $300

-Canadian Polar Commission Scholarship, ACUNS, 2012 $10,000

-President's Doctoral Prize of Distinction, University of Alberta, 2011 $5,000

-Association of Polar Early Career Scientists (APECS) IPY 2012 Conference From Knowledge to Action Partial Travel Assistance and Accommodation Awards $1,500

-Mitacs-Accelerate Internship (Mitacs, Campbell Scientific Canada, 2011-2012 $15,000

-President's Doctoral Prize of Distinction, University of Alberta, 2011 $5,000
-Alexander Graham Bell Canada Graduate Scholarship, NSERC, 2010-2013 $105,000
-President's Doctoral Prize of Distinction, University of Alberta, 2010 $10,000
-Science Graduate Scholarship, University of Alberta, 2010 $2,000
-University of Alberta Doctoral Scholarship, University of Alberta, 2010   Honorary
-Simon Fraser University Department of Geography Graduate Bursary, 2005 $4,000
-Simon Fraser University Geography Students' Union travel award, 2005 $100

Research grants

Circumpolar/Boreal Alberta Research (C/BAR; University of Alberta) and Northern Scientific Training Program (NSTP; Aboriginal Affairs and Northern Development Canada). Emmerton, C.A. and St. Louis V. 2011-12 ($5,500); 2012-13 ($6,900); 2013-14 ($3,500).

Northern Contaminants Program Grant. Mercury Input to the Beaufort Sea from the Mackenzie River. Graydon, J. and St.Louis, V. 2010-11 ($13,708; collaborator).

Northern Scientific Training Program (NSTP), Department of Indian and Northern Affairs grant. Summer 2003, 2004 (~$3,700/year).

Volunteering & Outreach

-Lab volunteer for Women In Science, Engineering & Technology Set Conference. 2012-13.
-International Polar Week Ask-a-scientist. 16-21 September, 2012.
-Northern Alberta Society for Animal Protection. Voting member and volunteer since 2007.

Media coverage

-Struzik, E. Into the hot zone. Up here. July-Aug 2010.
-Harbord, C. CBC Radio (Inuvik) interview (J. Graydon). 18-June-09.
-May, K. NWT News/North. Mercury levels high in Mackenzie river. 29-June-09.
-Brooymans, H. Mercury levels raise concerns. Edmonton Journal. 17-June-09.
-Murphy, B. Hg in Mackenzie R. delta higher than previously believed. Folio. 15-May-09.

Relevant professional experience

-Invited reviewer for the following journals: Global Biogeochemical Cycles, Environmental Technology, Chemistry and Ecology, Estuaries and Coasts, CJFAS

-Session chair at: International Polar Year Results Workshop (session Productivity) November 3-6, 2010; Alberta Environment Conference (session 34A,34B) April 21-23, 2008.

Training & skills

1. Certificate Courses
-Standard First Aid, May 2-3, 2012 (2-year certification); MATLAB Fundamentals, Mathworks. Jan. 23-25, 2012; Toronto, ON; LICOR Eddy Covariance Training, LICOR Biosciences. Oct. 23-25, 2011; Lincoln, NE.

2. Laboratory experience
-gas chromatography, ion chromatography, TOC analysis, spectrophotometry, fluorometry, trace mercury analysis (CVAFS), general water and soil quality

3. Environmental sampling experience
-water quality: physical chemistry, nutrients, trace organics and metals, pesticides and bacteria
-air quality/gas exchange: Eddy Covariance CO_2 flux tower; operation of CAPMoN station
-sediment quality: ^{14}C soil dating, Ekman dredge, Sipre and gravity corers
-water quantity: operation of Water Survey of Canada stream/lake stations; manual measurement
-meteorological: operation of long-term Environment Canada meteorological station
-biological: plant biomass, macrophytes, zooplankton/phytoplankton, periphyton, minnows
-pollution: lacustrine oil spill shoreline assessments
-technical: dataloggers, various environmental probes

4. Computing
-Statistical: Systat, SPSS, SAS, MATLAB. Productivity: Office, Illustrator, Photoshop, SigmaPlot, Webpage development. Spatial/Design: ArcGIS/ArcInfo, AutoCAD

5. General experience
- Safe boating, WHMIS, Radiation safety, Class 5 driver's license, AMA & Young Drivers Defensive Driving, outboard operation/maintenance, ATVs, snowmobiles, chainsaws, canoeing/kayaking, 1-ton trucks, general construction.